Cured-in-Place Pipe Pressure Liner Experimental Study

by

Olukayode Awe

A thesis
presented to the University of Waterloo
in fulfillment of the
thesis requirement for the degree of
Doctor of Philosophy
in
Civil Engineering

Waterloo, Ontario, Canada, 2023

Examining Committee Membership

The following served on the Examining Committee for this thesis. The decision of the Examining Committee is by majority vote.

External Examiner	Jayantha Kodikara, PhD. Professor, Civil Engineering, Monash University
Supervisor	Mark Knight, PhD. Associate Professor, Civil and Environmental Engineering, University of Waterloo
Internal Examiner	Mariana Polak, PhD. Professor, Civil and Environmental Engineering, University of Waterloo
Internal Examiner	Kunho Eugene Kim, PhD. Assistant Professor, Civil and Environmental Engineering, University of Waterloo
Internal-external Examiner	Xianguo Li, PhD. Professor, Mechanical and Mechatronics Engineering, University of Waterloo

Author's Declaration

This thesis consists of material all of which I authored or co-authored: see Statement of Contributions included in the thesis. This is a true copy of the thesis, including any required final revisions, as accepted by my examiners. I understand that my thesis may be made electronically available to the public.

Statement of Contributions

Chapters 2, 3, 4, and 5 of this PhD thesis have been incorporated into journal papers co-authored by myself and my supervisor, Prof. Mark Knight. In the experimental setup, Mr. Ahmed Abdel-aal was involved in my initial lab building. He also co-wrote and edited certain sections in the third journal paper (i.e., Chapter 4). Dr. Mark Knight supervised all the work completed in this thesis and provided technical and editorial feedback in preparing the research work.

Abstract

Long-term mechanical properties are critical parameters for the design and performance of thermoset Cured-in-Place Pipe (CIPP) gravity and pressure liners. These liners have been used extensively across North America; however, their long-term performance has not been extensively studied. The purpose of this research is to better understand CIPP liners by experimentally quantifying the mechanical response of the liner under flexure, tension, and internal pressure loading conditions. Non-reinforced and reinforced CIPP long-term (50-year) flexural modulus, tensile modulus, and flexural strength were estimated, and the Creep Retention Factors (CRF) and Strength Retention Factors (SRF) to be applied to the short-term flexural and tensile mechanical properties, were determined. It also provides CIPP short-term hydrostatic burst response for a 150-mm and 200-mm I-Main composite pressure CIPP liner. It estimates the Pressure Rating (PR) using the well-established Hydrostatic Design Basis (HDB) design approach. For flat plate testing, 10,000-hour flexural and tensile creep tests were conducted on I-Main test coupons under a stress level that is 25% of the liner yield strength, and 3,000-hour plus flexural creep-rupture tests were performed completed on various non-reinforced and reinforced CIPP flat coupon specimens. A customized burst facility was designed, constructed, and commissioned for full-scale pipe testing to obtain unique CIPP HDB test data to develop a CIPP HDB regression line. Results show that the long-term (50-year) flexural CRF does not correspond with the tensile CRF values. Also, the long-term (50-year) flexural SRF for both non-reinforced and reinforced test specimens were compared and found not to agree with the generalized SRF (50%) typically used for design. For the case of full-scale pipe testing, results found that the CIPP liner specimens, having no known physical defect, demonstrated significant variability, which was experimentally inferred to be due to the presence of invisible liner imperfections such as microscopic air voids. A regression analysis of CIPP HDB data found that the CIPP design factor, based on the ratio of the short-term burst strength to the 50-year Long-term Hydrostatic Strength (LTHS), agrees with previous research on thermoplastics and glass-reinforced pipes. The most important finding is that, for the particular pressure CIPP specimens used in this research, the 50-year LTHS and HDS, found by extrapolation of the experimental data, were comparable to similar thermoset and thermoplastic pressure pipes that use the HDB method. This finding implies that the HDB design approach has a high potential to advance CIPP testing and design to standardize all watermain CIPP products.

Acknowledgements

First, praise God for His grace and mercy and for bringing this amazing achievement my way. Next, I would like to thank my supervisor, Prof. Mark Knight, for his guidance throughout this research project. He has provided me with a career opportunity and tremendous mentoring.

I would also like to thank my PhD examination committee members, Prof. Xianguo Li, Prof. Mariana Polak, Prof. Kunho Eugene Kim, and Prof. Jayantha Kodikara, for their constructive contributions and comments.

This research would not be possible without the funding support provided by Insituform Technologies Limited in collaboration with the Ontario government (as Ontario Graduate Scholarship (OGS)), the University of Waterloo (as President's Graduate Scholarship (PGS)), the Natural Sciences and Engineering Council of Canada (NSERC), and Ontario Centres of Excellence (OCE).

I want to thank other colleagues who worked closely with me during my grad schoolwork: Ahmed Abdel-aal, Anelisa Silva Schmidt Zucco, and Jide Ogunbanjo. To the technicians who assisted in some aspects of this work: Peter Volcic, Robert Kaptein, Douglas Hirst, and Richard Morrison, thank you!

Finally, support from my family was needed throughout my studies. Shout out to my amazing wife, Demilade, and also to my wonderful and well-behaved kids – King, Joy, and Zoe. Thank you all for believing in me and cheering me up while working on this research.

Table of Contents

List of Figures

List of Tables

Chapter 1

Introduction

1.1 Background

The non-disruptive nature of the thermoset Cured-in-Place Pipe (CIPP) trenchless installation technique and its outstanding ability to increase the life of old underground pipelines make CIPP one of the most widely used products today. In North America, the Non-Mandatory Appendix X1 in ASTM F1216 [1], *"Standard Practice for Rehabilitation of Existing Pipelines and Conduits by the Inversion and Curing of a Resin-Impregnated Tube,"* is used as a method to design CIPP liners. This design method requires mechanical properties such as a long-term flexural modulus for Equations X1.1 and X1.3, long-term flexural strength for Equations X1.2 and X1.6, and long-term tensile strength for Equation X1.7 [1], [2]. Table 1.1 shows the ASTM F1216 equations used for design and identifies the parameters for long-term mechanical properties.

Table 1.1: Long-term parameters in ASTM F1216 design equations.

	ASTM F1216 Equations	Long-Term Parameters
X1.1	$P = \frac{2KE_L}{(1-\nu^2)} \cdot \frac{1}{(DR-1)^3} \cdot \frac{C}{N}$	E_L is the long-term flexural modulus
X1.2	$1.5\frac{\Delta}{100}\left(1+\frac{\Delta}{100}\right)DR^2 - 0.5\left(1+\frac{\Delta}{100}\right)DR = \frac{\sigma_L}{PN}$	σ_L is the long-term flexural strength
X1.3	$q_t = \frac{1}{N}\left[32\,R_w\,B'\,E'_s \cdot C\,(E_L I/D^3)\right]^{1/2}$	E_L is the long-term flexural modulus
X1.4	$\frac{E}{12(DR)^3} \geq 0.00064$	Not Applicable
X1.5	$\frac{d}{D} \leq 1.83\left(\frac{t}{D}\right)^{1/2}$	Not Applicable
X1.6	$P = \frac{5.33}{(DR-1)^2}\left(\frac{D}{d}\right)^2 \frac{\sigma_L}{N}$	σ_L is the long-term flexural strength
X1.7	$P = \frac{2\sigma_{TL}}{(DR-2)\,N}$	σ_{TL} is the long-term tensile strength

The required Type Tests include flexural, tensile and creep tests following applicable ASTM standards. However, testing is completed using flat plate specimens, which are not representative of field-installed CIPP and does not account for curvature effects, possible liner imperfections and surge pressures that will occur in a pressure pipe system.

Thermoplastic pressure pipes such as High-Density Polyethylene (HDPE) and Polyvinyl Chloride (PVC) and thermoset glass fibre reinforced pipe (GRP) use a Hydrostatic Design Basis (HDB) method to determine the pipe's long-term properties using full-scale pipe specimens. Owing to the need to provide a high tensile capacity to withstand internal pressure and surge pressures, Long-term Hydrostatic Strength (LTHS) and Hydrostatic Design Stress (HDS) are determined for the pipes. There is currently no reported framework to guide engineers and designers in determining LTHS and HDS for CIPP [3]. One strategy is to adopt well-established HDB test methods and its comprehensive pressure classification system to design thermoset watermain CIPP liners [4]. Using the HDB approach can allow industry professionals to make an engineering-appropriate forecast of the long-term strength of CIPP liners for pressure pipe applications [5].

This research aims to advance the testing and design of pressure CIPP liners for watermain renovation through an extensive experimental program.

1.2 Research Goal and Objectives

The goal of this study is to better understand the long-term mechanical properties of pressure CIPP liners, as well as, advance the design approach currently adopted for watermain CIPP liners. By experimentally quantifying the creep modulus, creep-rupture, and burst stresses in the liner when exposed to various loading conditions, the mechanical response of commercially available thermoset CIPP products using both flat coupon and full-scale pipe specimens is investigated.

This goal is achieved by pursuing four specific research objectives, which are as follows:

1. To determine short-term and long-term mechanical properties from coupon specimens to investigate the creep behaviour and determine Creep Retention Factor (CRF) for a composite CIPP liner.

2. To determine short-term and long-term mechanical properties from coupon specimens to investigate the creep-rupture behaviour and determine the Strength Retention Factor (SRF) for non-reinforced and reinforced CIPP liners.

3. To design, construct and validate a pressure testing facility to determine short-term mechanical properties using full-scale specimens, as well as, investigate CIPP pressure performance and determine the Pressure Rating (PR) for a composite CIPP liner.

4. To expand the constructed pressure testing facility to determine long-term pressure performance using full-scale specimens and develop a CIPP HDB regression line to determine the LTHS, HDS and PR for a composite CIPP liner.

1.3 Thesis Structure

Figure 1.1 presents a graphical description of the contents of this manuscript-based thesis. Chapters 2 to 5 address one or several of the thesis research objectives and are submitted journal papers that contribute to fundamental knowledge and engineering application. Chapter 6 presents the research findings and contributions from Chapters 2 to 5, as well as, recommendations for future work.

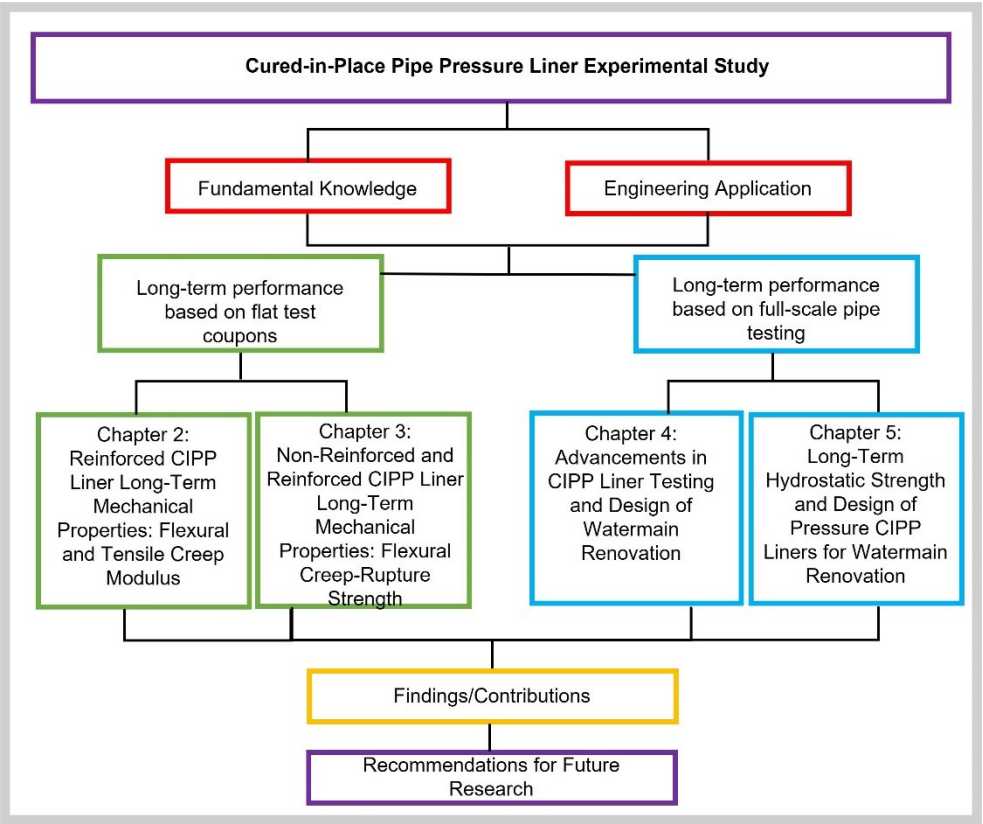

Figure 1.1: Thesis structure and outline for contributing to fundamental knowledge and engineering applications.

Chapter 2 details an experimental study of the flexural and tensile creep properties of a thermoset composite CIPP liner subjected to a stress level that is about 25% of the liner yield strength for 10,000 hours (14 months). The estimated 50-year creep properties of the liners are compared with results obtained using an accepted theoretical model from literature and current industry practice of a 50% CRF. A significant finding in this chapter was the high degree of difference observed when the flexural and tensile CRF were compared to the generalized 50% CRF adopted for CIPP design.

Chapter 3 presents an experimental study of the flexural creep-rupture response of a thermoset non-reinforced and reinforced CIPP liner using a linear displacement potentiometer attached to the top surface of coupon specimens. The long-term flexural strengths of the liners were determined and compared with the conventional flexural strength determination approach based on the use of creep modulus curves and a CRF value of 50%. A major finding in this chapter was the significant difference

observed when comparing the non-reinforced homogenous CIPP response with the fibre-reinforced composite CIPP product.

Chapter 4 presents the development of a unique pressure testing equipment and experimental procedure to study the short-term burst response of a thermoset composite CIPP liner when subjected to a uniformly increasing pressure to cause liner failure. An interesting finding in this chapter details how microscopic liner imperfections can cause significant variability when CIPP is subjected to hydrostatic pressure.

Chapter 5 gives an overview of the HDB methodology used to establish the long-term hydrostatic strength of thermoplastic and thermoset pressure pipes and its applicability to design CIPP reliably. It presents an experimental investigation of the mechanical response of a CIPP liner after setting, monitoring, and maintaining the CIPP internal pressure and determining the time burst failures occurred. CIPP product 50-year LTHS and the liner PR were determined.

Chapter 2

Reinforced CIPP Liner Long-Term Mechanical Properties: Flexural and Tensile Creep Modulus

2.1 Overview

Long-term mechanical properties of reinforced thermoset Cured-in-Place Pipe (CIPP) liners, which are critical parameters for completing the design of CIPP products, have not been extensively studied. In this study, CIPP long-term (50-year) flexural modulus and tensile modulus were estimated, and the Creep Retention Factors (CRF) to be applied to the short-term flexural and tensile mechanical properties were determined. 10,000-hour flexural and tensile creep tests were conducted on an I-Main composite pressure CIPP liner under a stress level that is 25% of the liner yield strength. Results show that the long-term (50-year) flexural CRF (35%) does not agree with the tensile CRF (50%). Despite the reductions made to CRF values to account for field conditions, curvature effects and possible liner imperfections, the CRF values were considered not to correspond to the generalized CRF (50%) typically used for design. Therefore, the anisotropic nature of reinforced thermoset CIPP pressure liners is critical to the long-term creep mechanical response. When loaded in flexure, their mechanical behaviour is significantly different from when loaded in tension.

2.2 Introduction

In North America, many buried pipelines transporting wastewater and potable water are old, deteriorated, and close to the end of their service lives [3]. Over the last 50 years, Cured-In-Place Pipe (CIPP) liners have been used to renovate gravity pipes (wastewater, stormwater, and culverts) and forcemains. Gravity CIPP liners developed in the 1970s consist of a tubular fabric impregnated with polyester or vinyl ester thermosetting resins [4]. The resin-impregnated fabric is cured within the pipe using an energy source (hot water, steam, or UV light) to form a tight-fit structurally stable pipe within the host pipe [1], [2], [6]. In later years, CIPP was developed to include a reinforcing fabric to prevent the liner from tearing apart when handling low-pressure (140 to 280 kPa) forcemains. Further development was made to CIPP, and in recent years, several CIPP systems for the renovation of pressure pipes were introduced to the trenchless industry. Unlike gravity CIPP liners, CIPP for pressure

liners is subjected to internal working pressures that can range from 415 to 830 kPa, as well as, recurring and occasional surge pressures [16], [31], [32]. Watermain pressure CIPP liners are composite materials consisting of thermosetting resin and reinforcements, which are generally manufactured using strict quality control practices to be styrene free so that they can meet NSF 61 testing requirements [2]. Matthews et al. [7] provide details about the evolution of fully-structural reinforced pressure CIPP products introduced after the first watermain renovation at the Perry Nuclear Plant in Cleveland, Ohio, in the late 1990s. This evolution involved introducing unique lining products such as Aqua-Pipe®, AquaLiner, InsituMain™, and NordiPipe™ into the pressure pipe renovation market. Aqua-Pipe® CIPP was introduced in the early 2000s and comprised two concentric, tubular, plain woven seamless polyester jackets with a polymeric membrane bonded to the interior. The tubular jacket or tube is impregnated with a thermoset epoxy resin and cured using hot water. Another CIPP product developed around the same time as Aqua-Pipe® is the NordiPipe™ CIPP liner. It has a fibreglass layer between two non-woven felt layers. The tube is impregnated with epoxy, and a polyethylene coating is on the interior and cured with steam or hot water. AquaLiner and InsituMain™ are other CIPP products introduced during the late 2000s. AquaLiner involves the insertion of a fibre-reinforced polypropylene sock into a deteriorated pipe. A silicone rubber inflation tube pushes a heated pig through the composite, melting the sock against the pipe, which then cools to form a solid glass-reinforced thermoplastic liner. InsituMain™ is composed of an epoxy composite layer that is reinforced with glass and polyester materials. It has a polyethylene layer on the inside pipe surface, and the resulting composite materials are saturated with a thermosetting epoxy resin, which is cured using hot water [7]. Although all commercially available pressure pipe applications are reinforced to form a composite liner, their mechanical performance is typically significantly different. Currently, Canada has rapid growth and acceptance of the Aqua-Pipe® CIPP for watermain renewal, as reported by Knight et al. [4]. The City of Toronto replaces 35 to 50 km of watermain annually and renovates more than 130 km annually using Cathodic protection and CIPP linings. The CIPP lining program for both the City of Montreal and the City of Toronto is estimated to be around $150 million annually, which is more significant than the estimated $30 to $50 million for CIPP watermain market in the United States [4].

2.2.1 CIPP Design

CIPP design is well established for gravity applications having various methods in countries worldwide. In North America, the Non-Mandatory Appendix X1 in ASTM F1216 [1], *"Standard Practice for Rehabilitation of Existing Pipelines and Conduits By The Inversion And Curing Of A Resin-Impregnated Tube,"* has been extensively used to design CIPP liners. This design method involves completing design checks to obtain an optimum liner thickness required to support external groundwater loads. Also, the technique ensures the liner withstands the internal pressure in spanning holes in the original pipe wall and sustains operating pressures and external loads imposed by soil and traffic surcharge. Depending on the existing pipe to be lined, the required thickness is calculated from a series of design equations. The most significant thickness is then selected for the CIPP installation. In Europe, considerable work was completed by Glock [8] to develop a fully analytical design method for rigidly encased circular pipes subjected to external water pressure, focusing on the resistance to groundwater pressure. The design theories by Glock [8] have been adopted as the ATV-M 127 in Germany [9], [10], and as the 3R2014 in France [11]. All with relatively conservative theoretical assumptions. Their designs involve taking a rational account of quantifiable geometric imperfections (gap and ovality) arising from both the host pipe system and the characteristics of the lining [9], [10], [11]. Adopting the French liner design method, which was initially developed by Thépot [11] in the French National Project of Research and Experimentations Rehabilitation of Urban Sanitation Networks (RERAU), has led to the development of gravity liner design in North America. Currently, to design circular and non-circular close-fit CIPP liners for rehabilitating gravity pipes, the ASCE MOP 145 [12] design method has been used to address the limitations noted in the current ASTM F1216 design method. This method is based on a closed-form solution, which considers both the host pipe's current shape and the potential imperfections, such as an annular gap in the liner and cracking or fracturing of the host pipe [12]. While most CIPP gravity design methods use an analytical approach, there are other more complex approaches (e.g., ATV-M 127 [9]) that use finite element models.

Unfortunately, there is currently no ASTM standard method to design CIPP for pressure pipelines. Since introducing CIPP to the pressure market in North America, engineers have adopted the ASTM F1216 design method for watermain pressure liners. This design method, which covers sewage gravity pipelines, includes additional design checks for low-pressure forcemains [1], [3], [4]. This method was

not intended for the design of watermains, and none of the revisions made since 1989 have addressed the limitations of the design approach to account for higher pressure systems (for watermains). Only the ASTM F1216 Equation X1.3 was revised in 2007, with minor changes to the ovality parameter mainly to design a liner to support soil, hydraulic, and live loads [4]. Based on a 2011 United States Environmental Protection Agency (USEPA) study [13], the responsibility to address CIPP quality assurance and quality control now lies with project owners or engineers. This transfer of responsibility is because the ASTM F1216 design method is now considered well-established for the intended gravity application for sewers and forcemains [13]. As a result, the International Organization for Standardization (ISO) and American Water Works Association (AWWA) have created pressure CIPP liners such as ISO 11297-4 [14] (*Plastics piping systems for renovation of underground drainage and sewerage networks under pressure — Part 4: Lining with cured-in-place pipes*) and AWWA C623 [15] (*Plastics piping systems for renovation of underground drainage and sewerage networks under pressure — Part 4: Lining with cured-in-place pipes*), respectively. Currently, both organizations are working on standardized design methods for watermain renovation.

All design methods for CIPP require short-term and long-term mechanical properties of the liner to determine the design thickness for installing a liner that will have a design life of up to 50 years. Such mechanical properties are fundamental input parameters for design and include the material strength and modulus to withstand flexural and tensile loads for 50 years. Long-term mechanical properties are established by multiplying short-term values by a Creep Retention Factor (CRF). The CRF is typically calculated using the ratio of the 50-year creep modulus to the short-term tensile or flexural modulus. Based on the ASTM F1216 design method, Equation 2.1 (ASTM F1216 Equation X1.1) and Equation 2.2 (ASTM F1216 Equation X1.3) require a long-term (time-corrected) flexural modulus for CIPP.

$$P = \frac{2 \times K \times E_L}{(1-\nu^2)} \times \frac{1}{(DR-1)^3} \times \frac{C}{N} \qquad (2.1)$$

where:

P = groundwater load measured from the invert of the pipe,

K = enhancement factor of the soil and existing pipe adjacent to the new pipe,

DR = ratio of the pipe outside diameter to the pipe minimum wall thickness,

v = Poisson's ratio,

E_L = long-term (time corrected) modulus of elasticity for CIPP,

C = ovality reduction factor, and

N = Safety Factor.

$$q_t = \frac{1}{N}[32 \times R_w \times B' \times E'_s \times C \times (E_L \times I/D^3)]^{1/2} \quad (2.2)$$

where:

q_t = total external pressure on pipe,

R_w = water buoyancy factor,

B' = coefficient of elastic support,

E'_s = modulus of soil reaction,

C = ovality reduction factor,

E_L = long-term (time corrected) modulus of elasticity for CIPP,

I = moment of inertia of CIPP,

D = mean inside diameter of the original pipe, and

N = factor of safety.

When a pipe is subjected to internal pressure, pressure forces are exerted in all directions within the pipe, trying to tear it apart. The tensile strength, which refers to the resistance of the CIPP material to rupture when subject to pressure-induced tensile forces and the modulus of elasticity, which is a measure of the stiffness help to predict the behaviour of the CIPP material under any given load [14]. The typical approach taken by engineers and designers involves conducting long-term flexural tests to determine the CRF. However, pressure liners are typically designed with a focus on reinforcements in the hoop direction therefore tensile CRF can be used on the short-term tensile strength as required by Equation 2.3 (ASTM F1216 Equation X1.7).

$$P = \frac{\sigma_{TL}}{(DR-1)\times N} \quad (2.3)$$

where:

P = internal pressure,

σ_{TL} = long-term (time-corrected) tensile strength for CIPP,

DR = ratio of the pipe outside diameter to the pipe minimum wall thickness, and

N = factor of safety.

2.2.2 Creep Phenomenon

To design and assess the long-term performance of polymeric products such as CIPP, viscoelastic and creep behaviours are among the critical mechanical properties needed to be fully understood. Unlike metal pipes (steel and iron), polymers exhibit creep under constant stress due to polymer chain slippage, i.e., non-linear viscoelastic material response compared to metal pipe linear-elastic material response. This response means polymers will lose strength with time. Creep is a continuing deformation that occurs with time, typically resulting from applied continuous stress below the material yield stress [15]- [16]. Figure 2.1 illustrates an idealized creep curve that shows three distinct regions polymers undergo. There can be a primary creep region immediately after the initial elastic and plastic strain, in which the creep strain increases rapidly with time. This region is followed by a secondary creep region, which is particularly important for analysis because the structure will remain serviceable while in this region. The creep strain increases at the tertiary creep region, and fracture occurs [14], [17].

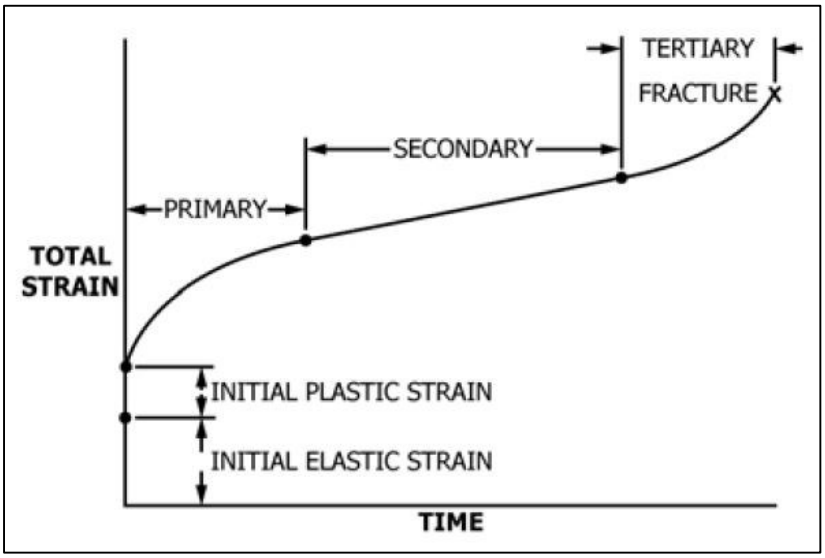

Figure 2.1: Idealized curve showing primary, secondary, and tertiary creep [14].

Depending on the magnitude and duration of the applied stress, creep deformation in CIPP can become so significant that the liner will lose its ability to withstand loads before the end of its estimated service life [18].

Generally, when a polymeric material is subjected to a constant load, the creep modulus, defined as the ratio of applied stress to creep strain, decreases with increasing time. 10,000 hours of testing is the standard industry practice for extrapolating test results to determine the 50-year creep properties following ASTM D2990 [14], *"Standard Test Methods for Tensile, Compressive, and Flexural Creep and Creep-Rupture of Plastics."* To determine the CIPP 50-year creep modulus, creep moduli values for multiple specimens are determined using linear regression of the observed values and projecting to 50 years. The linear regression models are often used for simplicity because some polymeric materials generally display linear creep responses for different durations after loading [19]. Curve-fitting techniques such as models developed by Findley (1944) can be used for creep data extrapolation. Findley's Power Law is a non-linear regression model that was successfully used by Straughan et al. [20] on reinforced polyester resin thermosetting materials and Batra [21] to evaluate glass fibre reinforced plastic (GRP) composites with vinyl ester and polyurethane-based resins [20], [21].

2.2.3 Reinforced CIPP Creep Modulus

Watermain CIPP liners typically require a high tensile capacity to withstand internal stress from operating pressures and pressure surges that will occur within the pipe network. Therefore, reinforcements such as glass, kevlar or carbon fibres are introduced into the matrix to form a reinforced composite CIPP product. Goertzen and Kessler [22] noted that, in a composite CIPP, the matrix (epoxy or polyurethane) experiences viscoelastic behaviour compared to the fibres (glass or kevlar). Thus, introducing such reinforcements into the matrix of CIPP can significantly change its mechanical behaviour as the resulting composite is anisotropic – having directionally dependent material properties.

It is common for unreinforced CIPP gravity liners to have a CRF between 40 to 50% for a 50-year design life. However, only a little testing is done on CIPP to determine material properties. Earlier research by Straughan et al. [23], Straughan et al. [20], Wang [24], Barbero and Rangarajan [25], Hazen [26] and Riahi [27] focused on characterizing the long-term properties of gravity liners that are typically not subjected to hoop stresses from internal pressure and are designed to resist external groundwater loads. These researchers completed testing to characterize the long-term creep modulus of CIPP liners in North America [23]- [27]. They used a linear regression model to estimate the currently adopted 50% CRF for gravity CIPP liners to complete an ASTM F1216 Non-Mandatory Appendix X1 design.

Gravity CIPP liners can also be reinforced to further withstand higher hydrostatic and external pressure loading in the longitudinal direction. In contrast, watermain CIPP liners are typically designed with a focus on reinforcements in the hoop direction to prevent the liner from tearing apart. Figure 2.2 illustrates the difference between the response of gravity CIPP from pressure CIPP. Gravity CIPP liners are designed to resist bending and buckling failure in the liner due to all external loads. However, pressure CIPP further considers the tensile force, F, a liner can provide to withstand internal stress induced by the internal pressure, P.

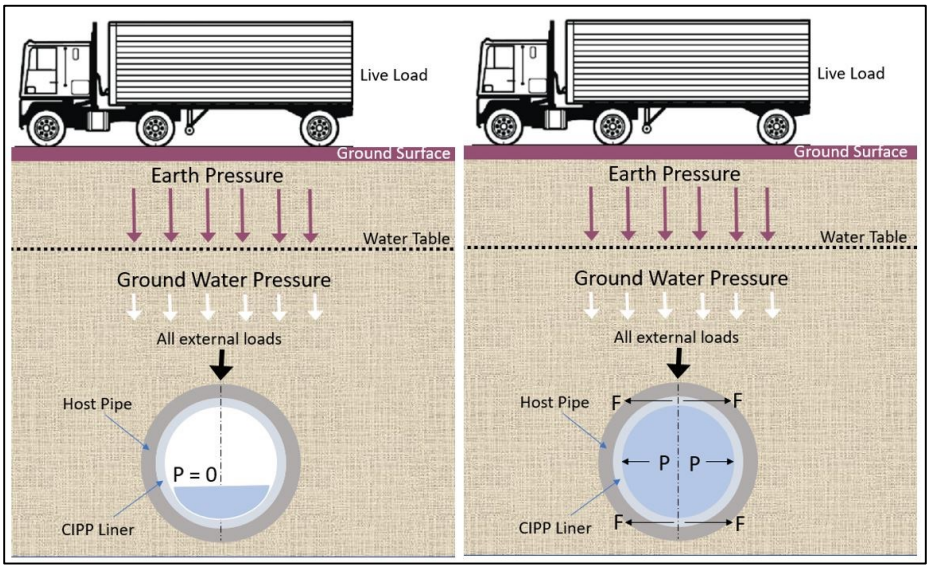

Figure 2.2: Difference between reinforced gravity CIPP (with zero internal pressure, P) and pressure CIPP liners (with internal pressure, P equal to the tensile force, F).

To date, it has not been established that the deformation of reinforced pressure CIPP mechanical properties under constant stress will be comparable to reinforced gravity CIPP, which also adopts a 40 to 50% CRF. Recent testing of reinforced pressure CIPP liners by Knight [28] has shown that reinforced CIPP CRF can be lower than the typical CRF for gravity CIPP liners. CRF was derived based on standard creep testing conducted on CIPP under controlled temperature and humidity, and data extrapolation was completed to determine the long-term CRF of the CIPP liners. Flexural creep testing of different reinforced watermain CIPP products found that flexural CRF can vary from 20 to 50% depending on the liner reinforcement and resin composition. This inherent variability shows that watermain CIPP 50-year liner design can be completed using long-term material properties with as low as 20% of their short-term modulus [3].

The long-term 50-year mechanical creep properties of a reinforced pressure CIPP is also a critical parameter when considering a high-pressure watermain system. For most commercially available pressure composite CIPP, the range of the tensile CRF has not been established owing to the complexity and difficulty of completing tensile creep testing. Therefore, the typical flexural CRF of 50% has often been used for pressure pipe design. In 1998, Straughan et al. [20] investigated the tensile creep properties of coupon specimens made from polyester resin-based fibre-reinforced

gravity CIPP liners. The CIPP tensile CRF value was determined to be 38%, which agrees with the flexural CRF range of 20 to 50% reported by Knight [28]. Shannon [29] recently (in 2022) reported the tensile creep behaviour of a widely tested CIPP liner, which may be Aqua-Pipe®. The tested liner showed tensile CRF values that ranged from 11 to 27%, which agrees with the flexural CRF range of 20 to 50% reported by Knight [28]. However, this tensile CRF range is significantly lower than the tensile CRF of 38% reported by Shannon [29] and the typical CRF of 50% used for liner design. It is unclear why the tested liner showed a tensile CRF value as low as 11%.

This study presents two aspects of CIPP testing. The first involves short-term tests to quantify mechanical properties and evaluate the flexural and tensile behaviour of an Insituform I-Main composite CIPP product. The second involves long-term testing to investigate and estimate CIPP 50-year behaviour. The ASTM D2990 testing procedure was used to evaluate both flexural and tensile CIPP creep response using linear and non-linear extrapolation methods and to investigate the appropriateness of using the traditional 50% CRF value.

2.3 Materials and Test Apparatus

2.3.1 CIPP Specimen Preparation

CIPP liner plates for this study were manufactured and supplied by Insituform Technologies Limited. The reinforced CIPP product is a redesigned version of the InsituMain™ and is called the I-Main CIPP. The reinforcing tube incorporates short fibreglass strands in a layered form, which provides a construction improvement for improved liner wetting out and good expandability, thereby ensuring a close-fit liner can be formed within the host pipe. Figure 2.3 shows a cross-section of the fibre-reinforced CIPP liner investigated in this research. The zoomed image shows how the discontinuous short fibreglass strands are placed on top of each other in the hoop direction.

The I-Main is designed so that the primary fibres are a $0^o/90^o$ glass in the hoop direction with an area weight of approximately 1 kg/m^2. It has an extra layer of randomly placed fibres on the bottom and has an area weight of approximately 0.2 kg/m^2. After constructing the I-Main, the final product is an epoxy composite with no distinct layers as a regular composite that uses reinforcing fabric.

To reduce possible product variability and enhance test data consistency, CIPP test specimens were manufactured in a plant and cured at 71°C. Flat rectangular plates, 275 x 280 mm in dimension, were also manufactured for type testing. One side of the plates was the coating side (with Elantas epoxy), while the other was a felt side (with fibreglass). The nominal thickness of the flat plate was approximately 4.5 to 4.6 mm.

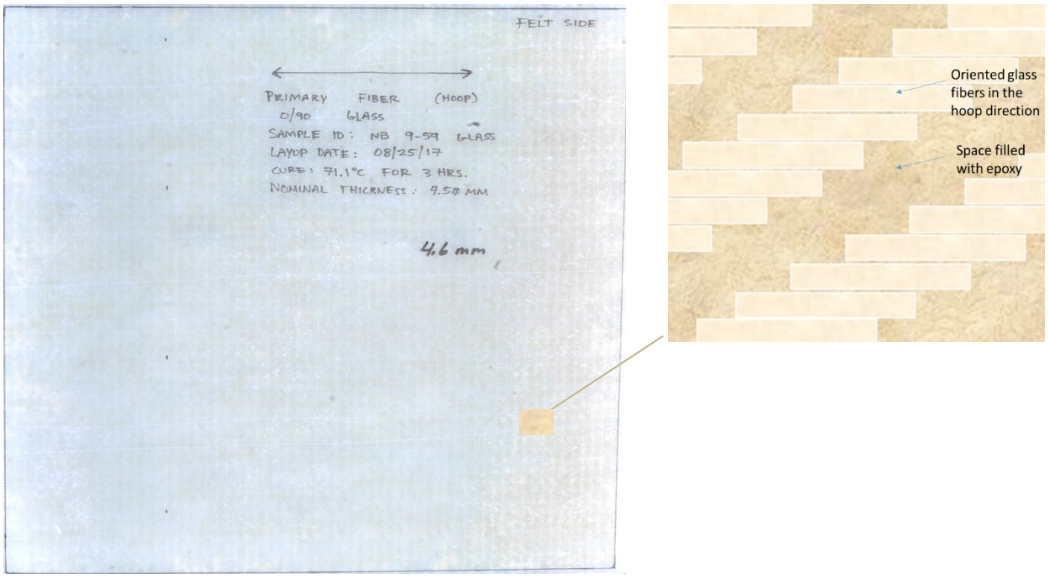

Figure 2.3: Cross-section of the CIPP flat plate and the orientation of fibreglass reinforcements in the composite CIPP liner.

In 2018, I-Main CIPP flat plates were manufactured and shipped to Waterloo. Unfortunately, the plates were noted to be distorted and were not acceptable for testing. Insituform then manufactured a second set of plates ensuring they were flat. Test specimens were waterjet cut from a direction parallel to the CIPP plate reinforcement, as this is the liner hoop direction. Labelling was done so that "SF" and "ST" represented short-term flexure and tension tests, respectively. In addition, "LF" and "LT" represented long-term tests to determine creep in flexure and tension, respectively.

2.3.2 Test Apparatus

To complete long-term flexural creep testing per ASTM D2990, test racks made of steel were designed per the Canadian Handbook of Steel Construction specifications [32] and fabricated to withstand

hanging test loads up to 0.5 kN for five specimens. Using a stirrup, each specimen was loaded flat-wise at the mid-span by hanging steel weights, as shown in Figure 2.4. Mechanical dial gages, accurate to 0.01 mm and mounted on top of the test frame, were used to monitor the deflection of the specimens. For verification purposes, the deflection of one of the test specimens was monitored for up to 1,000 hours using a displacement transducer connected to a commercially available data acquisition system (SoMat eDaQ). All tests were conducted in a room with a constant temperature of 20-23°C, and relative humidity of 50-55%RH.

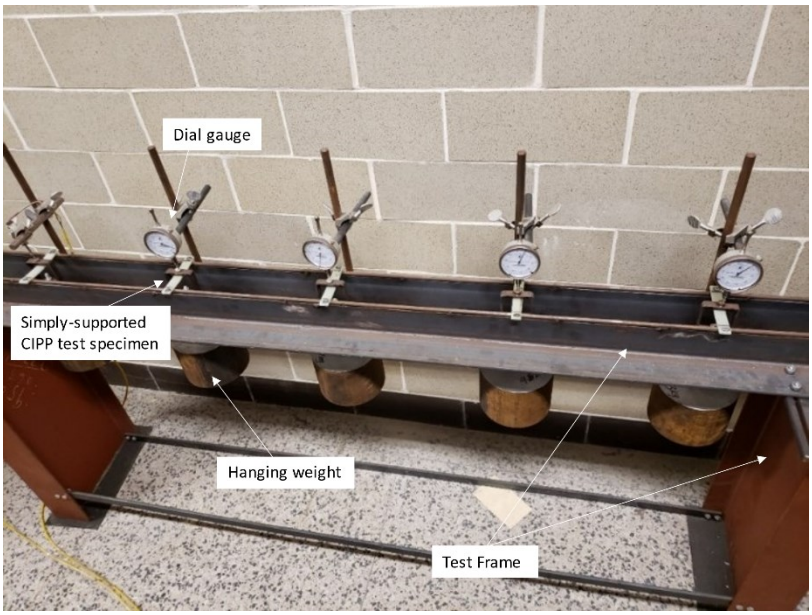

Figure 2.4: Flexural creep test setup located in a vibration-free and constant temperature room.

To investigate the long-term tensile creep properties of the CIPP test specimens, test equipment designed and constructed by the Gas Technologies Institute (GTI) in Chicago was used. This test setup was originally developed to determine the creep response of Medium Density Polyethylene (MDPE) pipes used in gas pipeline applications but was customized to test CIPP specimens. The GTI equipment consists of a controlled environmental chamber that applies a constant load to the specimens using a hydraulic cylinder. The applied load and specimen nominal displacement was measured every second and recorded using a load cell and displacement transducer connected to a data acquisition system. Figure 2.5 shows the tensile testing setup to obtain elongation readings for CIPP creep strain computing.

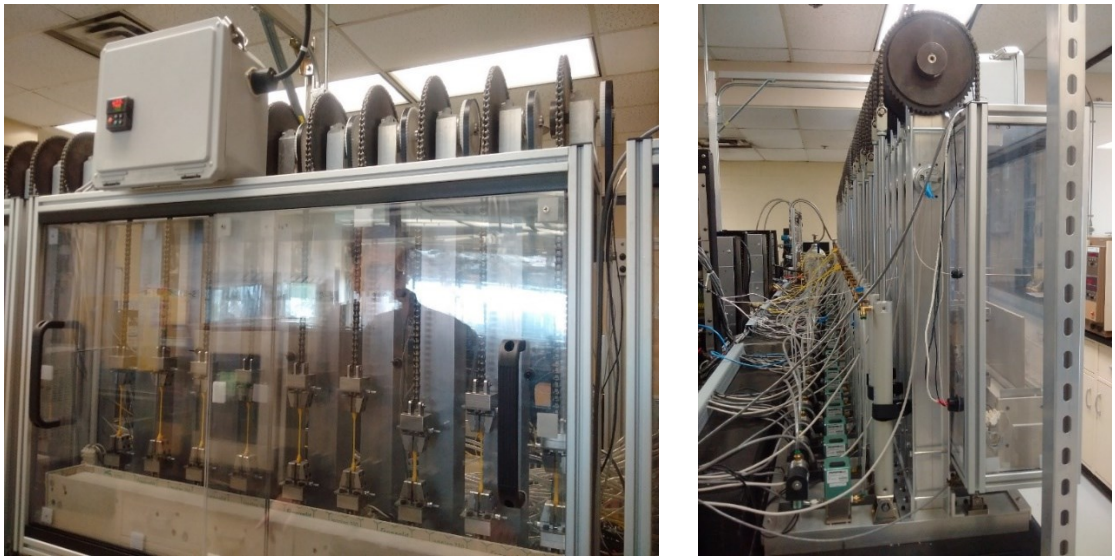

Figure 2.5: Tensile creep test equipment customized to evaluate the tensile creep response of CIPP [30].

2.4 Results and Discussions

2.4.1 Short-Term Flexural Test

CIPP specimens were prepared for short-term flexural testing using the MTS Citerion™ machine with a maximum rated force capacity of 10 kN. The specimen size was determined using a span-to-depth ratio of 16:1 per ASTM D790 [31], *"Standard Test Methods for Flexural Properties of Unreinforced and Reinforced Plastics and Electrical Insulating Materials."* Section 7 and Note 8 of the ASTM standard suggest that a 32:1 or 40:1 span-to-depth ratio may be required for composite to avoid the occurrence of shear failure within the test specimens. Figure 2.6 shows the test specimens prepared for three-point flexural testing. For the I-Main CIPP specimens, the typical testing span-to-depth ratio of 16:1 was experimentally checked and determined to be long enough for flexural testing as the specimens have a uniform cross-section, and no shear failure was anticipated. Figure 2.7 shows a cross-section of the composite CIPP coupon specimen showing no clear distinction in the reinforcement layers.

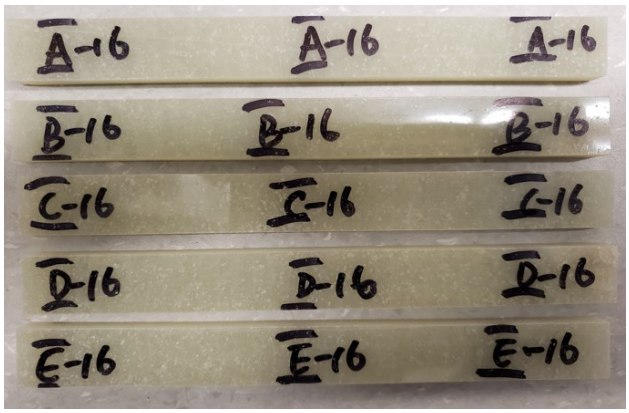

Figure 2.6: Flexural test specimens prepared for ASTM D790 testing.

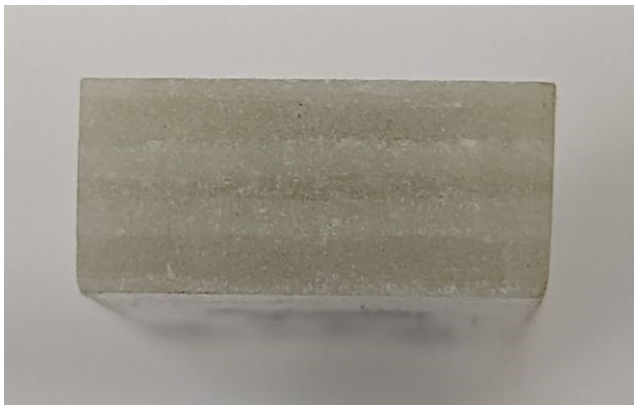

Figure 2.7: Cross-section of the composite I-Main CIPP liner having a uniform cross-section with no distinct reinforcement layers.

Short-term flexural testing consisted of placing the five rectangular specimens flat-wise on two supports and loading the specimens flat-wise at mid-span in flexure as a beam until failure or 5% strain in their outer fibres. Figure 2.8 shows typical flexural stress (σ_f) versus flexural strain (ε_f) curves used to determine the flexural strength of the test specimen response as described by ASTM D790. Curve "a" represents a specimen that breaks before yielding, curve "b" represents a specimen that yields and then breaks before the 5% strain limit, and curve "c" represents a specimen that neither yields nor breaks before the 5% strain limit. Flexural Strength (σ_{fM}) is the maximum flexural stress sustained by the test specimen during a bending test and Flexural Strain (ε_{fM}) is the corresponding strain rate. Flexural Stress at Break (σ_{fB}) is the flexural stress at break of the test specimen during a bending test and Flexural Strain (ε_{fB}) is the corresponding strain rate. Flexural Stress at 5% strain (σ_{fC}) is the flexural

stress at the 5% strain limit of the test specimen during a bending test – the testing is stopped at the corresponding Flexural Strain (ε_{fB}).

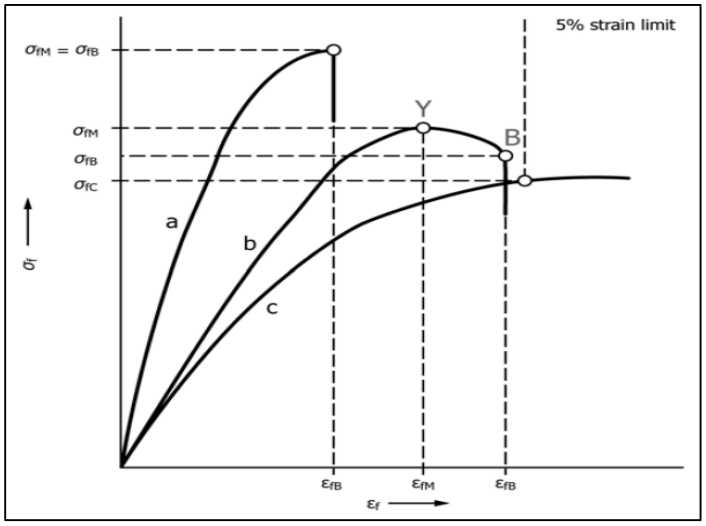

Figure 2.8: Typical flexural stress-strain curves [31].

Figure 2.9 shows the reinforced CIPP stress-strain response subjected to three-point flexural testing. The figure indicates that the liner behaviour is similar to a homogeneous liner and is noted to follow curve “c” in Figure 2.8. No specimen failed during the testing, and the test was stopped after the ASTM D790 prescribed limit of 5% strain was reached. Figure 2.8 shows that the liner flexural stress gradually increased up to approximately 140 MPa at a strain rate of 3.8%, where the specimen cracked and the reinforcing fibres were energized. This phenomenon resulted in a load increase during the testing and can be interpreted as the sudden shifts in the stress-strain behaviour of the CIPP specimens.

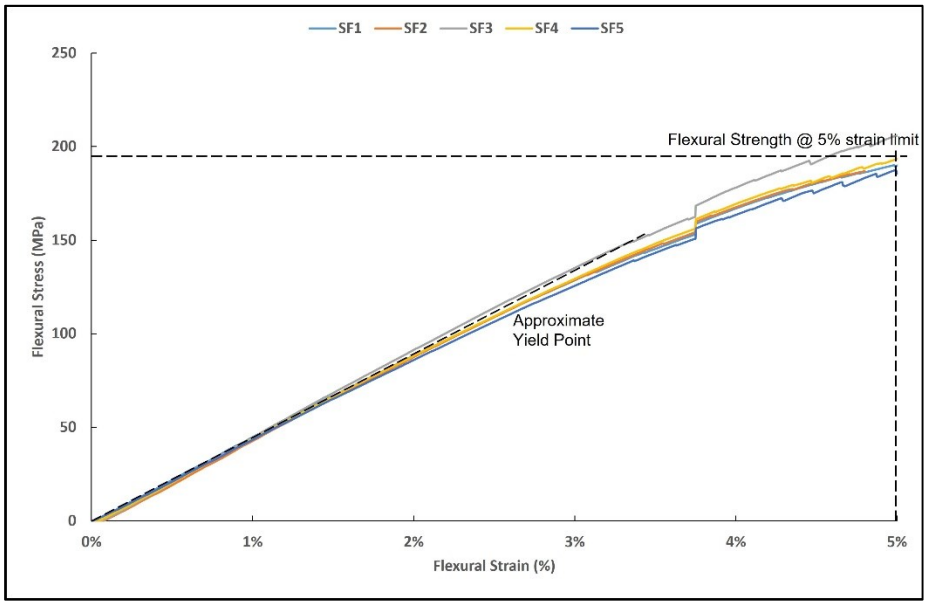

Figure 2.9: Flexural stress-strain curves for specimens cut from the CIPP flat plate.

Mechanical properties such as the flexural strength, flexural strain, initial tangent modulus of elasticity and yield strength were determined for all five CIPP specimens. ASTM D790 [31] defines flexural strength as the maximum flexural stress sustained by the test specimen during a bending test. The flexural strain is defined as the nominal fractional change in the length of an element of the outer surface of the test specimen at midspan, where the maximum strain occurs. The initial tangent modulus of elasticity is defined as the ratio, within the elastic limit, of stress to corresponding strain calculated by drawing a tangent to the steepest initial straight-line portion of the load-deflection curve. Yield strength occurs at the first sudden deviation from the initial linear portion of the stress-strain plot [31].

Table 2.1 provides the flexural test results for tested CIPP specimens. No failure occurred in the test specimens, and maximum flexural strength was defined at the ASTM D790 strain limit of 5% when the test was stopped. The flexural strength varied between 185.8 and 205.7 MPa, with a mean value of 192.3 MPa and a standard deviation of 8.04 MPa. The yield strength ranged between 106.1 and 151.4 MPa, with a mean value of 131.2 MPa and a standard deviation of 17.1 MPa. The yield strain varied between 2.5 and 3.6%, with a mean value of 3.1% and a standard deviation of 0.4%. The initial tangent modulus of elasticity values ranged between 4,182 and 4,539 MPa, with a mean value of 4,356 MPa

and a standard deviation of 129 MPa. From a pressure pipe design standpoint, designing the tested reinforced liner based on the mean flexural strength values at the 5% strain limit may be unreasonable, as CIPP will not be strained up to 5% in the field. Therefore, the tensile yield mechanical properties were considered more appropriate for designing the I-Main CIPP liner.

Table 2.1: Flexural test results for specimens cut from the CIPP flat plate.

Description	Unit	Specimen Identification					Statistics	
		SF1	SF2	SF3	SF4	SF5	Mean	Std. Dev
Mean Depth	mm	4.5	4.5	4.5	4.5	4.5	4.5	-
Test Span	mm	71.8	71.3	71.7	71.8	72.7	71.9	0.5
Span-to-depth ratio	-	16:1	16:1	16:1	16:1	16:1	-	-
Specimen Length	mm	99.9	100	99.9	100	99.9	99.9	0.03
Specimen Width	mm	14.9	14.9	14.9	14.9	14.9	14.9	0.02
Flexural Strength	MPa	189.8	186.8	205.7	193.4	185.8	192.3	8.04
Flexural Strain	%	5.0	4.8	5.0	5.0	5.0	4.96	0.1
Yield Strength	MPa	132.6	151.4	143.5	136.4	106.1	131.2	17.1
Yield Strain	%	3.1	3.6	3.1	3.1	2.5	3.1	0.4
Tangent Modulus of Elasticity	MPa	4,348	4,182	4,539	4,391	4,319	4,356	129
Peak Load	N	496	497	539	506	497	507	18

2.4.2 Short-Term Tensile Test

Five Type II test specimens were prepared and tested per ASTM D638 [32], *"Standard Test Method for Tensile Properties of Plastics."* An MTS Criterion™ tensile testing equipment with a maximum rated force capacity of 10 kN and a 50-mm gage length extensometer was used. Figure 2.10 shows the test specimens after testing. Specimen dimensions were measured using a digital calliper accurate to 0.01 mm.

ASTM D638 [32] determines the tensile mechanical properties of a specimen based on the stress-strain curves using Figure 2.11. Depending on the curve, the specimen's tensile strength and

elongation (or strain) at “break,” tensile strength and elongation at “yield,” tensile stress and elongation at “break,” and tensile stress and elongation at “yield” can be determined.

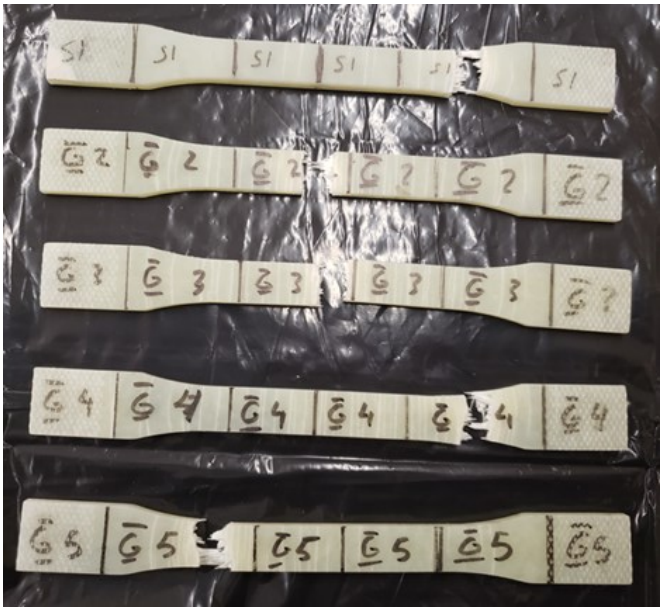

Figure 2.10: Composite CIPP tensile test specimens after testing.

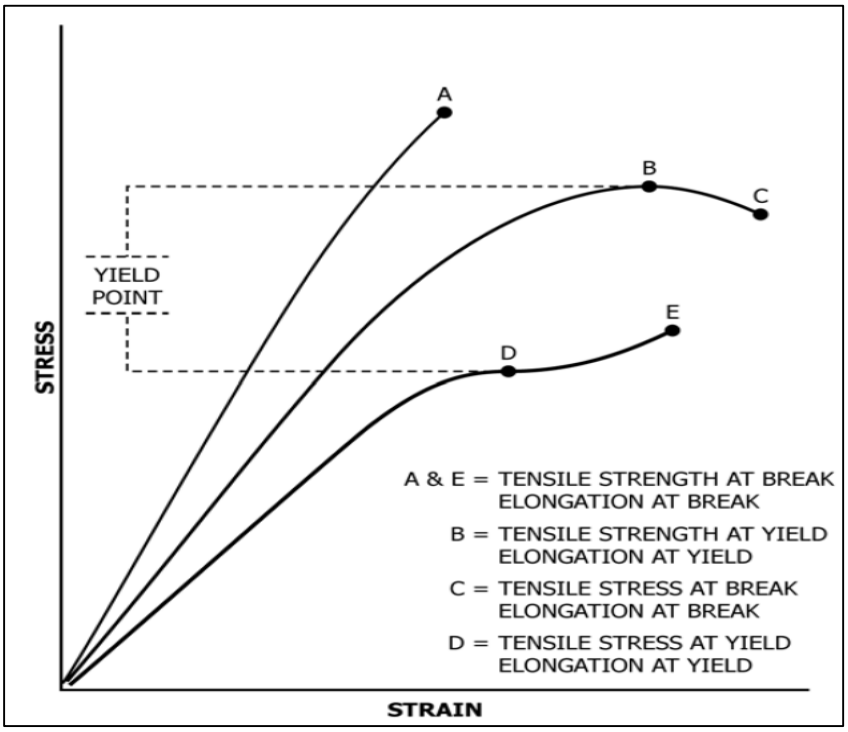

Figure 2.11: Typical tensile stress-strain curves [32].

Figure 2.12 provides the stress-strain curves for the I-Main CIPP test specimens. The trend of the curves shows that tensile stress and elongation at yield (i.e., point D) and tensile strength and elongation at break (i.e., point E) are required to be determined. Figure 2.12 shows a split in the stress-strain response for all test specimens. Two specimens (ST1 and ST5) showed similar responses with tensile strength (at break) between approximately 100 to 120 MPa and a strain rate between 0.9 and 1.2%. Conversely, two specimens (ST2 and ST3) showed similar responses having a tensile strength of approximately 154 to 155 MPa at a strain rate between 2.2 to 2.3%, and specimens ST4 displayed the highest tensile strength of about 175 MPa at a strain of 1.9%. It can be inferred that those test specimens ST1 and ST5 reached their tensile strength (at break) prematurely. This specimen behaviour may have been due to a flaw in the specimens as ST1 and ST5 are observed to have similar load rates with ST4 (which has the highest tensile strength at 175 MPa).

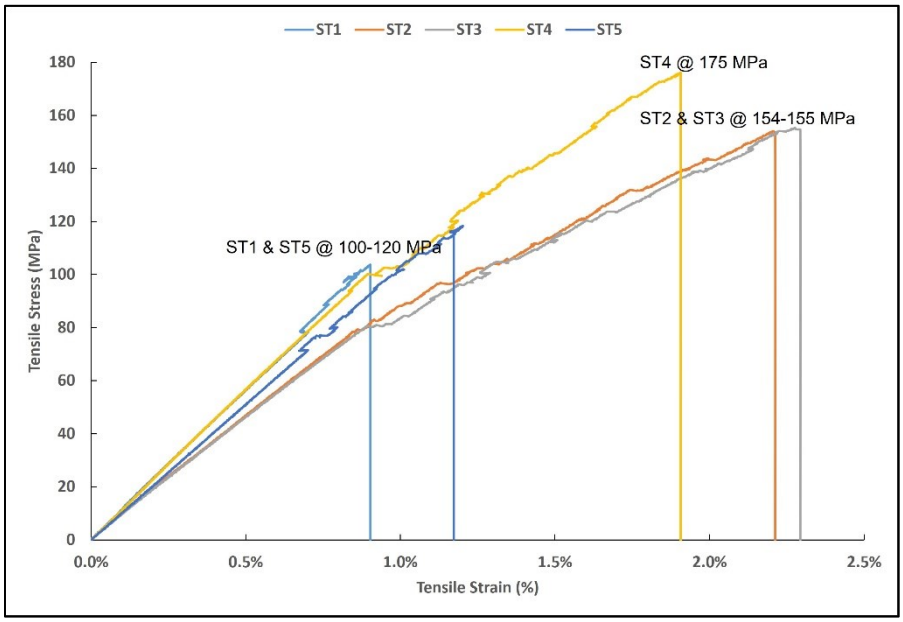

Figure 2.12: Tensile stress-strain curve for specimens cut from the CIPP flat plate.

Table 2.2 provides the tensile test results for the CIPP specimens. The table provides the tensile strength (tensile strength at break), yield strength (tensile stress at yield), initial tangent modulus of elasticity, strain values and a description of where the breakage occurred (i.e., within or outside the gage length). The tensile strength varied between 103.8 and 176.2 MPa, with a mean value of 141.5 MPa and a standard deviation of 29.7 MPa. The tensile strain ranged between 0.9 and 2.3%, with a mean value of 1.3% and a standard deviation of 0.23%. The yield strength varied between 80 and 103 MPa with a mean value of 96.2 MPa and a standard deviation of 16.2 MPa. The yield strain ranged between 0.9 and 1.2%, with a mean value of 0.96% and a standard deviation of 0.14%. The initial tangent modulus of elasticity values varied between 9,230 and 11,366 MPa, with a mean value of 10,296 MPa and a standard deviation of 1,040 MPa.

These short-term test results reveal significant variability in the CIPP tensile mechanical properties. Engineers and designers are advised to use their sound engineering judgements when determining mechanical properties to design watermain CIPP. Since tensile properties are critical for the design of reinforced pressure CIPP, the mechanical properties at the yield point are considered in this research. From a pressure pipe design standpoint, designing the tested reinforced liner based on the mean values may be misleading and unrealistic. The mean tensile strength (141.5 MPa) was computed with

the inclusion of specimens that failed outside the extensometer gage length, which is not compliant with the ASTM D638 test method. Specimen failures were observed to be within the gage length in specimens ST2 and ST3 (shown in Figure 2.10). For pressure pipe applications, the consequence of failure is very high; therefore, CIPP designs should be completed based on the liner yield strength.

Table 2.2: ASTM D638 tensile properties for specimens cut from the CIPP flat plate.

Description	Unit	Specimen Identification					Statistics	
		ST1	ST2	ST3	ST4	ST5	Mean	Std. Dev
Break within the Gage Length	-	No	Yes	Yes	No	No		
Width	mm	12.5	12.6	12.6	12.6	12.6	12.6	0.02
Thickness	mm	4.6	4.4	4.5	4.4	4.5	4.5	0.05
Tensile Strength at Break	MPa	103.7	154.1	155.3	176.2	118.3	141.5	29.6
Load (Break)	N	6,411	9,028	9,316	10,491	7,212	8,492	1,653
Elongation at Break (Strain)	%	0.9	2.2	2.3	1.9	1.2	1.3	0.2
Tensile Strength at Yield	MPa	103	80	80	100	118	96.2	16.2
Load (Yield)	N	6,354	4,892	5,084	6,205	7,182	5,943	951
Elongation at Yield (Strain)	%	0.9	0.9	0.9	0.9	1.2	0.96	0.14
Tangent Modulus of Elasticity	MPa	11,366	9,335	9,230	11,351	10,196	10,296	1,040

2.4.3 Test Stress Selection

ASTM D2990 does not specify the test load to create the required stresses in test specimens. Hence, a test stress value below the yield strength, reflecting the maximum stresses anticipated for pressure pipe applications, was considered appropriate. Watermain CIPP liners are typically restrained within a metallic host pipe and are not expected to be excessively strained in the field. Thus, the test specimens were evaluated within their elastic region by applying stresses that are approximately 25% of the short-term yield strength values (i.e., 25% × 192.3 MPa = 48.1 MPa for flexural testing and 25% × 96.2 = 32.8 MPa for tensile testing). Based on a review of North American practices, this approach

agrees with the prescribed stress level adopted by previous researchers such as Riahi [27] and Guice [33].

2.4.4 10,000-hour CIPP Flexural Creep

Four CIPP test specimens were placed in the flexural creep apparatus and loaded to create a stress of approximately 25% of the short-term yield strength. Per the ASTM D2990 test procedure, deflection measurements for each test specimen were taken at around 1, 6, 12, and 30 minutes and 1, 2, 5, 10, 30, 60, 100, 300, and 500 hours. Also, measurements were taken at 1,000-hour intervals up to 10,000 hours [14].

The creep modulus, $E_{c,}$ at a given time in each specimen was estimated as the initial applied stress (σ_o) ratio to the creep strain (ε) at that given time using Equation 2.4.

$$E_c = \frac{\sigma_0}{\varepsilon} \qquad (2.4)$$

Table 2.3, Figure 2.13 and Figure 2.14 provide the flexural creep test data for strain and modulus up to 10,000 hours. All test specimens appeared not to show a smooth strain profile to determine the transition from primary creep to the secondary creep stage (see Figure 2.1). However, the strain profiles for each specimen (shown in Figure 2.13) suggest that the secondary creep (i.e., steady state) stage began between 500 and 1,000 hours, as all specimens displayed a change in the creep strain rate. The mean 10,000-hour flexural creep strain (1.31%) for the tested specimen was noted to increase by about 35% from the initial flexural creep strain (0.85%) upon load application. No tertiary creep was noted in the tested specimens.

It can be observed from Figure 2.14 that there are discontinuities between 10 and 2,000 hours for both LF1 and LF2 specimens. This missing data was due to an unforeseen inability to take test readings caused by the COVID-19 worldwide pandemic lockdown. Despite the incomplete data, the LF1 and LF2 test data were noted to agree with LF3 and LF4 test data. In all specimens, it was observed that the creep modulus decreased with time, as the flexural modulus at 10,000 hours was significantly lower than the flexural modulus at the onset of loading. The mean flexural creep modulus at 10,000 hours was 2,353 MPa, 2,569 MPa, 2,706 MPa and 2,416 MPa in the LF1, LF2, LF3 and LF4 specimens, respectively. A similar trend was observed at the onset of loading in all specimens except specimen

LF3. It is unclear why specimen LF3 displayed a significantly high initial modulus. Possible causes may be a human error when taking dial gauge readings at the start of the test. Time delays from manually reading off dial gauges for multiple test specimens may have induced a slight increase in the initial deflection readings, which compounded over time. Despite this discrepancy, specimen LF3 displayed a similar creep modulus with specimens LF1, LF2 and LF4. This general trend suggests that the liner displayed linear viscoelastic behaviour under the stress levels investigated (25% of the yield strength) since in a linear viscoelastic material, as explained by Findley [34], the applied stress is proportional to the creep strain at any given time.

Compared with the ASTM D790 short-term flexural modulus, all specimens' mean initial creep modulus (at one minute) was found to be 3,853 MPa. This value is about 12% lower than the short-term flexural modulus of 4,356 MPa.

Table 2.3: CIPP 10,000-hour flexural creep test data.

LF1			LF2			LF3			LF4		
Time (hours)	**Strain (%)**	**Creep Modulus (MPa)**	**Time (hours)**	**Strain (%)**	**Creep Modulus (MPa)**	**Time (hours)**	**Strain (%)**	**Creep Modulus (MPa)**	**Time (hours)**	**Strain (%)**	**Creep Modulus (MPa)**
0.02	0.85	3,838	0.02	0.86	3,854	0.02	0.81	4,058	0.02	0.89	3,662
0.05	0.86	3,807	0.05	0.87	3,823	0.05	0.82	4,024	0.05	0.89	3,634
0.08	0.87	3,776	0.08	0.88	3,792	0.08	0.82	4,007	0.08	0.90	3,619
0.25	0.88	3,716	0.53	0.89	3,733	0.50	0.84	3,923	0.50	0.91	3,550
1.13	0.90	3,658	1.13	0.90	3,704	1.08	0.84	3,891	1.02	0.92	3,509
3.13	0.91	3,602	3.17	0.91	3,634	3.17	0.86	3,812	3.05	0.94	3,444
5.85	0.92	3,547	5.88	0.92	3,593	6.08	0.87	3,766	5.55	0.95	3,406
10.42	0.94	3,494	10.43	0.93	3,566	12.17	0.88	3,736	12.05	0.97	3,356
23.38	0.95	3,443	23.42	0.93	3,553	24.03	0.89	3,678	24.38	0.98	3,320
73.38	0.99	3,321	73.40	0.94	3,540	72.20	0.91	3,594	72.08	1.01	3,227
118.67	1.00	3,274	118.68	0.95	3,488	166.92	0.94	3,513	166.80	1.03	3,161
4875.67	1.29	2,531	4875.67	1.20	2,778	240.27	0.94	3,487	240.15	1.04	3,118
6288.72	1.33	2,464	6288.72	1.25	2,655	720.42	0.99	3,315	720.32	1.09	2,977
7085.00	1.36	2,413	7085.00	1.27	2,626	1012.27	1.01	3,269	1012.15	1.11	2,921

LF1			LF2			LF3			LF4		
Strain (%)	**Creep Modulus (MPa)**	**Time (hours)**	**Strain (%)**	**Strain (%)**	**Creep Modulus (MPa)**	**Time (hours)**	**Strain (%)**	**Strain (%)**	**Creep Modulus (MPa)**	**Time (hours)**	**Strain (%)**
7997.17	1.37	2,389	7997.17	1.27	2,611	1943.00	1.05	3,139	1942.90	1.15	2,831
9002.17	1.39	2,365	9002.17	1.29	2,583	3070.92	1.07	3,077	3070.80	1.19	2,731
10103.17	1.39	2,353	10103.17	1.29	2,569	4131.17	1.10	2,980	4131.07	1.22	2,652
-	-	-	-	-	-	5092.17	1.11	2,961	5092.05	1.23	2,637
-	-	-	-	-	-	5982.17	1.13	2,906	5982.05	1.25	2,592
-	-	-	-	-	-	7056.82	1.15	2,871	7056.72	1.28	2,536
-	-	-	-	-	-	7991.67	1.15	2,853	7991.55	1.30	2,501
-	-	-	-	-	-	9123.53	1.19	2,769	9123.42	1.32	2,455
-	-	-	-	-	-	10000.00	1.21	2,706	10000.00	1.34	2,416

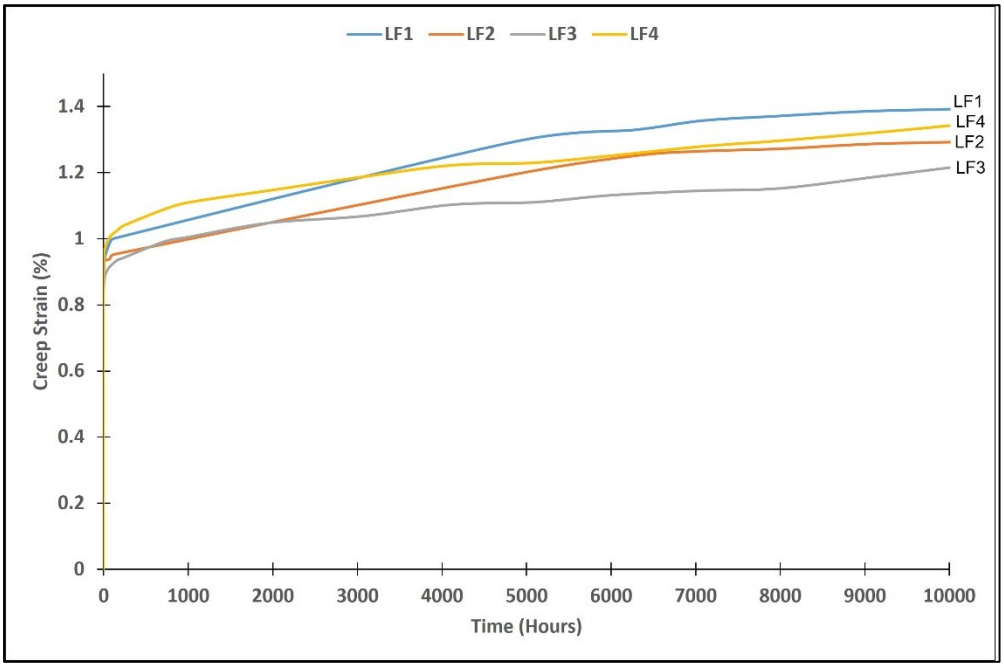

Figure 2.13: CIPP Flexural creep strain up to 10,000 hours.

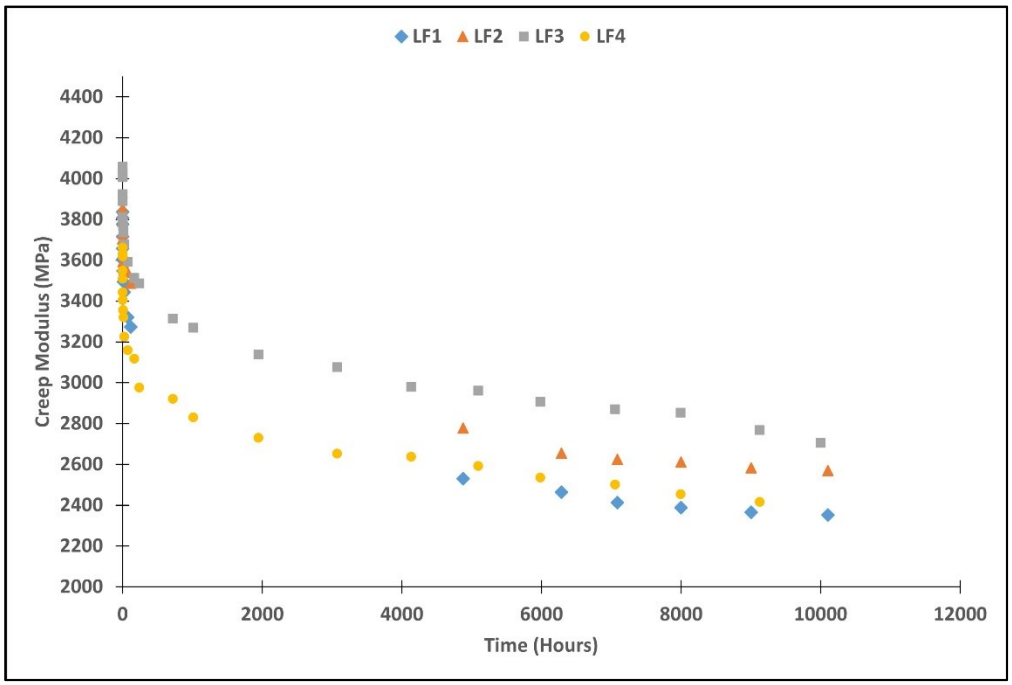

Figure 2.14: CIPP Flexural creep modulus up to 10,000 hours.

Two models were used to fit the 10,000-hour experimental test data to estimate the CIPP 50-year creep modulus. The approaches involve 1) Normal-log linear regression analysis and 2) Non-linear regression using Findley's power law.

2.4.4.1 Linear Regression Analysis

Equation 2.5 was used for creep modulus prediction using experimental data to complete linear regression.

$$E_c = a \times \text{Log}(t) + b \qquad (2.5)$$

where:

E_c = creep modulus, MPa,

t = time after loading, hr,

a and b are regression constants.

The constants a and b were obtained by developing the normal-log plot of creep modulus (y-axis) against time (x-axis), and the creep modulus was then extrapolated to 50 years.

Hazen [26] and Riahi [27] have previously advised that using all test data for linear extrapolation can be misleading as the significant weighting of the early time data (before 1,000 hours) on the regression analysis shifts the predicted 50-year creep modulus upwards [26], [27]. This claim was investigated for the I-Main CIPP specimens as the regression of the 1,000-to-10,000-hour data was compared with the predicted 50-year creep modulus using all data.

2.4.4.2 Findley's Non-linear Extrapolation

The I-Main CIPP 50-year flexural creep modulus was also predicted using Findley's Power Law, which is a non-linear extrapolation approach that can estimate the creep modulus of a composite liner after 50 years of service. Findley's Power Law was first developed in 1944 to study the viscoelastic properties of polymers using a model that describes a simple relationship between creep strain and time [20], [35]. Findley's power law is a curve-fitting technique that has been extensively used to describe the viscoelastic behaviour of various fibre-reinforced polymer composites under constant stress [36].

Findley's power law is a simple relationship between creep strain and time using Equation 2.6 to determine a theoretical strain, ε.

$$\varepsilon = \varepsilon_o + mt^n \quad (2.6)$$

where:

ε_o = initial strain,

t = time after loading, hr.

Findley's creep parameters, n and m, were obtained by expressing Equation 2.6 in logarithmic form and performing a linear regression analysis on the normal-log plot of strain against the log of time given by Equation 2.7.

$$\text{Log}(\varepsilon - \varepsilon_o) = n \times \text{Log}(t) + \text{Log}(m) \quad (2.7)$$

The experimental strain obtained at one minute was assumed to be the instantaneous strain upon loading. Therefore, the strain values used on the ordinate are the difference between the total strain (i.e., experimental strain at time t and the initial strain). Once the Findley constants were obtained, the creep strain at 50 years (i.e., 438,000 hours) was then extrapolated, and the corresponding creep modulus was estimated based on the ratio of the initial applied stress (σ_o) to the creep strain (ε) at that given time (see Equation 2.4). A sample calculation illustrating the procedure used to obtain the Findley parameters can be found in Appendix A.

2.4.4.3 CIPP 50-year Flexural Creep Modulus

Table 2.4, Figure 2.15, Figure 2.16, and Figure 2.17 provide the extrapolated 50-year ASTM D2990 flexural creep modulus values using all test data and the data from 1,000 to 10,000 hours. The table also provides Findley's non-linear extrapolations for the 50-year creep modulus for flexural testing. Flexural creep modulus predictions based on a linear regression of all data ranged from 2,030 to 2,556 MPa with a mean of 2,290 MPa and a standard deviation of 217 MPa. When only 1,000 to 10,000 hours of data was used, the flexural creep modulus ranged from 1,379 to 1,906 MPa with a mean of 1,604 MPa and a standard deviation of 225 MPa. Findley's flexural creep modulus predictions ranged from 1,182 to 1,642 MPa, with a mean of 1,427 MPa and a standard deviation of 190 MPa.

Thus, the theoretical creep modulus estimated using Findley's law showed good agreement (i.e., approximately 12% difference) with linear extrapolation of experimental data using 1,000 to 10,000

hours of data. However, the linear regression prediction using all data sets was noted to be significantly different (i.e., approximately 60% difference) from the theoretical modulus estimated using Findley's law.

Table 2.4: CIPP 50-year flexural creep test results.

Specimen ID	**All Data**		**1,000 to 10,000-hour data**		**Findley's Law**
	Creep Modulus (MPa)	**R^2 Value**	**Creep Modulus (MPa)**	**R^2 Value**	**Creep Modulus (MPa)**
LF1	2,030	0.92	1,379	0.97	1,182
LF2	2,322	0.89	1,506	0.92	1,472
LF3	2,556	0.92	1,906	0.96	1,642
LF4	2,254	0.92	1,626	0.98	1,412
Maximum	2,556	0.92	1,906	0.98	1,642
Minimum	2,030	0.89	1,379	0.92	1,182
Mean	2,290	0.91	1,604	0.96	1,427
Standard Deviation	217	-	225	-	190

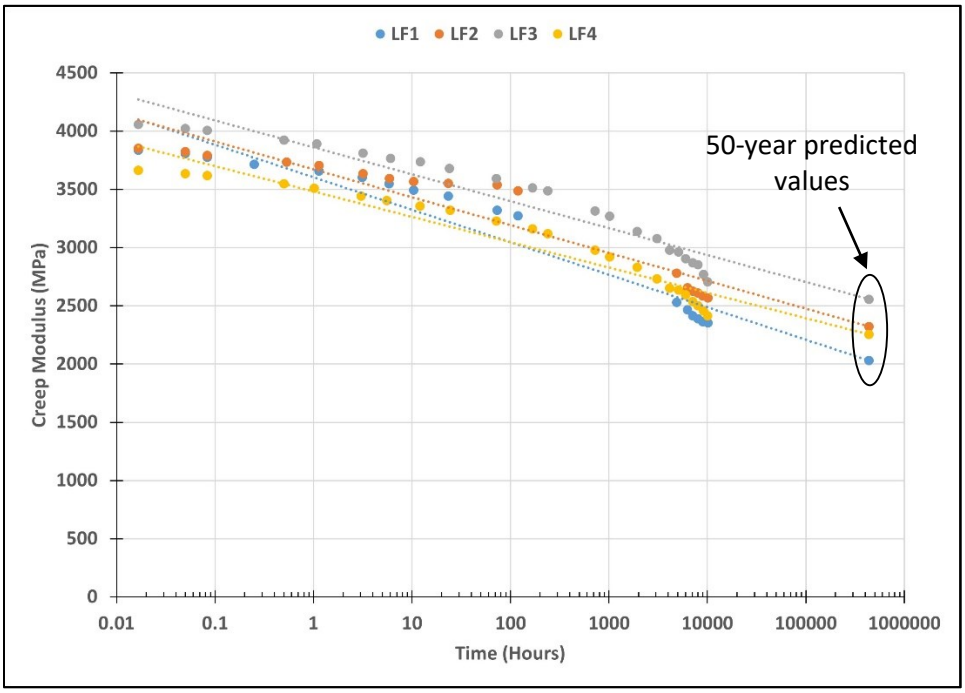

Figure 2.15: Extrapolated flexural creep modulus using all specimens cut from the CIPP flat plate.

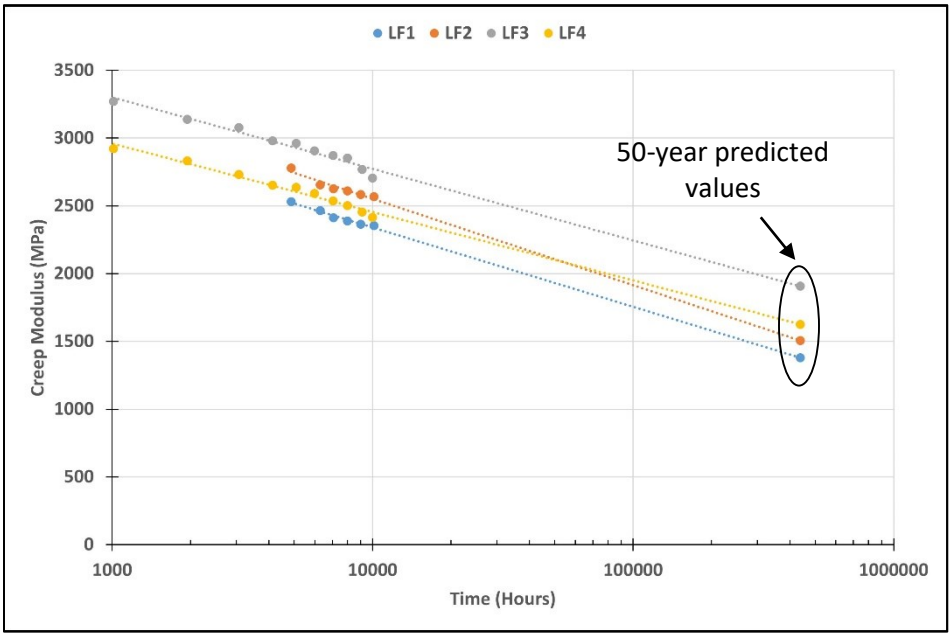

Figure 2.16: Extrapolated flexural creep modulus using values at only 1,000-to-10,000-hour test data.

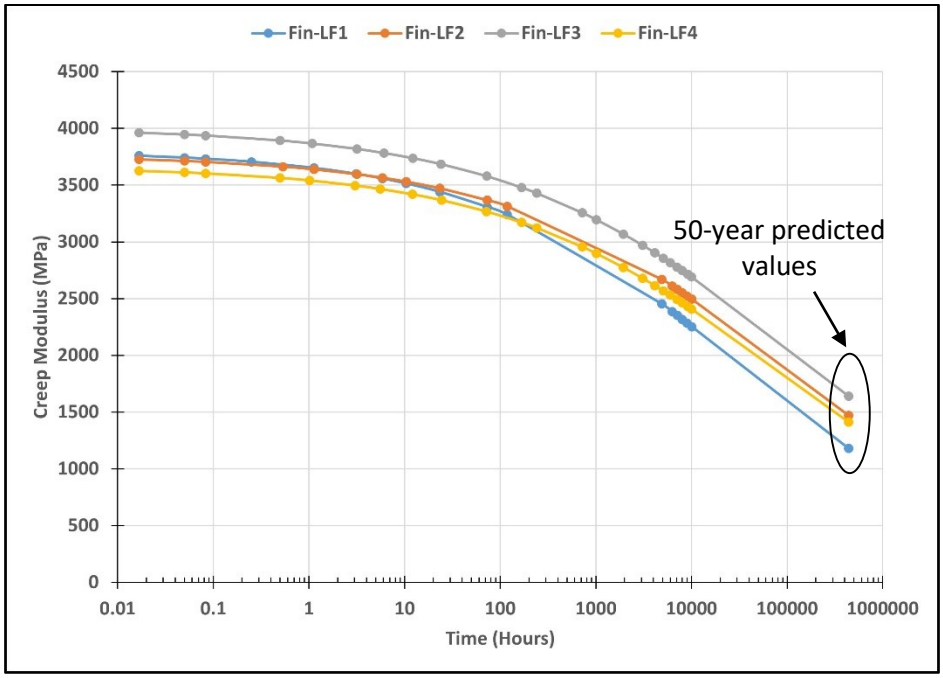

Figure 2.17: Extrapolated flexural creep modulus using Findley's law.

2.4.5 10,000-hour CIPP Tensile Creep

Three ASTM D638 Type II test specimens were loaded in the GTI tensile apparatus. A stress that is approximately 25% of the ASTM D638 yield strength (i.e., 25% × 96.2 MPa = 24.1 MPa) was used on the GTI test rig. Before the test was started, the load cells were calibrated, and a record of the specimen elongation was taken at one-second intervals using a data acquisition system. The GTI creep data was then down-sampled to agree with ASTM D2990 [14], which specifies that the elongation measurements for each test specimen to be taken at approximately 1, 6, 12, and 30 minutes and 1, 2, 5, 10, 30, 60, 100, 300, and 500 hours and at 1,000-hour intervals up to 10,000 hours.

Using Equation 2.1 (previously discussed in Section 2.4.3), the creep modulus, E_c, at a given time in each specimen was estimated as the ratio of the initial applied stress (σ_o) to the creep strain (ε) at that given time. Table 2.5, Figure 2.18 and Figure 2.19 provide the tensile creep test data over 10,000 hours. All test specimens appeared not to show a smooth strain profile to determine the transition

from primary creep to the secondary creep stage (see Figure 2.1). However, the strain profiles for each specimen (shown in Figure 2.18) suggest that the secondary creep (i.e., steady state) stage began between 200 and 500 hours, as all specimens displayed a change in the creep strain rate. The mean 10,000-hour strain (0.32%) in each tensile specimen was about 30% larger than the initial tensile strain (0.22%) upon load application. No tertiary creep was noted in the tested specimens. The mean tensile creep modulus at 10,000 hr was 7,617 MPa, 7,347 MPa and 7,636 MPa in the LT1, LT2 and LT3 specimens, respectively. A similar trend was observed at the onset of loading in all specimens. Compared with the ASTM D638 short-term tensile modulus, the mean initial creep modulus (at 0.02 hours) for all specimens was found to be 10,996 MPa. This percentage difference is about 6%, which is significantly close and due to the use of a data logging system as opposed to manual dial gauge reading in Section 2.4.4 flexural creep discussions.

While the general trend in Figure 2.19 suggests that the liner displayed linear viscoelastic behaviour under the stress levels investigated (25% of the yield strength), unusually high mean initial creep modulus may be due to the specimen variability noted in the short-term results. Despite this behaviour, all specimens' mean initial creep moduli were observed to be significantly close to the one-minute short-term tensile modulus.

Table 2.5: CIPP 10,000-hour tensile creep test data.

Time (hours)	LT1		LT2		LT3	
	Strain (%)	Creep Modulus (MPa)	Strain (%)	Creep Modulus (MPa)	Strain (%)	Creep Modulus (MPa)
0.02	0.21	11,227	0.22	10,853	0.22	10,907
0.1	0.22	10,728	0.23	10,650	0.23	10,626
0.2	0.22	10,728	0.23	10,455	0.23	10,405
0.5	0.22	10,728	0.23	10,455	0.23	10,405
1	0.22	10,728	0.24	10,267	0.23	10,405
2	0.22	10,728	0.24	10,267	0.24	10,194
5	0.22	10,728	0.24	10,084	0.24	10,194
10	0.23	10,526	0.24	10,084	0.24	10,194
20	0.23	10,526	0.24	9,908	0.24	9,990
50	0.24	10,144	0.25	9,573	0.24	9,990
100	0.24	9,963	0.26	9,413	0.25	9,794
200	0.25	9,788	0.26	9,258	0.25	9,605
500	0.25	9,566	0.26	9,156	0.26	9,356
700	0.26	9,417	0.27	8,866	0.27	9,016
1000	0.26	9,247	0.28	8,746	0.27	8,938

Time (hours)	LT1		LT2		LT3	
	Strain (%)	Creep Modulus (MPa)	Strain (%)	Creep Modulus (MPa)	Strain (%)	Creep Modulus (MPa)
2000	0.27	8,959	0.28	8,480	0.28	8,618
3000	0.27	8,793	0.29	8,208	0.28	8,480
4000	0.28	8,617	0.30	8,124	0.29	8,391
5000	0.29	8,334	0.30	8,007	0.29	8,310
6000	0.29	8,228	0.30	7,967	0.30	8,172
7000	0.29	8,200	0.31	7,743	0.30	8,038
8000	0.30	8,090	0.32	7,636	0.31	7,782
9000	0.31	7,789	0.32	7,531	0.32	7,660
10000	0.32	7,617	0.33	7,347	0.32	7,636

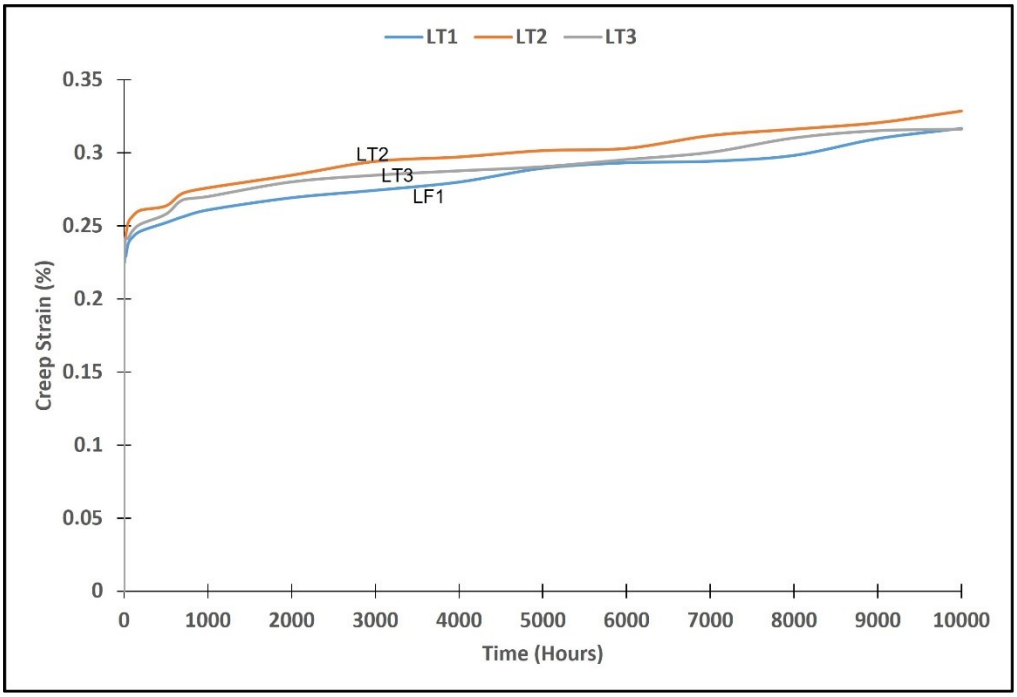

Figure 2.18: CIPP tensile creep strain up to 10,000 hours.

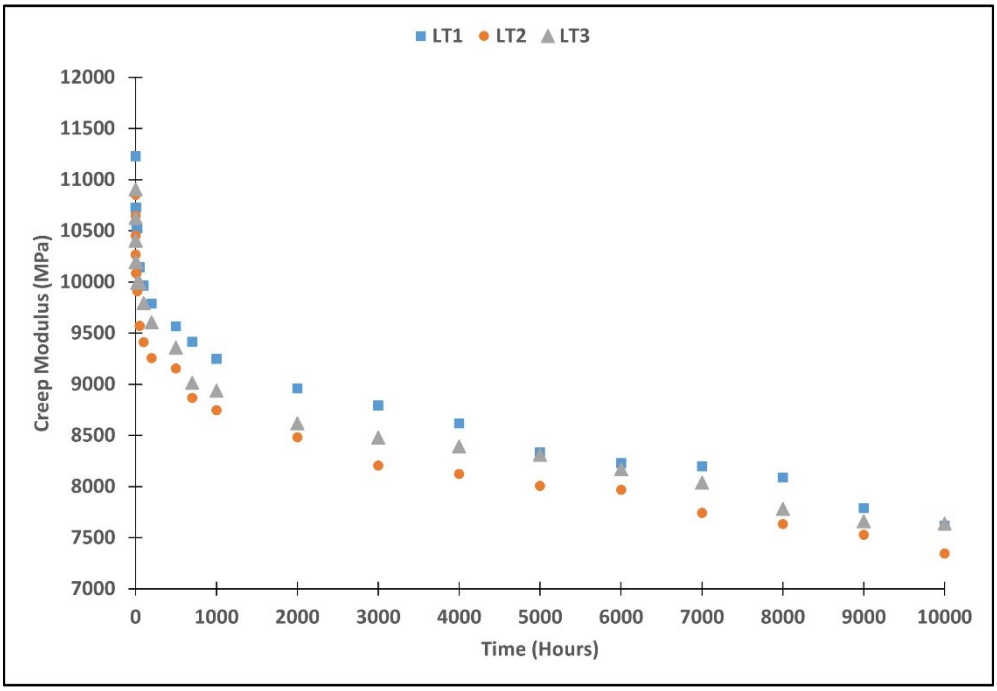

Figure 2.19: CIPP tensile creep modulus up to 10,000 hours.

2.4.5.1 CIPP 50-year Tensile Creep Modulus

Similar to flexural creep testing, linear and non-linear models were used to fit the 10,000-hour experimental test data to estimate the CIPP 50-year creep modulus. Table 2.6, Figure 2.20, Figure 2.21 and Figure 2.22 provides the extrapolated 50-year ASTM D2990 tensile creep modulus values using all test data and the data from 1,000 to 10,000 hours. Table 2.6 also provides Findley's non-linear extrapolations for the 50-year creep modulus for tensile testing. Tensile creep modulus predictions based on a linear regression of all data ranged from 7,022 to 7,530 MPa with a mean of 7,306 MPa and a standard deviation of 259 MPa. When only 1,000 to 10,000 hours of data were used, the tensile creep modulus ranged from 5,535 to 5,766 MPa with a mean of 5,614 MPa and a standard deviation of 132 MPa. Findley's tensile creep modulus predictions ranged from 5,203 to 6,027 MPa, with a mean of 5,714 MPa and a standard deviation of 446 MPa.

Thus, the theoretical creep modulus estimated using Findley's law showed very strong agreement (i.e., approximately 2% difference) with linear extrapolation of experimental data from 1,000 to 10,000 hours. However, the linear regression prediction using all data sets was noted to be significantly different (i.e., approximately 25% difference) from the theoretical modulus estimated using Findley's law.

Table 2.6: CIPP 50-year tensile creep test results.

Specimen ID	All Data		1,000 to 10,000-hour data		Findley's Law
	Creep Modulus (MPa)	R^2 Value	Creep Modulus (MPa)	R^2 Value	Creep Modulus (MPa)
LT1	7,366	0.90	5,766	0.91	5,912
LT2	7,022	0.94	5,535	0.97	5,203
LT3	7,530	0.88	5,539	0.95	6,027
Maximum	7,530	0.94	5,766	0.97	6,027
Minimum	7,022	0.88	5,535	0.91	5,203
Mean	7,306	0.90	5,614	0.94	5,714
Standard Deviation	259	-	132	-	446

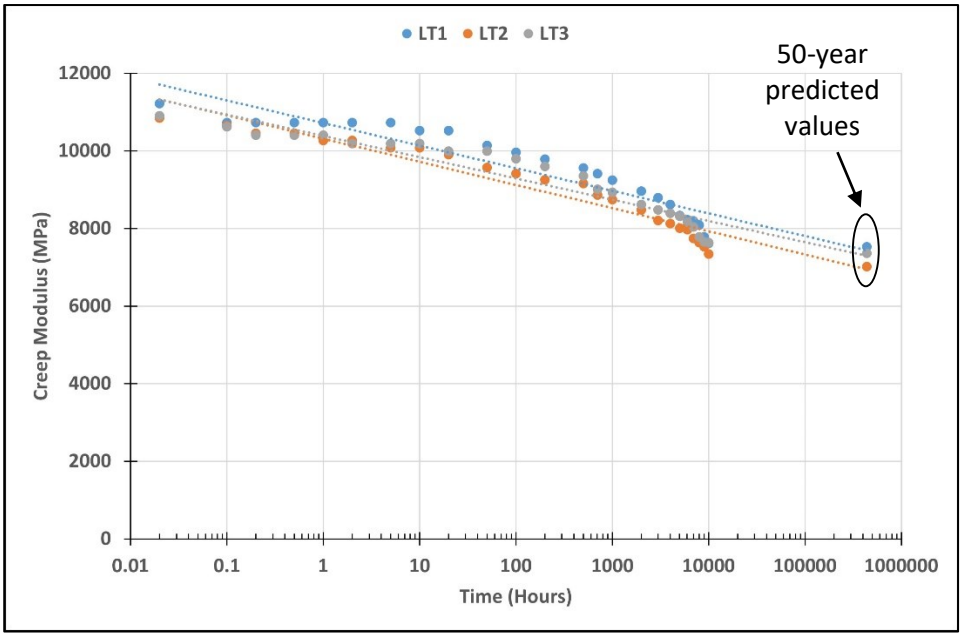

Figure 2.20: Extrapolated tensile creep modulus using all specimens cut from the CIPP flat plate.

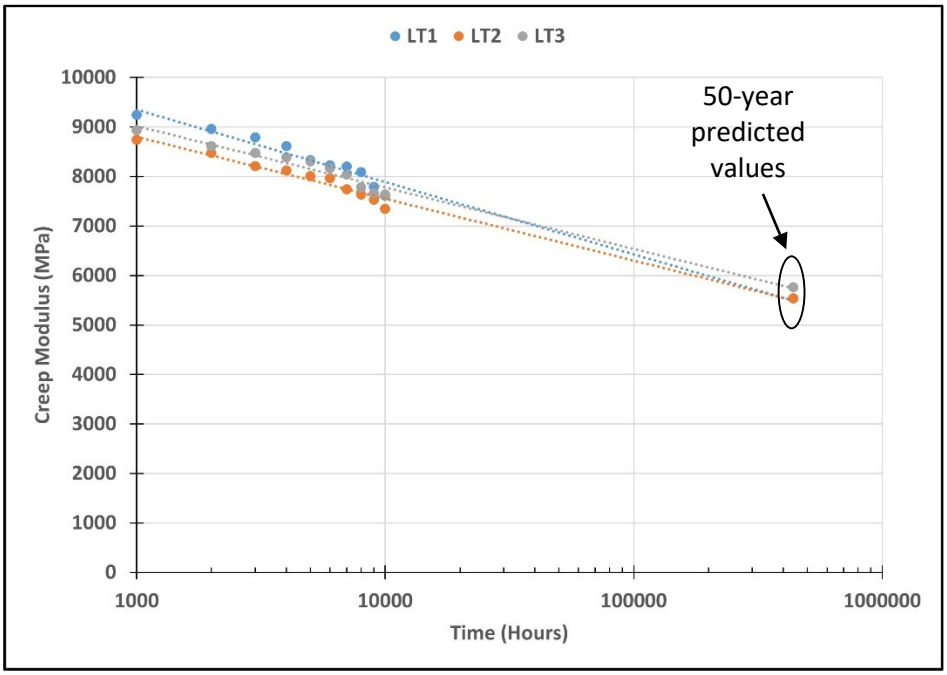

Figure 2.21: Extrapolated tensile creep modulus using values at only 1,000-to-10,000-hour test data.

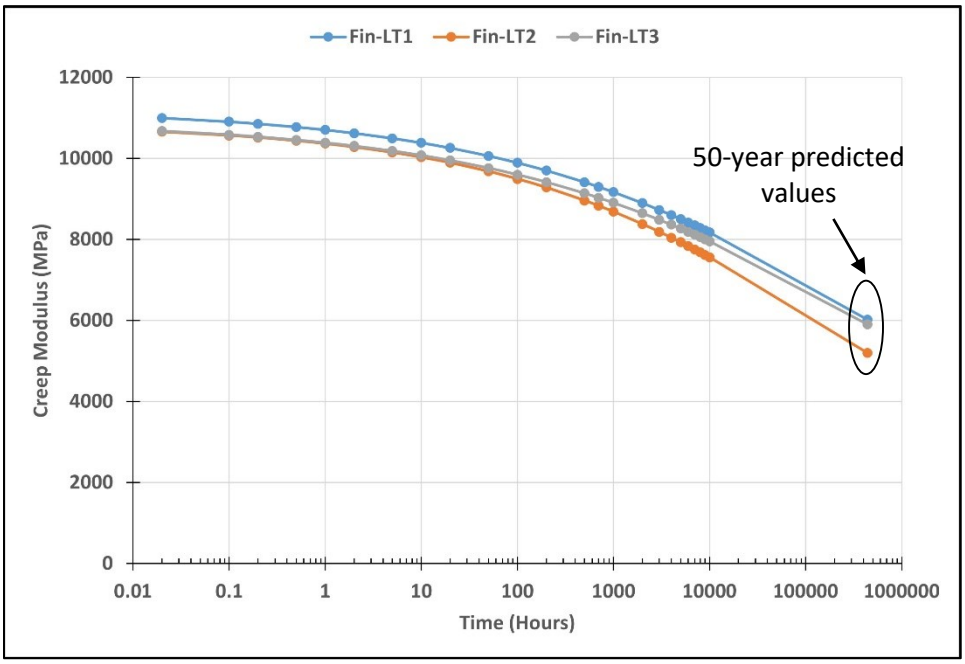

Figure 2.22: Extrapolated tensile creep modulus using Findley's law.

2.4.6 Long-Term Flexural and Tensile CRF

The 50-year CRF for each CIPP specimen was estimated using the ratio of the creep modulus to the short-term modulus using Equation 2.8, and the results were compared to the 50% CRF commonly used in industry.

$$\text{CRF} = \frac{E_L}{E} \tag{2.8}$$

where:

E_L = 50-year creep modulus, and

E = Short-term flexural or tensile modulus.

Table 2.7 provides the mean short-term and 50-year creep modulus and the CRF for both specimens tested in flexure and tension. Table 2.7 shows the I-Main CIPP liner had a flexural CRF of 59% when all data was regressed, which is significantly different from CRF predictions using 1,000 to 10,000-hour data (42%) and Findley's non-linear extrapolation (37%). A strong agreement was observed between the linear regression method using 1,000 to 10,000-hour data and Findley's non-linear extrapolation. For tensile creep testing, a tensile CRF of 66% was predicted using all data. This value was significantly higher than the 51% and 53% CRF based on 1,000 to 10,000-hour data and Findley's non-linear extrapolation, respectively.

Table 2.7: Mean short-term and long-term tensile and flexural modulus and CRF.

Creep Test	**Short-term values**	**Creep Modulus at 10,000 hours**			**CIPP 50-year CRF**		
	Initial Tangent Modulus (MPa)	Using All data (MPa)	Using 1,000-to-10,000-hour data (MPa)	Using Findley's Law (MPa)	All data (%)	1,000-to-10,000-hour (%)	Findley's Law (%)
Flexural	4,356	2,290	1,604	1,427	59	42	37
Tensile	10,296	7,306	5,614	5,714	66	51	53

The use of the typical 50% CRF to estimate the 50-year service life for a reinforced liner could produce misleading results as composite CIPP flexural CRF can fall within the range of 37 to 42%, which is lower

by approximately 10%. In comparison with flexural creep findings by Straughan et al. [20] and Knight [28] on various reinforced CIPP specimens, the I-Main CIPP fell within the CRF range of 20 to 50%. However, this study determined the flexural CRF to be at 42% using the last equally spaced 1,000-hour data; therefore, a CRF range of 20 to 40% can be used when determining long-term 50-year flexural mechanical properties for reinforced pressure CIPP. Tensile CRF values ranged from 51 to 53% and were in agreement with the generalized 50% CRF. While this is true, it is not clear if all CIPP will have a 50% since CIPP typically offers various kinds of products using different liner configurations to form composite liners. Tensile creep research by Shannon [29] found a reinforced watermain CIPP CRF range of 11 to 27%. This range is significantly different from the tensile results presented herein. While testing of the I-Main CIPP determined that reinforced CIPP can have a CRF that is approximately 50%, Shannon [29] stated that some CIPP liners could have CRF as low as 11%. This wide range may be due to the different resin and fibre reinforcements evaluated. Therefore, from a pressure pipe design standpoint, all CIPP products must be tested to determine their CRF.

In this study, the CRF values were determined using flat plate specimens, which are not representative of field conditions and have curved surfaces. From a pressure pipe design standpoint, the determined long-term mechanical properties can be reduced to account for liner imperfections and specimen shape differences. Thus, 35% and 50% creep retention factors would be appropriate for the I-Main CIPP liner. Despite the reductions to account for field conditions, curvature effects and possible liner imperfections, the determined CRF values do not agree with the typical 50% value that is currently used for design.

Watermain CIPP can show different long-term material responses when loaded as a beam in flexure compared to when pulled apart in tension. The I-Main CIPP flexural CRF value (35%) was found to be significantly lower than the tensile CRF value (50%). This anisotropic nature of the composite CIPP liner is a critical consideration for the design of pressure CIPP liners. Therefore, the anisotropic nature of CIPP pressure liners is critical to the long-term creep mechanical response as their behaviour when loaded in flexure is significantly different from when loaded in tension. Liner designers are advised to design based on each liner's mechanical properties and projected behaviour.

2.5 Conclusions

This research presents a unique set of data providing critical short-term and long-term design parameters that can be used by engineers, researchers, and numerical modelling experts to predict or validate pressure CIPP long-term mechanical properties. Multiple coupon specimens fabricated in the hoop direction of a reinforced composite CIPP liner were tested for approximately 10,000 hours using a stress level corresponding to 25% of the yield strength of the liner, and the long-term 50-year flexural and tensile modulus was determined. The following conclusions can be drawn:

1. In all specimens tested to determine long-term flexural and tensile mechanical properties, it was observed from the strain profiles that the secondary creep (i.e., steady state) stage began beyond the 500 to 1,000 hours of testing as all specimens displayed a change in the creep strain. Both flexural and tensile creep strains increased with time from the onset of loading. The mean 10,000-hour creep strain in the flexural and tensile creep test specimens was approximately 35% larger than the mean initial flexural strain and 30% larger than the mean initial tensile strain, respectively.

2. Compared with the short-term modulus values, the mean initial creep modulus (at one minute) was approximately 12% lower for flexural creep testing. In contrast, for tensile creep testing, the percentage difference was observed to be about 6%. All specimens were considered to exhibit a behaviour that suggests that the reinforced CIPP liner displays linear viscoelasticity within the investigated range of stress that is 25% of the yield strength (i.e., approximately 48 MPa and 33 MPa, respectively).

3. A comparison of regression approaches used for extrapolating experimental creep data for flexural and tensile properties using the composite CIPP specimens was completed. The theoretical modulus estimated using Findley's model showed better agreement (approximately a 12% difference for flexural creep testing and only a 2% difference for tensile creep testing) with the linear regression method using 1,000 to 10,000-hour data. In comparison with a linear regression that considered all test data, Findley's model showed a 60% difference for flexural creep testing and a 25% difference for tensile creep testing. While

regression analysis helps a designer forecast long-term CIPP properties, it is critical to ensure the 50-year flexural, and tensile creep moduli are not overestimated.

4. The extrapolated flexural creep modulus using 1,000 to 10,000-hour linear regression and Findley's law showed that a creep modulus that is 35% of the liner ASTM D790 short-term flexural modulus can be obtained in a reinforced liner subjected to 25% of its yield strength for 50 years. Similarly, a tensile creep modulus that is approximately 50% of the ASTM D638 short-term tensile modulus of the reinforced liner can be obtained when subjected to 25% of its tensile yield strength for 50 years. Thus, these findings provide the CIPP industry and researchers with data to show that the anisotropic nature of CIPP pressure liners is critical when investigating long-term creep mechanical properties. Using the generally accepted 50% CRF to estimate the 50-year CIPP creep modulus for reinforced pressure CIPP liners are direction dependent and do not apply to flexural and tensile testing.

Chapter 3

Non-Reinforced and Reinforced CIPP Liner Long-Term Mechanical Properties: Flexural Creep-Rupture Strength

3.1 Overview

For years, the long-term flexural strength of CIPP liners has been estimated by applying a generalized retention factor of 50% to the short-term flexural strength to complete the design of non-reinforced and reinforced polymeric CIPP products. There is currently an industry controversy over the validity of applying the typical 50% retention factor (based on flexural creep testing) to determine CIPP long-term flexural strength, as there are limited studies to support the adopted retention factor. This study provides CIPP Long-term (50-year) Flexural Strength ($LTFS_{50}$) and Strength Retention Factor (SRF) values for four commercially available CIPP products. 3,000-hour plus flexural creep-rupture tests were completed on non-reinforced and reinforced CIPP specimens at room temperature using a custom-built loading frame with lead-loaded steel boxes. Results show that the long-term (50-year) flexural SRF for the non-reinforced test specimens (55-65%) and SRF for the reinforced test specimens (80-85%) do not agree with the generalized SRF (50%) typically used for design. Therefore, using the appropriate long-term mechanical strength properties of CIPP is critical in design to avoid being over-conservative.

3.2 Introduction

Thermoset Cured-in-Place Pipe (CIPP) liners have been used to renovate buried pipelines since the 1970s and can be classified as either a non-reinforced or reinforced polymeric material. Non-reinforced CIPP consists of a needle-felt tube that is resin impregnated. The tube has sufficient strength to resist material tearing or stretching during installation. Reinforced CIPP consists of woven fabrics with glass or carbon fibres that are designed to produce a composite material (resin and reinforcement) [27], [37]. Reinforced CIPP liners are polymer matrix composites that have received significant attention in recent decades due to their ability to provide high tensile capacity to the liner, thereby extending its application to large pipe diameters and pressure applications. CIPP resins are thermoset resins that form cross-linked polymers when the curing process is complete. Therefore,

under constant and continuous stress, the cross-linked polymers exhibit a non-linear viscoelastic material response and creep due to polymer chain slippage [2], [4]. To assess the long-term performance of polymeric products such as CIPP and thermoplastic pipes, viscoelastic creep and creep-rupture behaviours must be fully understood.

3.2.1 Flexural Creep and Creep-Rupture

Creep is a continuing deformation that occurs with time when a plastic or similar material is subjected to constant stress. Polymers typically demonstrate three different creep regions, which include primary, secondary and tertiary creep (see Figure 3.1). Primary creep occurs immediately after the initial elastic and plastic strain. This region is followed by a secondary creep region, where the polymer structure remains serviceable as long-term stress exposure is below the material yield stress [15]-[16]. At the tertiary creep region, creep-rupture occurs in the polymer structure as the creep strain increases rapidly and fractures [14], [17]. The creep-rupture of a polymer is the result of combined events, such as viscoelastic deformation, primary and secondary bond rupture, shear yielding and crazing, chain slippage, void formation, and growth leading to fracture [15].

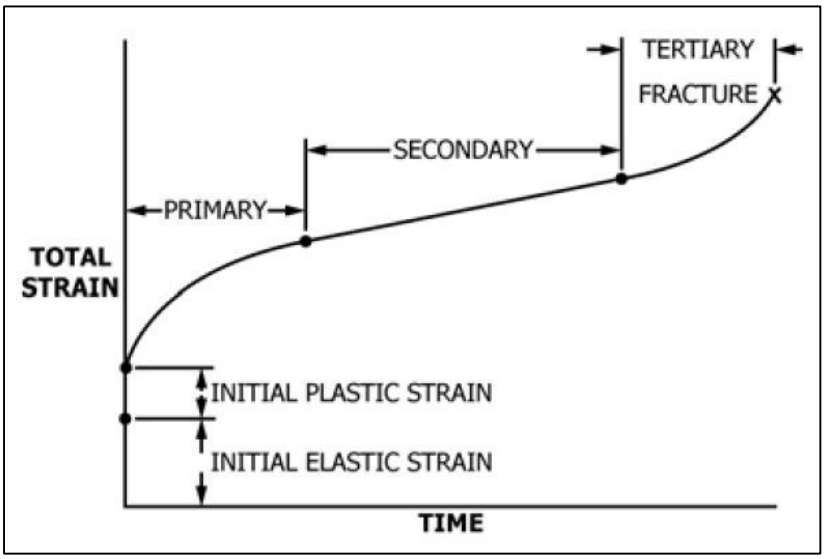

Figure 3.1: Idealized curve showing primary, secondary, and tertiary creep [14].

3.2.2 CIPP Mechanical Properties

In North America, the Non-Mandatory Appendix X1 in ASTM F1216 [1], *"Standard Practice for Rehabilitation of Existing Pipelines and Conduits by The Inversion and Curing of a Resin-Impregnated Tube,"* has been extensively used to design CIPP liners. This method involves completing multiple design checks to obtain an optimum liner thickness that ensures the liner supports external groundwater loads, withstands the internal pressure spanning across holes in the original pipe wall, and sustains other pressures, including those imposed by soil and traffic surcharge [1]. Depending on the existing pipe to be lined and the criteria listed above, the required thickness is calculated from a series of design equations. The largest thickness is then selected for the installation.

Based on the ASTM F1216 design method, Equation 3.1 (ASTM F1216 Equation X1.2) and Equation 3.2 (ASTM F1216 Equation X1.6) require a long-term (time-corrected) flexural strength for CIPP. Also, Equation 3.3 (ASTM F1216 Equation X1.7) require a long-term (time-corrected) tensile strength for CIPP.

$$1.5\frac{\Delta}{100}\left(1+\frac{\Delta}{100}\right)DR^2-0.5\left(1+\frac{\Delta}{100}\right)DR=\frac{\sigma_L}{PN} \qquad (3.1)$$

where:

DR = ratio of the pipe outside diameter to the pipe minimum wall thickness,

Δ = ovality of the host pipe,

σ_L = Long-term Flexural Strength,

P = external pressure on the liner, and

N = Safety Factor.

$$P=\frac{5.33}{(DR-1)^2}\times\left(\frac{D}{d}\right)^2\times\frac{\sigma_L}{N} \qquad (3.2)$$

where:

DR = ratio of the pipe outside diameter to the pipe minimum wall thickness,

D = mean inside diameter of the original pipe,

d = diameter of the hole in the original pipe,

σ_L = long-term (time-corrected) flexural strength for CIPP, and

N = factor of safety.

$$P = \frac{\sigma_{TL}}{(DR-1)\times N} \quad (3.3)$$

where:

P = internal pressure,

σ_{TL} = long-term (time-corrected) tensile strength for CIPP,

DR = ratio of the pipe outside diameter to the pipe minimum wall thickness, and

N = factor of safety.

Similar to design methods in Australia [41] and Europe [42], the F1216 design method requires the use of both short-term and long-term mechanical properties of the liner to determine the design thickness for installing a liner that will have a service life of up to 50 years. Such mechanical properties are key input properties for design and include the long-term 50-year flexural strength. Flexural strength refers to the ability of a CIPP material to withstand bending. It is determined using short-term tests based on ASTM D790 [31], *"Standard Test Methods for Flexural Properties of Unreinforced and Reinforced Plastics and Electrical Insulating Materials."* The long-term flexural strength of CIPP can be determined using creep-rupture flexural tests. Creep-rupture tests measure the time-to-rupture for a specimen subjected to constant stress and obtained from a coupon specimen under specified environmental conditions (i.e., constant temperature and humidity).

Another critical long-term mechanical property used in the design of CIPP is the long-term 50-year flexural modulus. Typically, a Creep Retention Factor (CRF) of 50% is applied to the short-term flexural modulus of CIPP material properties to determine the liner's long-term modulus using creep testing. The CRF applied on CIPP is the ratio of the 50-year predicted modulus to short-term modulus according to ASTM D2990 [14] and is derived based on standard creep testing conducted under controlled temperature and humidity. There is currently an industry controversy over the appropriateness of using the typical 50% CRF on material properties to determine the long-term flexural strength required by the ASTM F1216 design method [38]. While some think that adopting

this 50% CRF is flawed and may be misleading when used to estimate CIPP long-term flexural strength, others believe in being conservative and reducing the long-term strength by half without any engineering backing [27], [31], [39], [40]. Estimating the long-term strength of CIPP by applying CRF defined from creep modulus curves to the short-term experimental flexural strength data by Lee and Ferry [19], Matthews et al. [6], and Riahi [27] may be misleading. Zhao and Whittle [41] and Moser et al. [42] have shown that for most plastic pipe liners, the modulus does not degrade with time [41], [42]. Since using the CRF appears not to be an accurate estimate of strength retention, there arises the need to establish CIPP long-term strength using a different testing method or design approach.

3.2.3 CIPP 50-year Flexural Strength

ASTM D2990 [14], *"Standard Test Methods For Tensile, Compressive, And Flexural Creep And Creep-Rupture Of Plastics,"* ISO 11296-4 [43], *"Plastics piping systems for renovation of underground non-pressure drainage and sewerage networks — Part 4: Lining with cured-in-place pipes"*, and ISO 11298-4 [44], *"Plastics piping systems for renovation of underground water supply networks — Part 4: Lining with cured-in-place pipes"* details testing procedures to characterize the long-term strength and stiffness of coupon specimens fabricated from gravity and pressure CIPP liners under dry or wet conditions [44]. Despite the availability of the experimental procedures in these standards, there are currently limited studies completed to determine CIPP long-term 50-year flexural strength using creep-rupture tests. Gumbel and Chrystie-Lowe [38] discussed testing done in Europe to investigate the long-term strength of glass fibre reinforced plastic (GRP) and further presented work done in the UK to determine the long-term flexural strength values and Strength Retention Factor (SRF) for three different CIPP liners using the flexural creep-rupture test in a sulphuric acid environment. They tested one unreinforced and two reinforced CIPP specimens in three-point loading, and their results found the SRF values to be 68% and 60-76% for the non-reinforced and reinforced CIPP specimens, respectively. In Australia, Shannon [29] completed a tensile creep-rupture test to develop long-term creep-rupture curves after subjecting a watermain CIPP liner to various stresses. Their results showed that the short-term strength of the liner remained close to the initial tensile strength, and the resulting retention in tensile modulus did not correlate with the reduction in strength. The testing was conducted for up to 400 hours, and the liner was reported to have a tensile SRF was approximately

70% [29]. To the author's knowledge, literature on determining long-term 50-year flexural strength for CIPP liners is challenging to find in North America. There is currently no comprehensive study that compares the creep-rupture behaviour of non-reinforced CIPP to reinforced CIPP liners.

This study estimates the long-term 50-year flexural strength for various commercially available CIPP liners in North America using 3,000 hours plus experimental creep-rupture data. Three-point flexural creep-rupture tests were completed on non-reinforced and reinforced CIPP specimens at room temperature using a custom-built loading frame with lead-loaded steel boxes.

3.3 Materials and Test Apparatus

3.3.1 CIPP Specimen Preparation

CIPP liner plates for this study were manufactured and supplied by Insituform Technologies Limited. Two commercially available CIPP liners were provided for non-reinforced (homogeneous) and reinforced (composite) CIPP liners. The Non-reinforced CIPP (NC) liners mainly contain a matrix made up of epoxy, while the Reinforced CIPP (RC) liners incorporate two layers of fibreglass to form an epoxy-fibreglass composite CIPP product.

To reduce product variability and enhance test data consistency, the CIPP specimens were manufactured in a laboratory under controlled conditions and cured at 71^{o}C. The CIPP liners were made to produce flat rectangular plates that were 275 x 280 mm in dimension. The nominal specimen thickness of the resulting flat plates was approximately 5.6 mm for the non-reinforced CIPP specimens and about 12.8 mm for the reinforced CIPP specimens. Specimen labelling was done to indicate a non-reinforced CIPP (NC) or reinforced CIPP (RC) and also include the product names of the supplied commercially available CIPP products. Thus "NC-L721" and "NC-L758" represented the two non-reinforced CIPP specimens while "RC-IPLUS" and "RC-IMAIN" represented the two reinforced CIPP specimens.

CIPP specimens were waterjet cut, and each specimen size was based on ASTM D790 [31]. Flat plate rectangular specimens were each prepared for both non-reinforced and reinforced CIPP products using a span-to-depth ratio of 16:1. Although ASTM D790 suggests that a 32:1 or 40:1 span-to-depth ratio may be required for reinforced plastic to avoid the occurrence of shear failure within the test

specimens, the typical testing span-to-depth ratio of 16:1 was experimentally determined to suffice. Figure 3.2 shows the specimens prepared for testing.

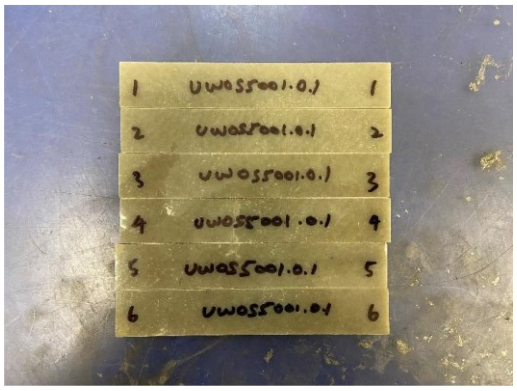

(a) NC-L721 test specimens.

(b) NC-L758 test specimens.

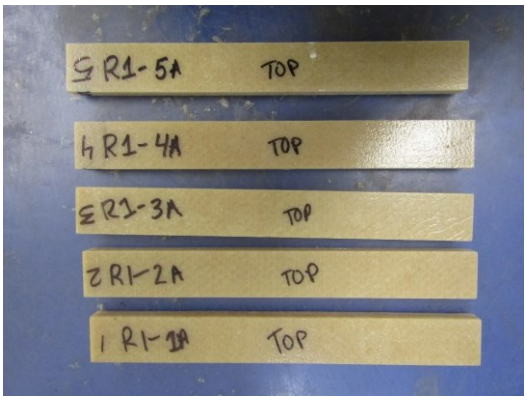

(c) RC-IPLUS test specimens.

(d) RC-IMAIN test specimens.

Figure 3.2: Flexural test flat plate coupons for both Non-reinforced CIPP (NC) and Reinforced CIPP (RC) test specimens.

3.3.2 Flexural Creep Rupture Test Procedure and Apparatus

To complete flexural creep-rupture testing at various stress levels on CIPP, flat rectangular specimens were simply supported and loaded as a beam to rupture. Linear potentiometers were acquired and mounted on each specimen to monitor abrupt changes in liner deflection and determine the time to rupture for various specimens. Before the test was started, each linear potentiometer was calibrated,

and a record of the specimen deflection over time was taken at one-second intervals using a SoMat eDAQ data acquisition system. Loading the CIPP specimens involved adding lead shots into fabricated steel-based cylinders or boxes to reach the required stress level. Figure 3.3 shows the hanging weights manufactured to induce test stresses based on the maximum flexural strength determined from short-term ASTM D790 tests, and Figure 3.4 shows the lead shots required to complement the steel-based weights containers. The cylindrical-shaped hanging weights fabricated to test the non-reinforced CIPP specimens were designed to provide a dead load of approximately 0.5 kN, while the box-shaped hanging weights manufactured to test the reinforced CIPP specimens were designed to provide a load of approximately 2.5 kN. All creep-rupture tests were conducted in a temperature-controlled room, where the room temperature was maintained at 20-23°C, and relative humidity was at 50-55%RH.

(a) Cylindrical-shaped hanging weight fabricated to test non-reinforced CIPP specimens.

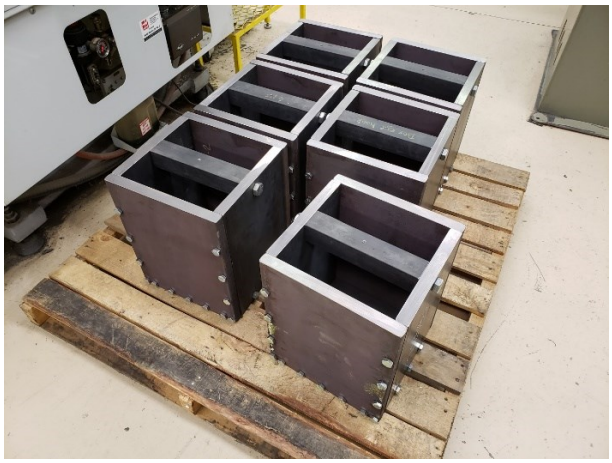

(b) Box-shaped hanging weight fabricated to test reinforced CIPP specimens.

Figure 3.3: Hanging weight containers designed and fabricated to test both non-reinforced and reinforced CIPP specimens in flexure.

Figure 3.4: Lead shots obtained to adjust container weight to create various equivalent stresses on multiple CIPP specimens.

Test racks were constructed using channel bars and I-beam sections to ensure that both NC and RC specimens were loaded flat at mid-span in a simply supported position. The test frames were designed per specifications in the Handbook of Steel Construction [32] to withstand concurrent test load (dead load).

Short-term flexural testing consisted of placing twenty-four rectangular specimens flat-wise on two supports and loading the specimens at mid-span in flexure as a beam until they ruptured or reached 5% strain in their outer fibres. Mechanical properties such as the flexural strength, flexural strain, initial tangent modulus of elasticity and yield strength were determined for all CIPP specimens. ASTM D790 [31] defines flexural strength as the maximum flexural stress sustained by the test specimen during a bending test. The flexural strain is defined as the nominal fractional change in the length of an element of the outer surface of the test specimen at midspan, where the maximum strain occurs. The initial tangent modulus of elasticity is defined as the ratio, within the elastic limit, of stress to corresponding strain calculated by drawing a tangent to the steepest initial straight-line portion of the load-deflection curve. Yield strength occurs at the first sudden deviation from the initial linear portion of the stress-strain plot [31].

Flexural creep-rupture tests were completed by rapidly and smoothly applying the load equivalent to the stress level of interest to the CIPP specimens. ASTM D2990 suggests conducting creep-rupture tests at a minimum of seven stress levels selected to produce rupture at approximately 1, 10, 30, 100, 300, 1,000, and 3,000 hours. Hence, the deformation measuring devices (Linear displacement potentiometer and SoMat eDaQ) were mounted and started before mounting the test specimens. The loads were prepared by gradually filling up the custom-fabricated steel cylindrical or rectangular weights containers with lead shots required to get the desired weight. Depending on the weight size, the loads were manually attached below the loading nose or using a material handler. Three replicates were made for each stress level, and test specimens were allowed to be rapidly strained within 1 to 5 seconds. Specimens were noted to have failed or ruptured if they cracked under the loading nose and fell off the test rack supports.

3.4 Results and Discussions

3.4.1 Short-Term Flexural Test

3.4.1.1 Non-reinforced CIPP Specimens

Twelve non-reinforced CIPP test specimens were loaded flat-wise at mid-span in flexure, as a simple beam, until they ruptured or reached the maximum 5% strain limit per ASTM D790 [31]. Figure 3.5 and Figure 3.6 provides the liner stress-strain plots. The plots show that both NC-L721 and NC-L758 test specimens had similar stress-strain responses, and the yield stress occurred at approximately 2.5% strain. After the specimens reached their yield, persistent fractures occurred within them, causing a continuous drop in the liner strength. However, the specimens were observed to show a good level of toughness (evidenced by “saw tooth waves” in the graphs), allowing them to have an increased ability to withstand the bending stress until rupture occurred.

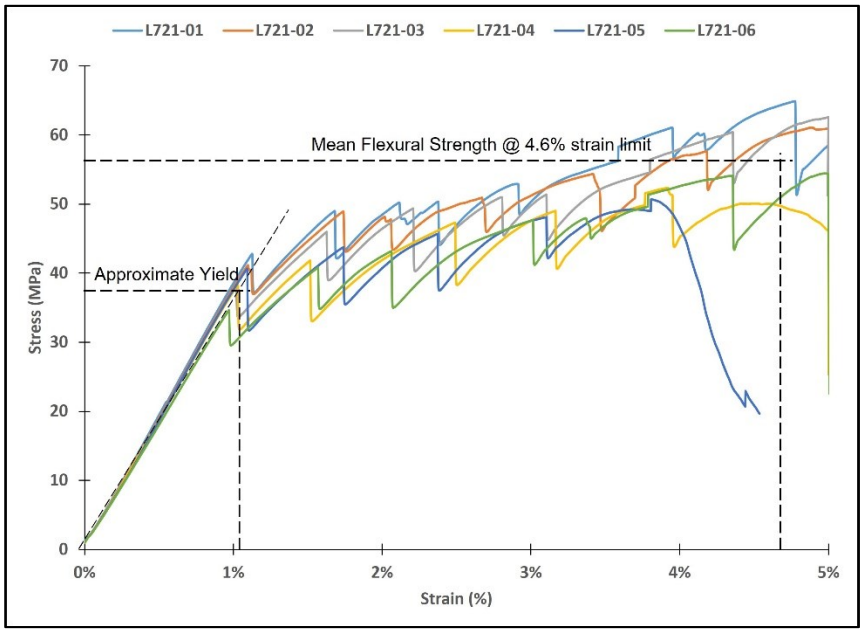

Figure 3.5: Stress-strain plot for six NC-L721 specimens (L721-01 to L721-06).

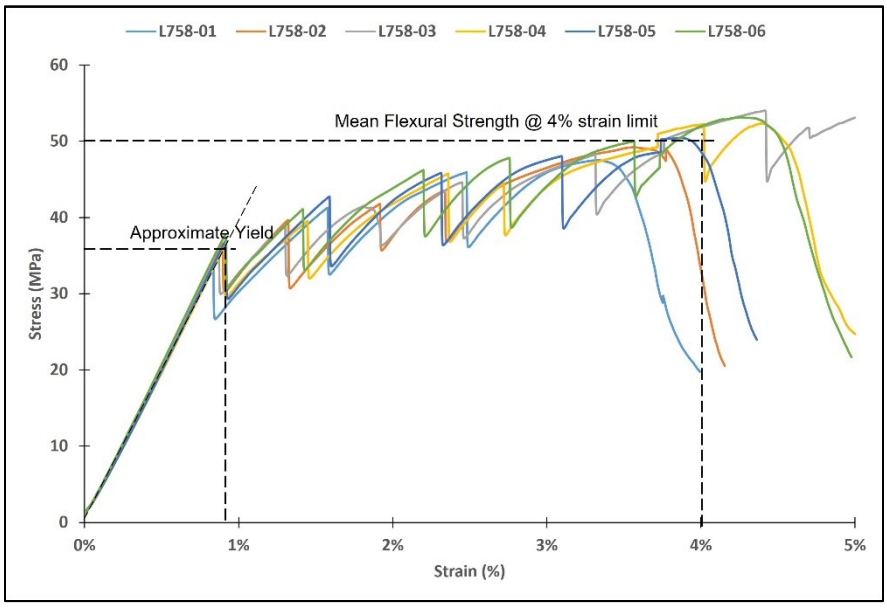

Figure 3.6: Stress-strain plot for six NC-L758 specimens (L758-01 to L758-06).

Table 3.1 provides the mean flexural test results for the non-reinforced tested CIPP specimens (see Appendix B for the complete dataset). The mean flexural strength values for NC-L721 and NC-L758

specimens were approximately 56 MPa (with a standard deviation of 0.13 MPa) and 50 MPa (with a standard deviation of 2.49 MPa), respectively. The mean flexural strain values for NC-L721 and NC-L758 specimens were 4.56% (with a standard deviation of 0.55%) and 3.97% (with a standard deviation of 0.46%), respectively.

Table 3.1: Non-reinforced CIPP short-term properties.

Flexural Properties	**Unit**	**NC-L721**		**NC-L758**	
			St. Dev		**St. Dev**
Width	mm	19.9	(0.01)	19.8	(0.02)
Thickness (depth)	mm	5.6	(0.13)	5.6	(0.03)
Span	mm	90	-	90	-
Span-to-depth ratio	-	16:1	-	16:1	-
Flexural Stress (Yield)	MPa	38.4	(3.20)	36.2	(2.81)
Flexural Strain (Yield)	%	1.0	(0.12)	0.9	(0.08)
Flexural Strength (Ultimate)	MPa	55.9	(0.13)	50.5	(2.49)
Flexural Strain (Ultimate)	%	4.56	(0.55)	3.97	(0.46)
Initial Tangent Modulus of Elasticity	MPa	3,747	(88)	4,016	(84)

3.4.1.2 Reinforced CIPP Specimens

While most NC test specimens were observed to reach failure before the 5% strain limit, no failure occurred in all RC test specimens except for specimen IMAIN-04. Figure 3.7 shows the back and side view of the RC specimens after the ASTM D790 three-point flexural tests, and Figure 3.8 and Figure 3.9 provides plots for the RC specimens. All specimens were considered free from any shear impact as deflection marks on the side and bottom were mainly straight.

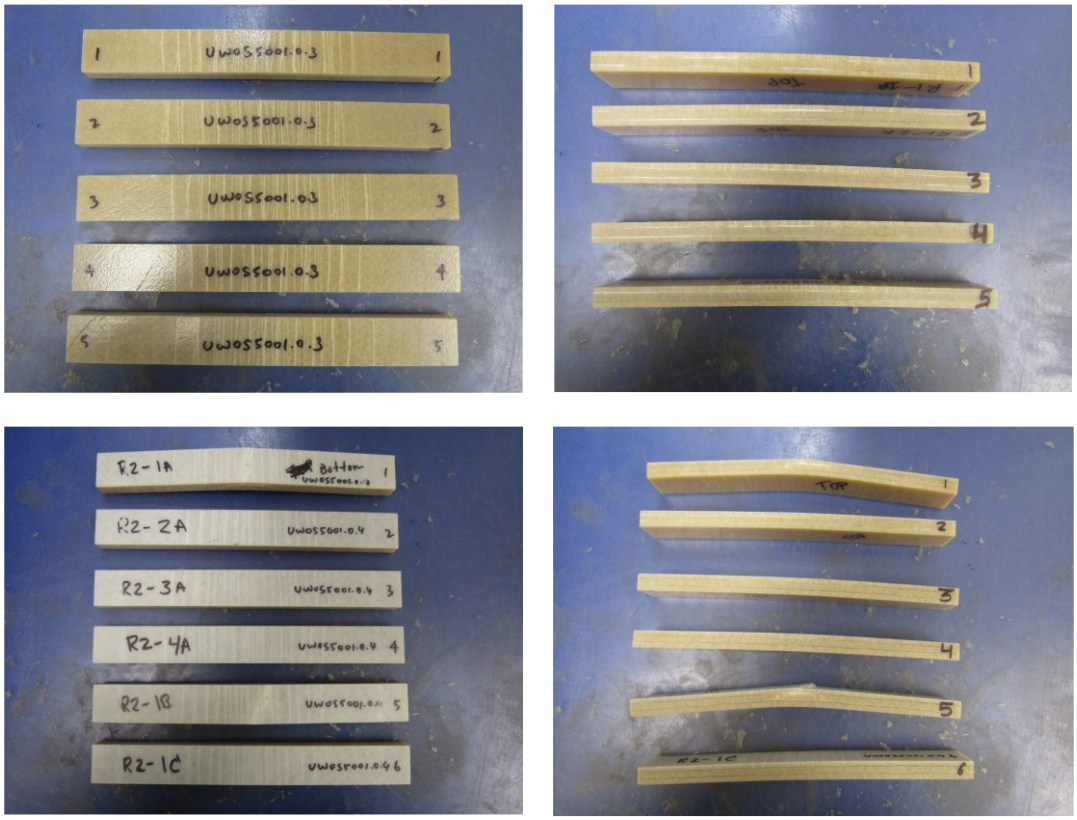

Figure 3.7: RC specimens after the ASTM D790 three-point flexural tests.

Twelve specimens were loaded flat-wise at mid-span in flexure, as a simple beam, until they ruptured or reached the maximum 5% strain limit per ASTM D790 [31]. Figure 3.8 and Figure 3.9 shows that both RC-IPLUS and RC-IMAIN test specimens exhibited similar stress-strain responses, and the yield point was not easily identified. Figure 3.9 shows that the liner flexural stress gradually increased up to approximately 160 MPa at a strain rate of 3.8%, where the reinforcing fibres were energized. This phenomenon resulted in a load increase during the testing and can be interpreted as the sudden shifts in the stress-strain behaviour of the CIPP specimens. No audible cracks were noted during testing, and the plots were observed to increase steadily until they reached the maximum ASTM D790 strain limit of 5%. Specimens were observed to reach their maximum flexural strength between 190 to 200 MPa with one case of rupture. Thus, a maximum stress level starting at 90% of the determined ASTM D790 flexural strength was considered to investigate the CIPP creep-rupture mechanical behaviour.

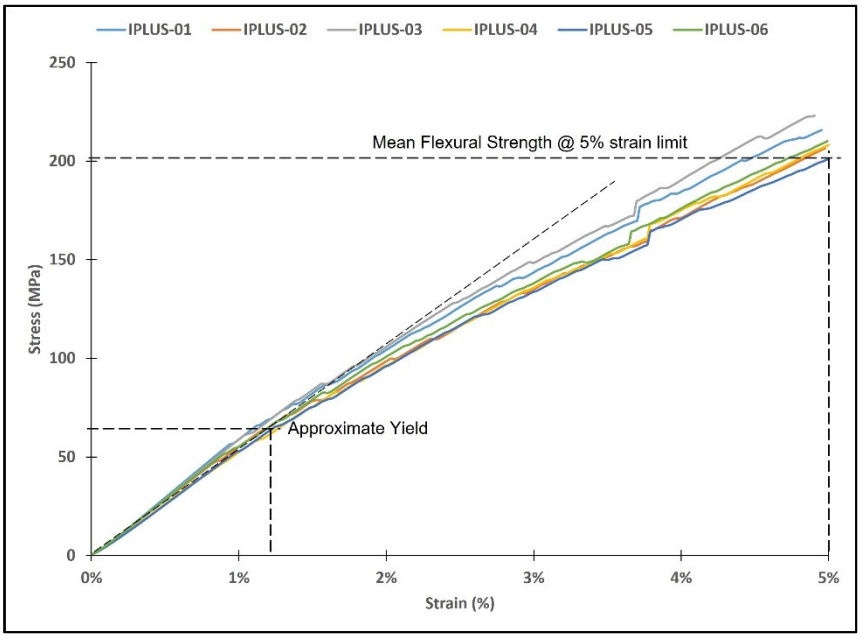

Figure 3.8: Stress-strain plot for six RC-IPLUS test specimens (IPLUS-01 to IPLUS-06).

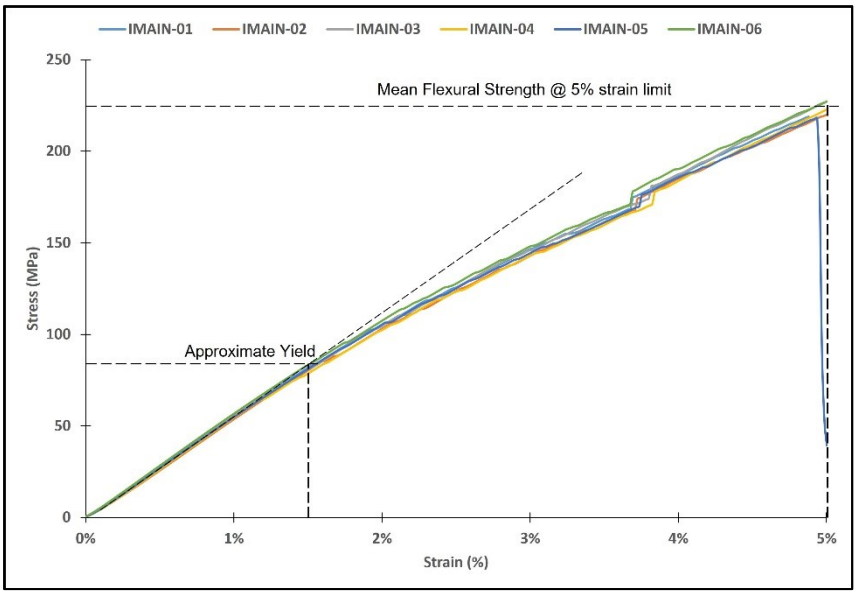

Figure 3.9: Stress-strain plot for six RC-IMAIN test specimens (IMAIN-01 to IMAIN-06).

Table 3.2 provides a summary of the flexural test results for the reinforced tested CIPP specimens (see Appendix B for the complete dataset). The mean flexural strength values for the RC-IPLUS and RC-IMAIN test specimens were approximately 201 MPa (with a standard deviation of 7.73 MPa) and 219

MPa (with a standard deviation of 3.88 MPa), respectively. The mean flexural strain values for NC-L721 and NC-L758 specimens were approximately 5%.

Table 3.2: Reinforced CIPP short-term properties.

Flexural Properties	Unit	RC-IPLUS		RC-IMAIN	
			St. Dev		St. Dev
Width	mm	30.1	(0.02)	30.0	(0.02)
Thickness (depth)	mm	12.7	(0.18)	12.8	(0.21)
Span	mm	205	-	205	-
Span-to-depth ratio	-	16:1	-	16:1	-
Flexural Stress (Yield)	MPa	69.8	(4.07)	83.5	(6.20)
Flexural Strain (Yield)	%	1.18	(0.35)	1.54	(0.15)
Flexural Strength (at 5% strain)	MPa	201	(7.73)	219	(3.88)
Initial Tangent Modulus of Elasticity	MPa	5,489	(273)	5,477	(115)

3.4.2 Test Stress Selection

Per the ASTM D2990 test procedure, a creep-rupture test is similar to a creep test. However, the creep-rupture test is continued until the specimen fails [14]. To determine the long-term 50-year flexural strength of the CIPP specimens, higher stresses were considered at the initial testing stage to induce a higher specimen creep rate to make the material fail in a shorter time. Based on observations from the short-term flexural test stress-strain plots (see Figure 3.5 to Figure 3.9), stress levels between the yield point and the ASTM D790 flexural strength were considered. A minimum of three repetitions of each stress level were completed. Thus, 90% of the ASTM D790 flexural strength was selected as the first stress level and subsequently reduced by 2.5 or 5%, depending on the CIPP response.

3.4.3 NC Long-Term Flexural Strength Testing

Based on the stress-strain response for each specimen, test stress levels were selected with a testing start point using 90% of the ASTM D790 flexural strength and subsequently reduced by 5% or 2.5% to extrapolate to 50 years. Figure 3.10 shows the test apparatus and the loaded non-reinforced CIPP specimens during testing.

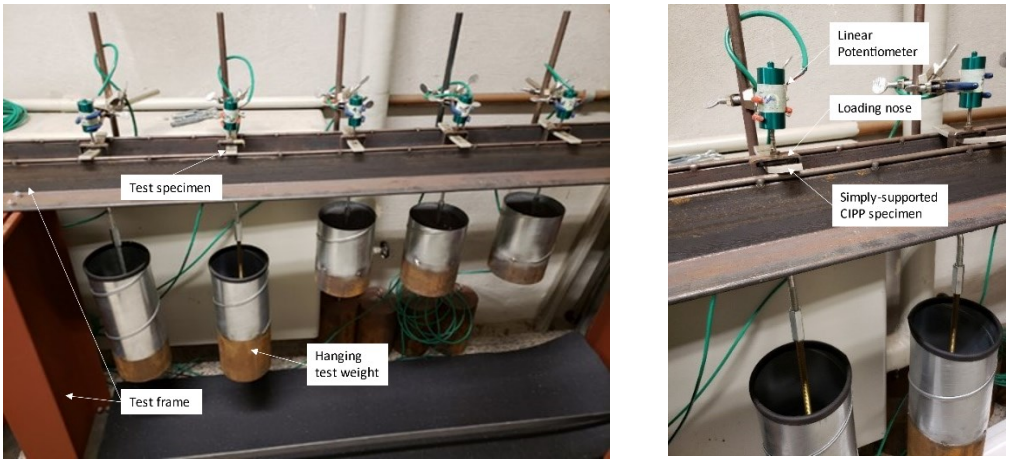

Figure 3.10: Test apparatus for a non-reinforced CIPP (NC) specimen tested with a load up to 0.5 kN.

The experiment was planned such that multiple failures occurred before 1 hour, between 1 and 100 hours, 100 and 1,000 hours, and then greater than 3,000 hours up to an approximate 10,000-hour period. Figure 3.11 shows the specimen rupture distribution observed for about 3,000 hours of testing. A total of fifteen and twenty-eight CIPP specimens were failed for the NC-L721 and NC-L758 test specimens, respectively. Within an hour of testing, fourteen creep-rupture failure points were noted for the NC-L721 test specimens and three for the NC-L758 test specimens. Between 1 and 100 hours of testing, six creep-rupture failure points were recorded for the NC-L721 test specimens and eight for the NC-L758 test specimens. Between 100 and 1,000 hours of testing, three creep-rupture failure points are noted for the NC-L721 test specimens and four for the NC-L758 test specimens.

Even though the NC-L721 and NC-L758 test specimens showed similar short-term flexural strengths (56 and 50 MPa), they showed significantly different rupture strengths. NC-L758 tested specimens were observed to have fewer rupture failures with time compared to the NC-L721 tested specimens.

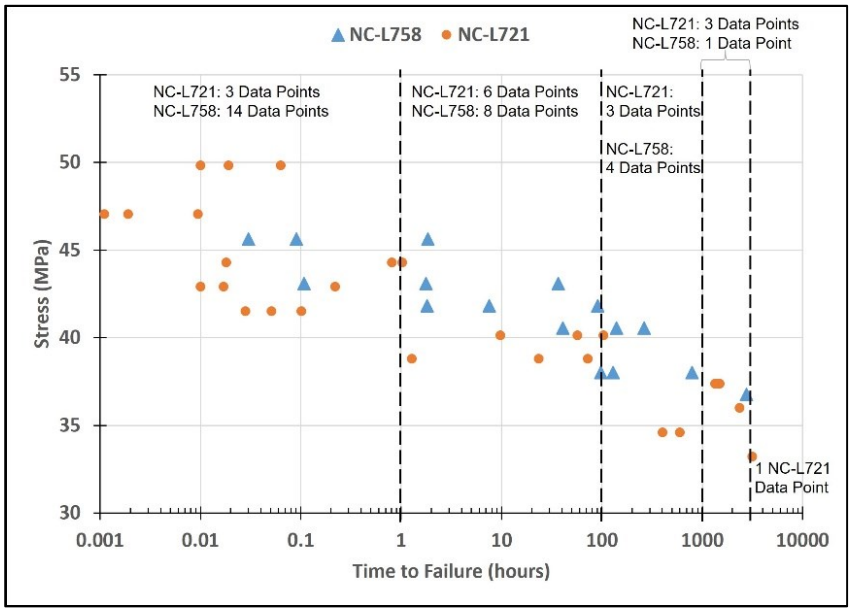

Figure 3.11: Rupture stress-time plots for NC-L721 and NC-L758 test specimens.

3.4.3.1 Linear Regression Analysis

Data analysis was completed using a logarithmic treatment on the test data. The least squares calculation was completed such that the rupture stress was on the independent variable (y-axis) and log time was the dependent variable (x-axis). Equation 3.4 was used to develop strength regression lines to predict the long-term 50-year flexural strength of the tested CIPP specimens.

$$\sigma = a \times \text{Log}(t) + b \qquad (3.4)$$

where:

σ = rupture stress, MPa,

t = time to rupture, hr,

a and b are regression constants.

Figure 3.12 and Figure 3.13 show strength regression plots illustrating the creep-rupture behaviour of two non-reinforced CIPP specimens subjected to the creep-rupture test at different stress levels. After developing the CIPP strength regression line, CIPP 50-year long-term flexural strength ($LTFS_{50}$) was

estimated to be 32 MPa and 34 MPa for the NC-L721 and NC-L758 test specimens, respectively. Since testing is still ongoing, this regression line will be validated with additional testing in the future.

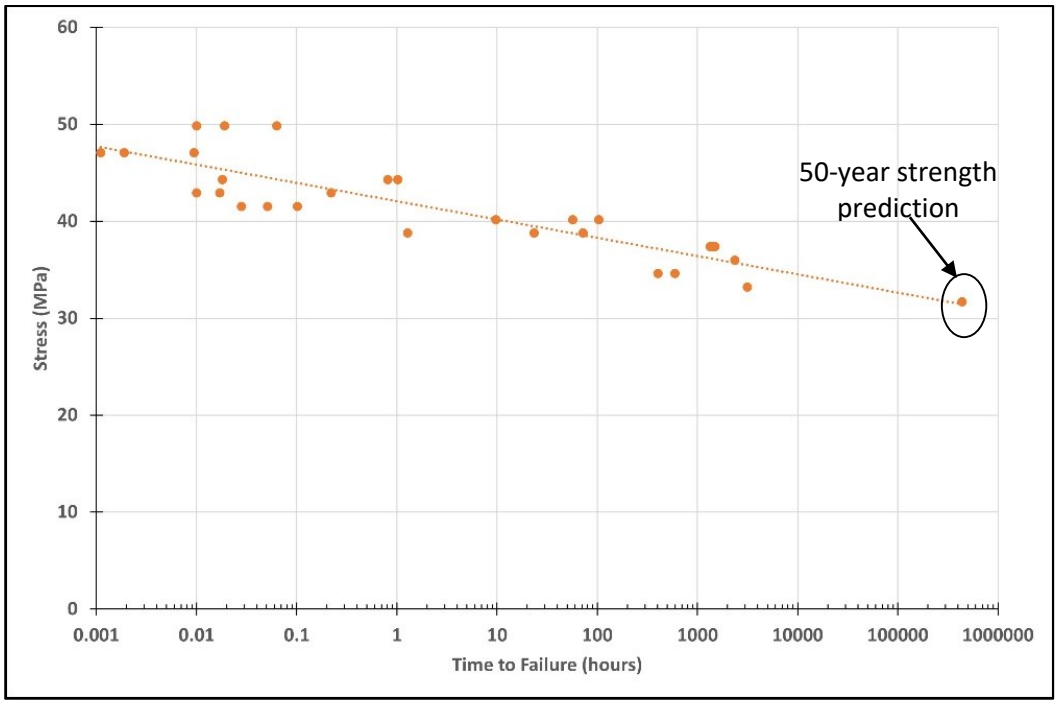

Figure 3.12: Regression line and extrapolation to determine long-term flexural strength for non-reinforced NC-L721 CIPP specimens.

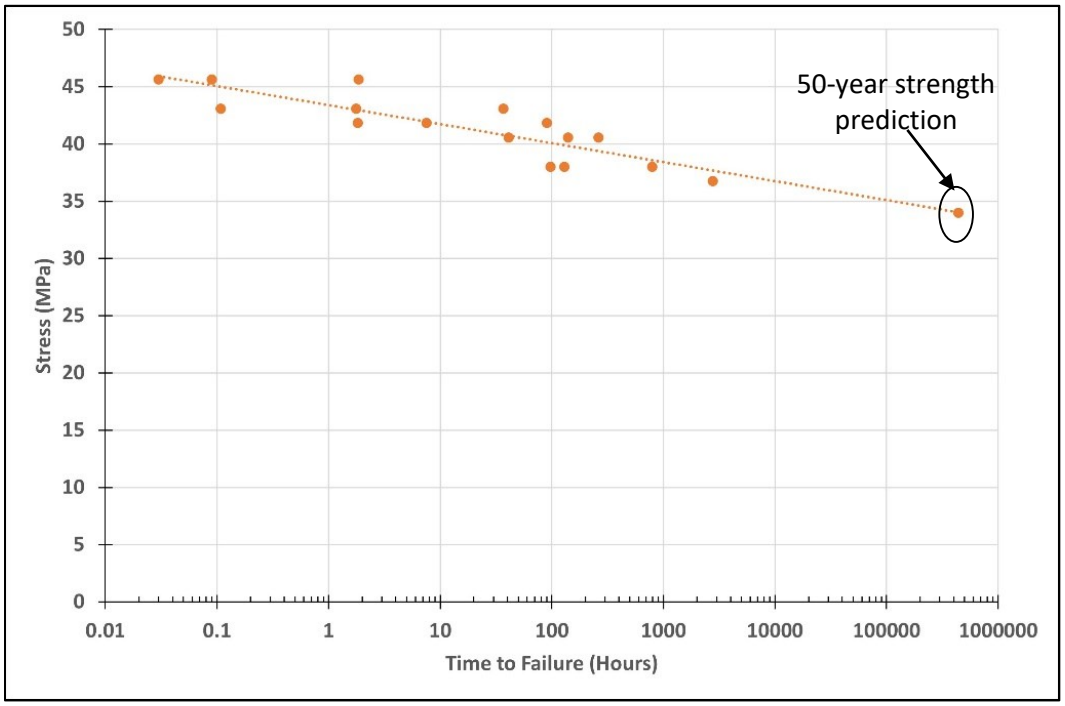

Figure 3.13: Regression line and extrapolation to determine long-term flexural strength for non-reinforced NC-L758 CIPP specimens.

3.4.3.2 Long-Term Flexural Strength Retention Factor (SRF)

The 50-year SRF for each CIPP specimen was estimated using the ratio of the long-term flexural strength to the short-term ASTM D790 strength using Equation 3.5, and the results were compared to the 50% value commonly used in the trenchless industry.

$$SRF = \frac{\sigma_L}{\sigma} \quad (3.5)$$

where:

σ_L = Long-term (50-year) flexural strength, and

σ = Short-term ASTM D790 flexural strength.

Table 3.3 provides the mean short-term flexural strength, 50-year flexural strength, and the SRF for both NC-L721 and NC-L758 test specimens. The table shows that, for the non-reinforced CIPP liners, the flexural SRF was approximately 59% and 68% for the NC-L721 and NC-L758 test specimens, respectively. Research completed by Gumbel and Chrystie-Lowe [38] on CIPP long-term flexural

properties found the SRF for a non-reinforced CIPP liner to be 68%. This SRF value agrees with the specimen NC-L758 results but is lower higher than the specimen NC-L721 results.

In this study, the strength retention factors were determined using flat plate specimens that are not representative of field conditions having curved surfaces. From a pressure pipe design standpoint, the determined long-term mechanical properties can be reduced to account for liner imperfections and shape differences. Thus, 55% and 65% strength retention factors would be appropriate for the NC-L721 and NC-L758 test specimens. Despite the reductions to account for field conditions, curvature effects and possible liner imperfections, the determined SRF values are higher than the typical 50% value that is currently used for design. Hence the need to conduct a CIPP creep-rupture test as test values can differ from the previously used 50% long-term value based on creep testing.

Table 3.3: Short-term, long-term flexural strength and SRF for NC test specimens.

Specimen ID	Maximum D790 Flexural Strength (MPa)	CIPP Long-term Flexural Strength (MPa)	CIPP 50-year SRF (%)
NC-L721	56	32	55
NC-L758	50	34	65

3.4.4 RC Long-Term Flexural Strength Testing

Similar to the methodology used for non-reinforced CIPP specimens, reinforced specimens (RC) were loaded to induce stress of up to 90% of the maximum flexural strength at 5% strain. Three rectangular flat CIPP specimens were set up for the RC-IPLUS CIPP and two specimens for the RC-IMAIN CIPP liner. Figure 3.14 shows the test apparatus and the loaded CIPP specimens during testing. Two stall mats were stacked below the hanging weights to allow the weights to drop safely should specimen failure occur.

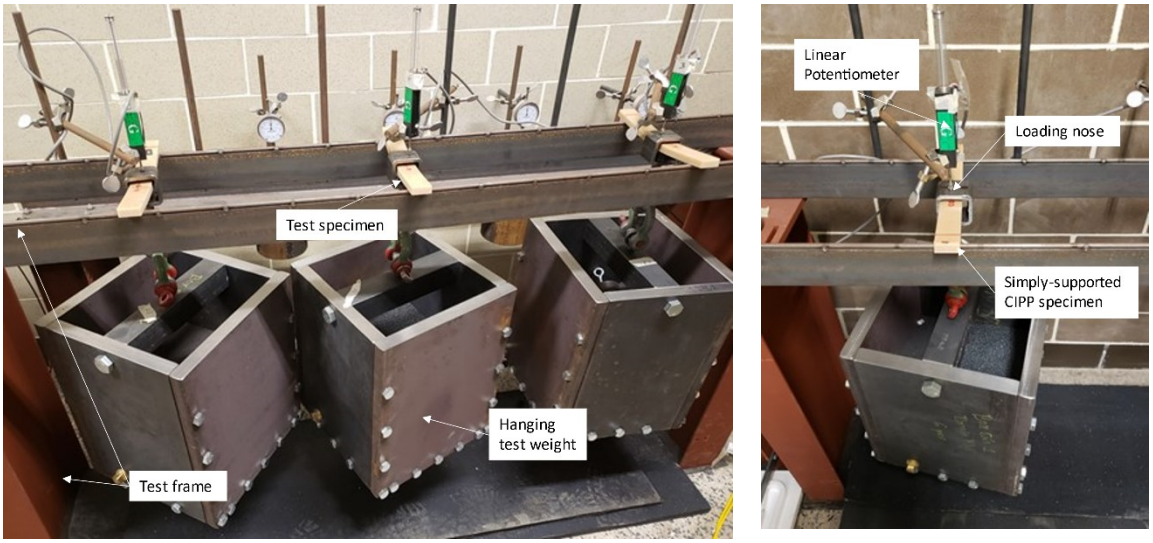

Figure 3.14: Test apparatus for a reinforced CIPP (RC) specimen tested with a load up to 2.5 kN.

Unlike the NC specimens that ruptured within the first hour of loading, there was no rupture failure in the RC-IPLUS and RC-IMAIN test specimens at and beyond one hour. Since CIPP is typically designed using flexural short-term mechanical properties obtained at a maximum of 5% strain, rupture failure was defined by the time it took the CIPP material to reach 5% strain [31]. For both reinforced test specimens, audible cracks were heard after a rapid increase in strain was experienced at the onset of loading. After that, steady strain occurs up to approximately 100 hours. Since the RC specimens did not crack and rupture, the trends of the strain increase with time were then observed to determine when the 5% strain limit was reached.

The RC specimens were noted to have a higher creep-rupture envelope than the NC specimens, as they sustained 181 MPa and 197 MPa (90% of maximum flexural strength at 5% strain) for a much extended period with minimal deflection.

3.4.4.1 RC Specimens Rupture Prediction

After 3,000 hours of testing, rupture prediction was made using linear regression on the stain data (from deflection measurements) and log of time. Figure 3.15 shows extrapolation plots and forecasts for the reinforced CIPP specimens loaded at 90% maximum flexural strength at 5% strain. At 50 years, the strain values at the ASTM D790 maximum flexural strength for the RC-IPLUS and RC-IMAIN were

estimated to be between 2.2 to 2.3% and 3.25 to 3.35%, respectively. These percentages are significantly lower than the ASTM D790 5% strain limit.

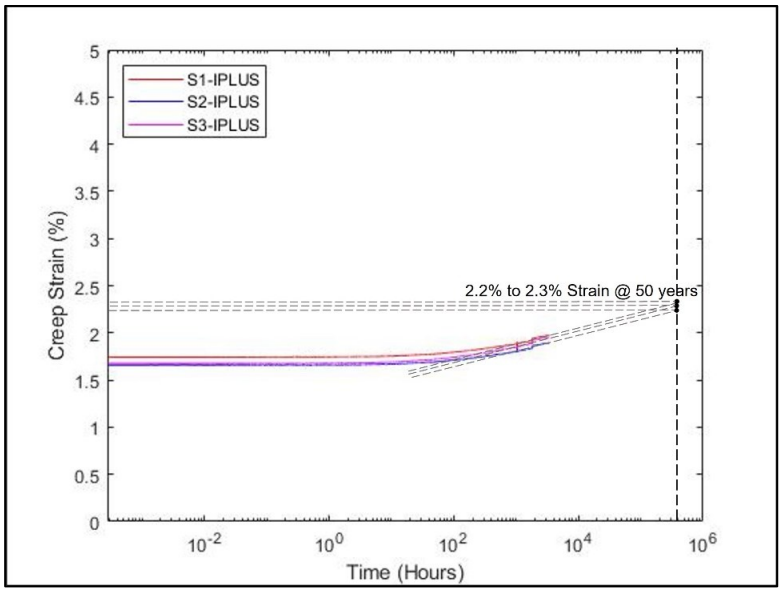

(a) RC-IPLUS prediction using strain measurements.

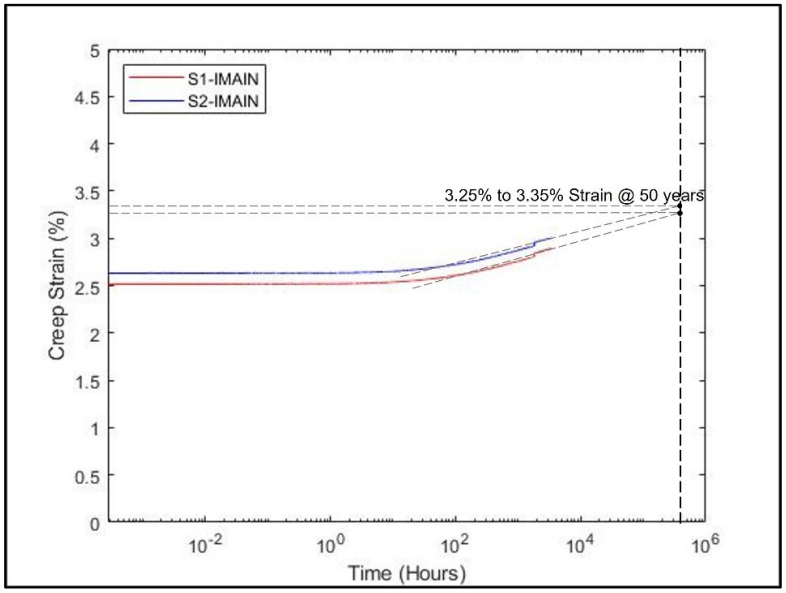

(b) RC-IMAIN prediction using strain measurements.

Figure 3.15: RC specimens Regression under 90% of the maximum short-term flexural strength.

Since no rupture failure occurred for RC-IPLUS and RC-IMAIN test specimens loaded at 90% of the maximum flexural strength, a higher stress level was investigated using a new set of specimens. The CIPP specimens were loaded to induce 197 MPa and 212 MPa stress, which is about 97% of the maximum flexural strength to ensure CIPP rupture occurred. Owing to the difficulty in fabricating additional experimental loading weights, no replicates were considered for the 97% stress level creep-rupture tests. Therefore, only one CIPP specimen was set up for RC-IPLUS and RC-IMAIN test specimens. After an hour of testing, no rupture failure occurred in either RC-IPLUS or RC-IMAIN test specimens. Stain data (from deflection measurements) was used to predict when a specimen rupture would occur after another 1,000 hours of testing. Figure 3.16 provides prediction data for the reinforced CIPP specimens loaded to 97% of the maximum short-term flexural strength. At 50 years, the strain values at the ASTM D790 maximum flexural strength for the RC-IPLUS and RC-IMAIN were estimated to be at approximately 2.45% and 3.8%, respectively. Table 3.4 details all extrapolation and prediction results for the reinforced CIPP specimens loaded at 90% and 97% stress levels. The RC test specimens were observed not to fail or rupture at 97% of the ASTM D790 maximum flexural strength at 5% strain.

Table 3.4: Extrapolation and prediction results to estimate failure time for RC test specimens.

Specimen ID	**Stress level (% maximum flexural strength)**	**Stress level (MPa)**	**Approximate strain at 10,000 hours (%)**	**Approximate strain at 50 years (%)**
RC-IPLUS	90	181	1.9	2.2
			2	2.25
			2.02	2.3
	97	195	2.2	2.45
RC-IMAIN	90	197	2.9	3.25
			3.1	3.35
	97	212	3.6	3.8

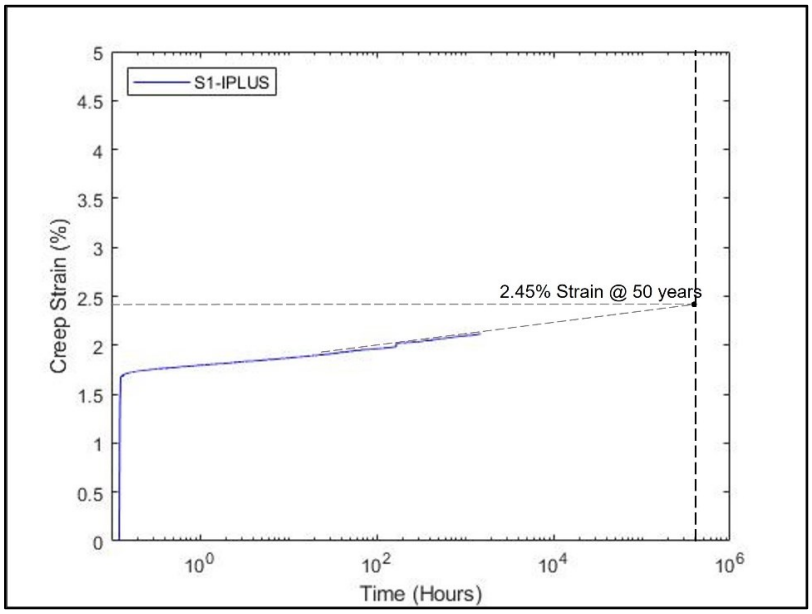

(a) RC-IPLUS prediction using strain measurements.

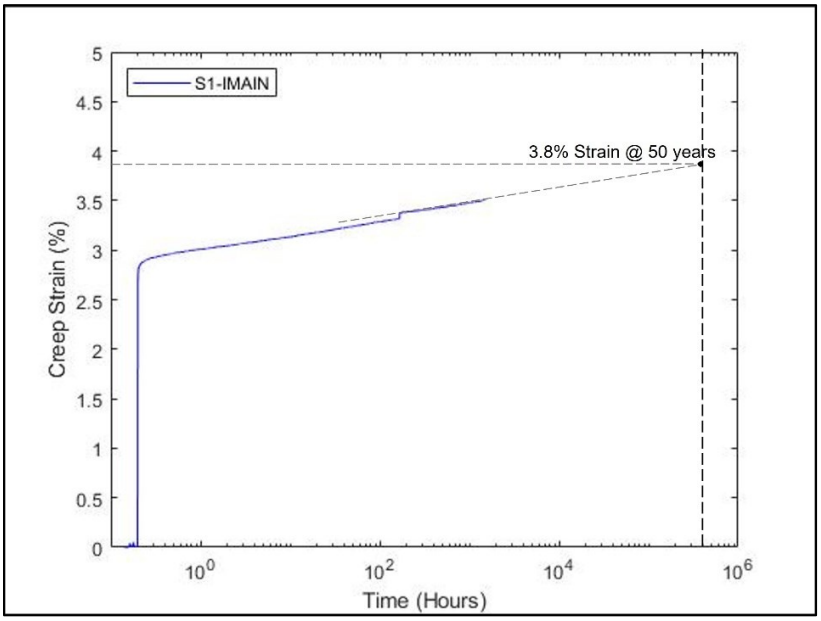

(b) RC-IMAIN prediction using strain measurements.

Figure 3.16: Regression completed to estimate rupture of RC specimens under 97% of the maximum short-term flexural strength.

3.4.4.2 Linear Regression Analysis

Similar to the data analysis completed for NC specimens, Equation 3.1 was used to develop strength regression lines to predict the long-term 50-year flexural strength of the RC test specimens. Figure 3.17 and Figure 3.18 shows the rupture stress of the CIPP specimens subjected to creep-rupture test at different stress levels to produce other rupture data points. The observed long-term mechanical response may be due to the presence of fibreglass in the RC specimens, which took more proportional stress than the resin.

From the development of the CIPP strength regression line, CIPP 50-year long-term flexural strength ($LTFS_{50}$) was estimated to be 177 MPa and 188 MPa for the RC-IPLUS and RC-IMAIN specimens, respectively.

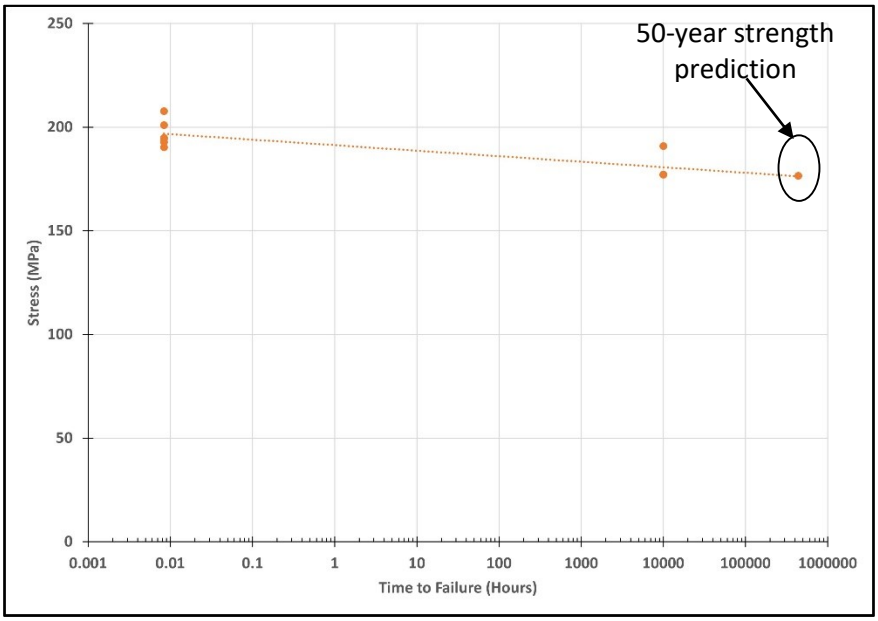

Figure 3.17: Regression line and extrapolation to determine long-term flexural strength for reinforced RC-IPLUS CIPP specimens.

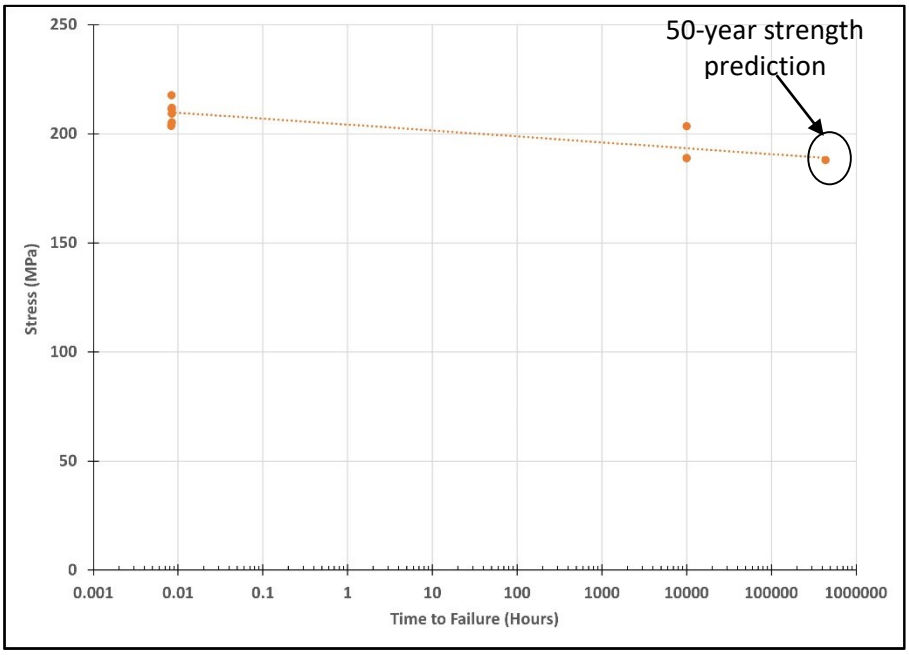

Figure 3.18: Regression line and extrapolation to determine long-term flexural strength for reinforced RC-IMAIN CIPP specimens.

3.4.4.3 Long-Term Flexural Strength Retention Factor (SRF)

The 50-year SRF for each CIPP specimen was estimated using the ratio of the long-term flexural strength to the short-term ASTM D790 strength (using Equation 3.2).

Table 3.5 provides the mean short-term flexural strength and 50-year flexural strength, as well as, the SRF for both RC-IPLUS and RC-IMAIN test specimens. The table shows that, for the reinforced CIPP liners, the flexural SRF was approximately 88% and 86% for the RC-IPLUS and RC-IMAIN test specimens, respectively. Research completed by Gumbel and Chrystie-Lowe [38] on CIPP long-term flexural properties found the SRF for two reinforced CIPP liners to be 60% and 76%. Shannon [29] determined the tensile SRF to be 70%. These values do not agree with the long-term flexural strength test results presented herein.

In this study, the strength retention factors were determined using flat plate specimens, which are not representative of field conditions and have curved surfaces. From a pressure pipe design standpoint, the determined long-term mechanical properties can be reduced to account for liner

imperfections and shape differences. Thus, 85% and 80% strength retention factors would be appropriate for the RC-IPLUS and RC-IMAIN test specimens. Despite the reductions to account for field conditions, curvature effects and possible liner imperfections, the determined SRF values do not agree with the typical 50% value that is currently used for design. This means that after 50 years of service, there can be about an 80 to 85% decrease in structural performance compared to the initial state of the CIPP liner. It was inferred that the glass reinforcement in the RC specimens introduced high short-term strength to the liner. These results highlight the value of the creep-rupture test as a differentiator of previously used 50% long-term value based on creep testing.

Table 3.5: Short-term, long-term flexural strength and SRF for RC test specimens.

Specimen ID	Maximum D790 Flexural Strength (MPa)	CIPP Long-term Flexural Strength (MPa)	CIPP 50-year SRF (%)
RC-IPLUS	201	177	85
RC-IMAIN	219	188	80

3.4.5 CIPP Design Consideration

Plotted creep-rupture stresses versus time-to-rupture data can be used directly for CIPP design. Figure 3.19 shows the wide range and unpredictability of the SRF for four CIPP liners tested under flexural creep-rupture. It can be observed from the lines that the creep-rupture failure envelope would decrease at different rates depending on each CIPP specimen. After extrapolating the strength of all non-reinforced CIPP liners, the regression line shows that the 50-year flexural strength retention would fall within approximately 55% to 65%. In comparison, reinforced CIPP flexural strength retention would range from 80% to 85%.

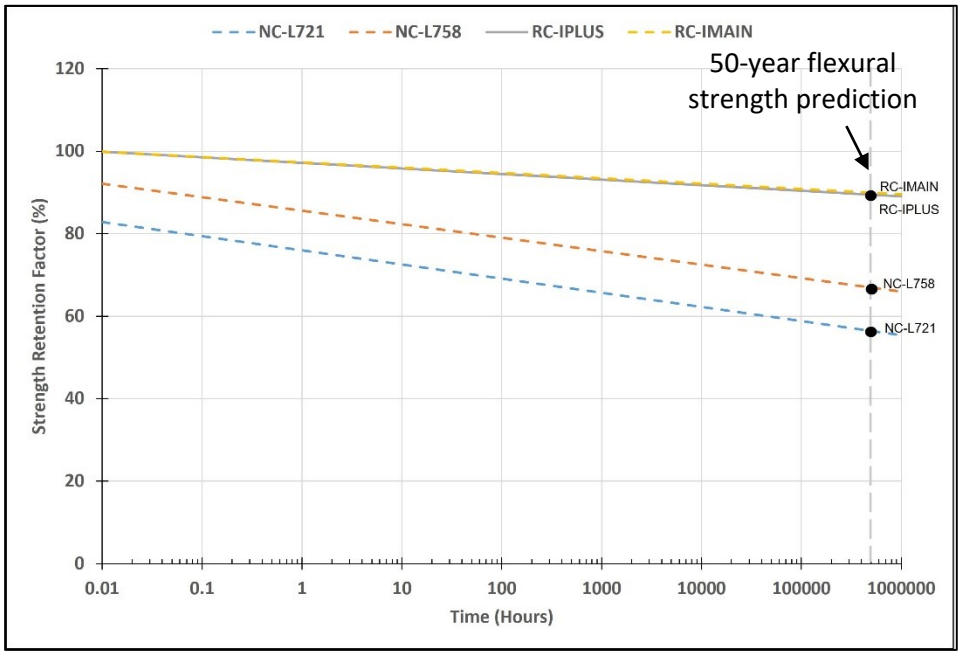

Figure 3.19: Strength regression line for four CIPP liners tested under flexural creep-rupture test to determine long-term 50-year strength.

As may be seen, the RC-IPLUS and RC-IPLUS specimens have SRF values significantly greater than the NC-L721 and NC-L758 specimens. Based on this data, safe stress can be determined below which it is safe to operate, given the time requirements of the end-use application.

In North America, ASTM F1216 Non-Mandatory Appendix X1 is used to design CIPP gravity and pressure liners. This design method covers gravity pipelines using Equations X1.1 to X1.4 and includes additional design checks for pressure pipelines using Equations X1.6 or X1.7. The ASTM F1216 Equations X1.2 and X1.6 require a long-term (time-corrected) flexural strength for CIPP. Considering the CIPP specimens investigated in this study, minimum SRF values (55% and 80%) in each case can be compared with traditional CIPP design (SRF = 50%) using Equation 3.1 and Equation 3.2 (see Section 3.2.2).

An example calculation (see Appendix C) shows that compared to the minimum thickness obtained using a 50% SRF, the minimum thickness value computed when a 55% SRF would be approximately 5% lower. When the 80% SRF was calculated, the minimum thickness obtained would be about 20% lower than the minimum thickness value obtained using the traditional 50% SRF. Using the

appropriate long-term mechanical strength properties of CIPP is critical in design to avoid being over-conservative, thereby using larger thickness values which can potentially cause liner constructability issues in the field.

3.5 Conclusions

This study evaluates the creep-rupture response and long-term 50-year flexural strength of both non-reinforced and reinforced CIPP specimens using creep-rupture testing. Multiple CIPP coupon specimens were tested to determine the rupture CIPP strength regression line using data points 3,000 hours. Based on the test results presented herein, the following conclusions can be drawn:

1. Short-term flexural testing found that for the non-reinforced CIPP test specimens (NC-L721 and NC-L758), some fractures developed inside the CIPP material, causing a persistent cracking evidenced by "saw tooth waves" in the stress-strain graphs until rupture occurred. However, no liner fracture was observed in the reinforced CIPP test specimens (RC-IPLUS and RC-IMAIN), and the stress-strain plots were observed to increase steadily until they reached the maximum flexural strain limit of 5% (per ASTM D790). Results show that the overall material composition (resin type and presence/absence of reinforcing fibres) of CIPP can play a major role in defining its mechanical behaviour. For the long-term creep-rupture tests, the presence of reinforcements in the RC test specimens was also observed to introduce high tensile capacity to the liner thereby preventing any event of rupture at the early stages (< 1 hour) that was observed in the NC test specimens.

2. Over the 3,000 hours plus test period, the RC-IPLUS and RC-IMAIN test specimens displayed no rupture failure after the initial cracking on the onset of loading. Forty-three rupture failures were observed in the NC-L721, and NC-L758 tested specimens. Strength regression lines were developed for the non-reinforced CIPP test specimens (NC-L721 and NC-L758) based on creep-rupture using stress levels from approximately 90% to 60% of the ASTM D790 maximum flexural strength, which found CIPP 50-year long-term flexural strength ($LTFS_{50}$) of 32-34 MPa. The $LTFS_{50}$ for the reinforced test specimens (RC-IPLUS and RC-IMAIN) was estimated to be 177-188 MPa using linear regression.

3. Specimens RC-IPLUS and RC-IMAIN showed no rupture failure throughout the test period considered in this experimental investigation. This specimen response was attributed to the high tensile capacity introduced to the liner by the reinforcements in the RC test specimens. CIPP strain extrapolation line showed that at the 97 and 90% stress levels, the creep strain for the reinforced test specimens would be below the 5% strain limit (per ASTM D790). Also, the strength regression line developed for the reinforced CIPP specimens using the data from testing estimated RC test specimens to be at approximately 80 to 85% of the short-term flexural strength. This research emphasized critical pressure pipe design considerations to reduce CIPP's long-term mechanical properties to account for liner imperfections and possible over-estimations in flat plate testing.

4. Strength regression lines were provided to show the distinctive and unpredictable CIPP long-term strength retention trend to design CIPP liners for 50 years. The tested non-reinforced CIPP liners exhibited the lowest short-term and long-term flexural strengths. They showed the lowest retention factors (55 and 65%), which are slightly lower than the available literature (SRF of 68%) on other non-reinforced specimens. In comparison, long-term strengths reinforced CIPP specimens reduced somewhat with time. Their strength retention factors were as high as 80% and 85% for the reinforced CIPP liners and were observed to be higher than available literature (SRF of 60-76%) on other reinforced specimens. All SRF values were higher than the generalized CIPP 50% retention factor. When analyzed using the applicable ASTM F1216 equations that require long-term flexural strength, it was observed that using the traditional 50% SRF value will produce a more conservative design output with a difference of about 5-20%.

Chapter 4

Advancements in CIPP Liner Testing and Design for Watermain Renovation

4.1 Overview

In North America, pressure testing is not typically performed on full-scale pressure cured-in-place pipe (CIPP) liners to determine their pressure performance. Instead, CIPP liners are designed using the ASTM F1216 Non-Mandatory Appendix X1 method using flexural and tensile properties from flat plate specimens. Thermoplastic and fibre-reinforced pipe renovation products have well-established methods that involve the determination of the pipe material Pressure Rating (PR) using the Hydrostatic Design Basis (HDB) method. In this study, CIPP short-term hydrostatic burst pressure was determined for a 150-mm I-Main composite pressure CIPP liner and the PR was estimated. A customized burst facility was constructed and commissioned at the University of Waterloo, which used a hydraulic cylinder and a gearbox-actuator pressurizing system in place of regular pumps. Test results found that the CIPP liner specimens, having no known physical defect, demonstrated significant variability in their burst pressures. The presence of invisible liner imperfections, such as microscopic air voids in the liner, decreased the burst pressure by approximately 50%. Therefore, the hydrostatic testing approach can be adopted as a North American standardized testing program to design and classify all watermain CIPP products in line with other pressure pipe products used in the trenchless industry.

4.2 Introduction

In North America, water distribution and transmission mains transport potable water from treatment plants to residents and businesses. Many of these pipelines are old, close to the end of their service lives, and are not easily accessible as they are mostly buried under metropolitan districts. Cured-In-Place Pipe (CIPP) liners consist of a tubular fabric impregnated with polyester or vinyl ester thermosetting resins [4]. The thermosetting resin-impregnated fabric is cured, within the pipe, using an energy source (hot water, steam, or UV light) to form a tight-fit structurally stable liner within the deteriorated host pipe.

Over the last 50 years, CIPP lining systems have been used to rehabilitate gravity pipes (wastewater, stormwater, and culverts), as well as, low-pressure (140 to 280 kPa) forcemains and siphons. Gravity CIPP liners are designed to resist hydrostatic, dead, and live loads. American Society of Testing Materials (ASTM) and the International Standards Organization (ISO) have developed industry-accepted standards for constructing gravity CIPP liners. In North America, the Non-Mandatory Appendix X1 in ASTM F1216 [1], *"Standard Practice for Rehabilitation of Existing Pipelines and Conduits by the Inversion and Curing of a Resin-Impregnated Tube,"* is used to design circular gravity CIPP liners. This method involves completing multiple design checks to obtain an optimum liner thickness required to support external groundwater loads. Also, the method ensures the liner withstands the internal pressure in spanning holes in the original pipe wall and sustains operating pressures and external loads imposed by soil and traffic surcharge. Depending on the existing pipe to be lined, the required thickness is calculated from a series of design equations. The most significant thickness is then selected for the CIPP installation. Gravity CIPP liners can be designed as non-structural or structural liners using the ASTM F1216 Non-Mandato0ry Appendix X1 design equations from Equations X1.1 to X1.4 [1].

4.2.1 CIPP Pressure Pipe Design

Over the last two decades, CIPP liners have been offered to renovate high-pressure pipelines (i.e., potable watermains). Matthews et al. [7] provide details about various CIPP products/technologies currently in the pressure pipe renovation market. While some CIPP liner product comprises two concentric, tubular, plain woven seamless polyester jackets, others involve using a fibreglass layer between two non-woven felt layers or simply forming a fibre-reinforced polypropylene sock within a deteriorated pipe [7]. Watermain pressure liners, in North America, are typically constructed using epoxy or vinyl ester resin-impregnated reinforced tubes to form a composite thermoset pipe [1], [2], [6]. Unlike gravity CIPP liners, watermain liners are subjected to internal working pressures ranging from 415 to 830 kPa [2]. They are also subjected to vacuum loads that can collapse the liner should they not have sufficient ring stiffness. In addition to working pressures and vacuum loads that exist with the water distribution system, CIPP liners can be subjected to surge pressures, which can be recurring and occasional surge pressures [2], [3], [45]. Marshall and Brogden [46] have shown that

surge pressure occurrences can increase or decrease the system pressure by 2 to 3 times the working pressure in a fraction of a second [46]. This surge pressure occurrence is a critical consideration for the design of watermain liners. Gravity CIPP can also be reinforced to withstand higher hydrostatic and external pressure loading in large-diameter applications.

Watermain CIPP liners are typically designed to focus on reinforcements in the hoop direction to prevent the liner from tearing apart. Figure 4.1 illustrates the difference between the response of gravity CIPP from pressure CIPP. Typically, gravity CIPP liners are designed to withstand bending and buckling failure in the liner due to all external loads. However, watermain pressure CIPP further considers the tensile force, F, a liner can provide to withstand internal stress induced by the internal pressure, P.

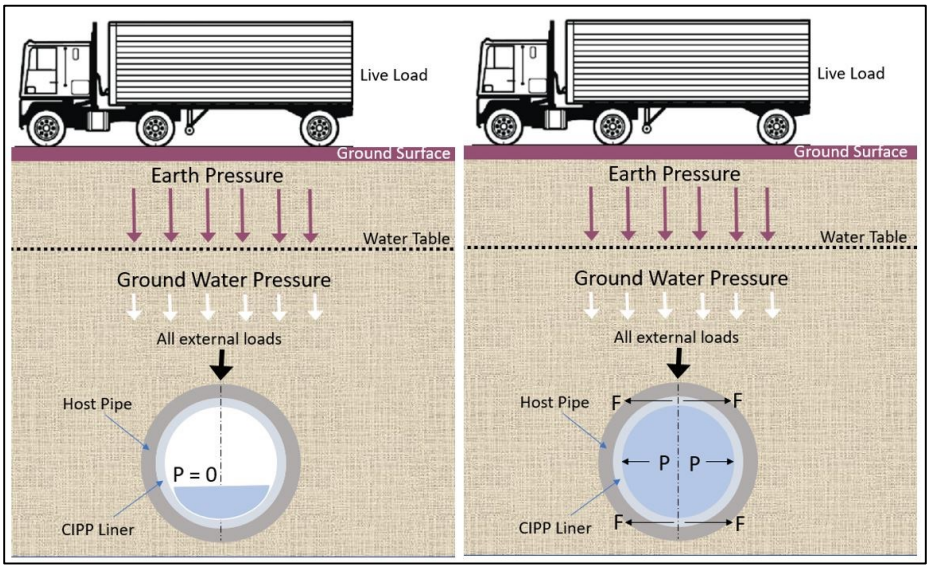

Figure 4.1: Difference between reinforced gravity CIPP (with zero internal pressure, P) and pressure CIPP liners (with internal pressure, P equal to the tensile force, F).

In North America, engineers and designers have adopted the ASTM F1216 Non-Mandatory Appendix X1 method to design watermain CIPP pressure liners. This design method covers sewage gravity pipelines (Equations X1.1, X1.2, X1.3, and X1.4) and includes additional design checks (Equations X1.5, X1.6, and X1.7) for sewage forcemain applications, which are typically lower than watermain pressures (550 to 1,035 kPa) [1], [3], [4]. Only the ASTM F1216 Equation X1.3 was revised in 2007, with minor changes to the ovality parameter mainly to design a liner to support soil, hydraulic, and

live loads [4]. It is also worth noting that ASTM F1216 designs are completed using a Safety Factor of 2 with no consideration for pressure surges that often result from pumps and valves turning on and off in water distribution systems. The ASTM F1216 design method was not intended for the design of watermains, and none of the revisions made since 1989 have addressed the limitations of the design approach to account for high-pressure systems (such as watermains).

4.2.2 Plastic Pipe Design

Pipe renovation products such as High-Density Polyethylene (HDPE) and Polyvinyl Chloride (PVC) pipes are designed to withstand all internal pressure loads by determining the material Pressure Rating (PR) using established stress values called the Hydrostatic Design Basis (HDB). Based on ASTM D2837 [47], *"Standard Test Method for Obtaining Hydrostatic Design Basis for Thermoplastic Pipe Materials or Pressure Design Basis for Thermoplastic Pipe Products,"* the pipe material (PR) is defined as *"the estimated maximum water pressure the pipe is capable of withstanding continuously with a high degree of certainty that failure of the pipe will not occur"* [47]. The pipe's Long-term Hydrostatic Strength (LTHS) is established and categorized to determine the HDB. The HDB refers to the categorized LTHS in the hoop direction for a given set of end-use conditions established by ASTM D2837. The LTHS is *"the estimated tensile stress in the wall of the pipe in the circumferential orientation that, when applied continuously, will cause the pipe failure at the intercept of the stress regression line with the 100,000-hour coordinate"* [47]. Figure 4.2 shows the stress regression line's typical development for thermoplastics and the LTHS. The figure also shows the lowest value of the LTHS based on a statistical analysis of the regression data, known as the Lower Confidence Limit (LCL) line. HDPE and PVC HDB regression lines are typically developed from a 10,000-hour pipe burst test using 25-mm extruded homogeneous and isotropic (same mechanical properties in the pipe hoop and longitudinal directions) unrestrained pipe specimens.

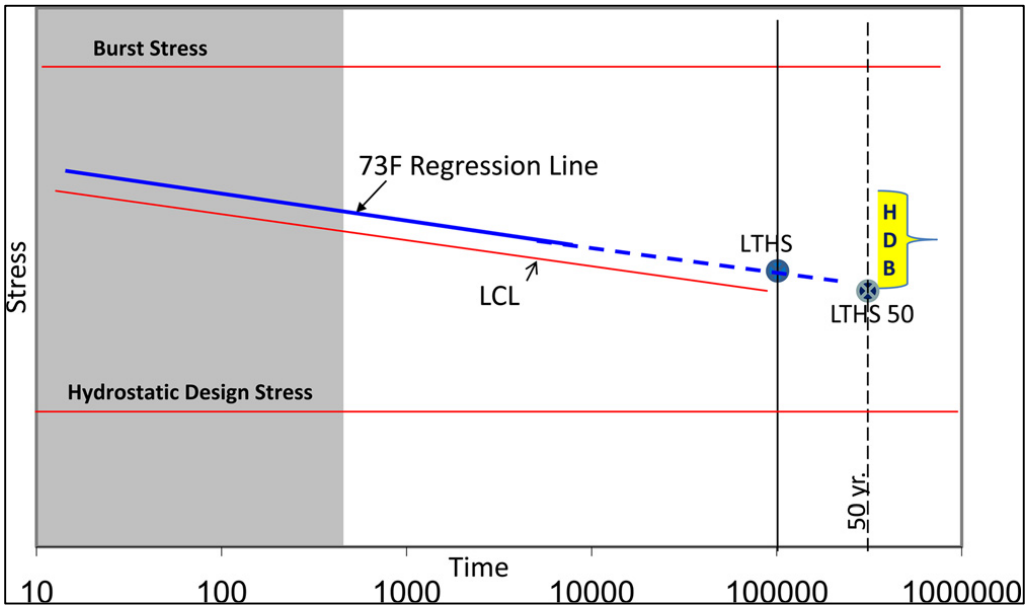

Figure 4.2: Typical regression line and extrapolation using ASTM D2837 [45].

Research conducted by Boros [45] to investigate the Hydrostatic Design Strength (HDS) of thermoplastic compounds found that the stress regression methodologies used for establishing LTHS are instrumental to the design of pipeline systems [45]. Table 4.1 provides PVC and HDPE HDS and HDB values allowing engineers and researchers to define the retention factor between the long-term and the short-term design strength value. The table shows that the HDB values are approximately 1.6 to 2 greater than the HDS and that HDS will be many times lower than the short-term burst strength (an approximate factor of 4).

Table 4.1: PVC and HDPE material HDS and HDB values in MPa at 23°C [48].

Pipe Material	Pipe Material Designation Code	Maximum HDS (MPa)	HDB (MPa)
PVC	PVC 1120	13.8	27.6
	PVC 2116	11.0	21.7
	CPVC 4120	13.8	27.6
HDPE	PE 3408	5.5	11.0
	PE 3608	5.5	11.0
	PE 3708	5.5	11.0
	PE 3710	6.9	11.0
	PE 4608	5.5	11.0
	PE 4708	5.5	11.0
	PE 4710	6.9	11.0

4.2.3 GRP Pressure Design

Pipe renovation products such as glass fibre reinforced polymer (GRP) pressure pipes are also widely used in the water industry. These composite pipes are often designed with layers of fibres at different locations in the pipe wall cross-section and have more fibres in the pipe hoop direction to resist internal hoop tensile stresses. For composite pipes, which typically have different mechanical properties in the hoop and longitudinal pipe directions, HDB regression lines have been developed using ASTM D2992 [49], "*Standard Practice for Obtaining Hydrostatic or Pressure Design Basis for "Fiberglass" (Glass-Fiber-Reinforced Thermosetting-Resin) Pipe and Fittings,"* using specimens with reinforcement layers that are larger than 25 mm. Sung and Jin [50], Faria and Guedes [51], and Rafiee et al. [52] have provided some information on the burst testing of in-plant manufactured GRP pipe specimens. Sung and Jin [50] measured burst pressure and time after applying sustained internal pressure for 10,000 hours and predicted the long-term behaviour of 400-mm GRP pipes that were 1.5 m long. The testing found that the correlation coefficient between the test results and the linear

equation was about 0.8, and the data was acceptable for linear regression. The regression equation developed by Sung and Jin [50] indicated that the 50-year burst pressure is approximately three times lower than the one-minute burst pressure. Faria and Guedes [51] presented valid long-term pressure test results for three GRP pipes. All in-plant manufactured pipe test specimens were 300 mm nominal diameter and 1.3 meters long. The reported regressions indicated that the 50-year burst pressure was 1.2 to 2.4 times lower than the one-minute short-term burst pressure [51]. Chen et al. [53] discussed the long-term hydrostatic strength of Kevlar fibre-reinforced flexible pipes that were also in-plant manufactured. Test specimens were 150 mm internal diameter and 1.1 m long. Using the mean reported regression, the 50-year burst pressure was 2.3 times lower than the one-minute short-term burst pressure [53].

4.2.4 Standardizing Pressure Pipe Design

Similar to GRP pipes, CIPP pressure liners are composite pipes with different mechanical properties in the hoop and longitudinal pipe directions. CIPP liners are manufactured and installed in the field, not in a manufacturing plant with tightly controlled manufacturing processes and conditions. Another additional complexity for CIPP liners is the presence of inherent features such as folds, wrinkles, and continuities that can form during the liner installation [2], [4]. Currently, there are no standards for testing or classifying CIPP pressure liners in North America using pipe burst testing approaches such as the HDB methodology. Hence, there is no available information regarding the ratio of CIPP 50-year burst pressure to the one-minute short-term burst pressure.

International Organization for Standardization (ISO) and American Water Works Association (AWWA) have created pressure CIPP liners such as ISO 11297-4 [14] (*Plastics piping systems for renovation of underground drainage and sewerage networks under pressure — Part 4: Lining with cured-in-place pipes*) and AWWA C623 [15] (*Plastics piping systems for renovation of underground drainage and sewerage networks under pressure — Part 4: Lining with cured-in-place pipes*), respectively. Currently, both organizations are working on standardized design methods for watermain renovation. An AWWA Committee report [37], *Structural Classifications of Pressure Pipe Linings; Suggested Protocol for Product Classification*, discussed the short-comings of using ASTM F1216 Non-Mandatory Appendix X1 for the design of pressure liners as a fully structural stand-alone (AWWA Class IV) CIPP product,

and the need for CIPP liners to undergo hydrostatic burst tests to follow the industry-accepted HDB design approach [37]. In general, a CIPP liner will be in contact with the inside of the existing pressure pipe. As internal pressure is applied, the liner will expand under pressure until either its resistance to expansion equals the internal pressure or its contact with the existing pipe stops the expansion. In most cases, the latter occurs first, and much of the internal pressure is transferred to the existing pipe. When the existing pipe remains structurally sound, the liner will feel only part of the internal pressure [4].

A few publications present the results from the independent pressure testing of CIPP liners to failure. Allouche et al. [54] presented results from internal pressure burst tests completed on a CIPP liner in an iron pipe with a fire hydrant tee. Before testing, the 100 mm hydrant feed pipe was removed. The CIPP liner spanned the hydrant opening, which was approximately 200 mm long and 150 mm wide. The CIPP liner was tested in a custom-made pressure cell. The internal pressure was increased to 3.8 MPa in 0.35 MPa increments and was held for at least five minutes. Testing was stopped due to cracking noises, end seal leakage, and the potential for catastrophic failure [54]. The CIPP liner was not tested independent of the host pipe. Knight and Bontus [2] discussed short-term burst testing for two commercially available CIPP liners per ASTM D1599 [55], *"Standard Test Method for Resistance to Short-Time Hydraulic Pressure of Plastic Pipe, Tubing, and Fittings."* They noted a possibility of CIPP liners exhibiting different tensile capacities to withstand internal pressure loads. The 1.2-meter-long test specimens were cast inside a 150 mm PVC pipe, which was removed after the liner was cured. Eleven burst tests were performed for one of the two CIPP liner products (Liner A), with a mean burst pressure of 5.45 and a standard deviation of 0.6 Mpa. Five burst tests were performed for the second CIPP liner (Liner B), exhibiting a significant testing variability and low mean burst pressure of 2.92 with a standard deviation of 0.7 MPa [2], [55]. Liner B is known to have visible wrinkles and folds. Almansour et al. [56] provided ASTM D1599 failure burst data for another commercially available CIPP liner. All test specimens were formed inside 150 mm PVC pipes and removed after curing. They evaluated CIPP specimens to investigate the effect of folds and compared them with two control specimens (with no folds). Test results indicated that inherent liner features such as folds could reduce CIPP burst pressure by 45% as the mean burst pressure was 2.65 with a standard deviation of 0.1 MPa with folds and 5.94 with a standard deviation of 0.01 MPa without folds [56]. Alam et al. [5] presented

burst pressure results for other commercially available CIPP glass-reinforced thermosetting-resin specimens. They evaluated CIPP specimens to investigate the effect of CIPP liner configuration. Nine 1.2-meter-long 300 mm diameter CIPP specimens with three different configurations were tested following the ASTM D1599 procedure. Their test results showed that a CIPP liner having variations in the configuration of the glass reinforcements can significantly reduce CIPP burst pressure by up to 45% [5]. As such, there is an urgent demand for an approach to develop a unified design method for the various pressure CIPP commercially available products.

This study presents two aspects of experiment-based research to advance the development of a standardized design method for watermain CIPP liners. The first involves constructing and developing a unique testing facility to evaluate the material behaviour of a commercially available Insituform I-Main CIPP liner. The second aspect consists of the test equipment validation and CIPP short-term burst testing, which can be used to develop the first known CIPP HDB regression line in subsequent research.

4.3 Watermain CIPP Liner Burst Facility

4.3.1 Burst Facility Design Framework

Burst testing laboratories specifically for CIPP liner testing are not common in the water utility industry as they are challenging to set up. Hence the need for a customized burst facility to be designed and constructed at the University of Waterloo. The test facility was built to determine the following: 1) CIPP short-term hydrostatic burst pressure, 2) CIPP pressure rating using long-term HDB testing, and 3) CIPP response to pressure cycles and fatigue life.

To achieve the above design requirements, the following equipment design objectives were set:

1) Ability to test full-scale CIPP liners specimens with an Outer Diameter (OD) of up to 250 mm and longitudinal specimen length at least five times the pipe OD.
2) Maximum burst pressure capacity of 14 MPa.
3) Controllable uniform pressure loading ramp rate with no pressure surges.
4) Modular components for maintenance and upgrading.

5) Condition and burst multiple CIPP liner specimens in a controlled temperature water bath at 23°C.

6) Data acquisition system that monitors and collects pressure sensor data at a minimum of 100 samples/sec.

7) A computer-controlled pressure monitoring system that can maintain multiple test specimen pressures to within 5% of the target set pressure for at least 10,000 hours (approximately 14 months) and specimen failure.

8) Ability to apply controlled pressure cycles to CIPP liner specimens for up to 10 million cycles or liner failure.

4.3.2 Burst Testing Equipment

The burst testing equipment (shown in Figure 4.3) was set up so that a water pressurization system was connected to a high-pressure manifold. The manifold connects to multiple CIPP test specimens laid horizontally in a controlled-temperature water bath. Solenoid valves between each test specimen and the manifold allowed each test specimen to be pressurized or disconnected from the manifold internal pressure when required. Pressure in each test specimen and the manifold were monitored and recorded using a custom-built LabVIEW data acquisition system. Should a test specimen pressure decrease below the target value, the manifold pressure was set to the target pressure and the solenoid valve was opened. Once the test specimen reached the target value, the solenoid was closed. This design involved developing a computer-controlled automated system to continually monitor and maintain each test specimen at the target value of up to 10,000 hours of testing.

The water pressurization system consisted of an electric-driven motor-actuator system that was connected to a hydraulic water-filled cylinder connected to the manifold. The pressurization system was designed to apply a continuous linearly increasing internal pressure up to 14 MPa. Water pressure was generated by moving the piston cylinder with the actuator forward. Pressure cycles can be generated by moving the piston backward and forward at a controlled frequency. Figure 4.4 shows the electrically driven actuator that consists of a screw-controlled actuator, gearbox, and electric motor. The gearbox is connected between the actuator and the electric motor. A motor controller

device was set up to control the motor speed at a constant variable pressure rate or to create a continuous pressure cycle. The stainless-steel hydraulic water-filled cylinder was custom manufactured and had an 82.5 mm bore and 50.8 mm rod size, and 200 mm stroke. Figure 4.5 shows the hydraulic actuator connected to the electric motor-controlled actuator.

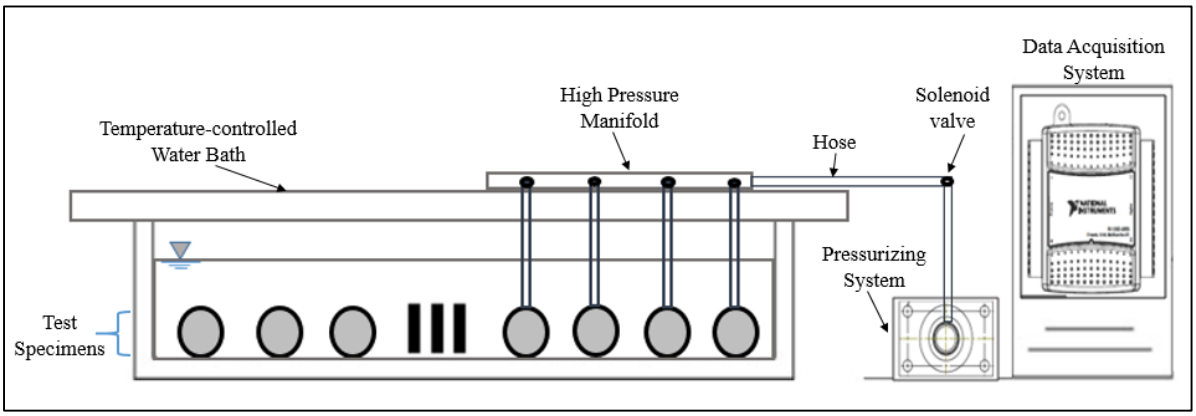

Figure 4.3: The University of Waterloo CIPP liner burst testing laboratory schematic.

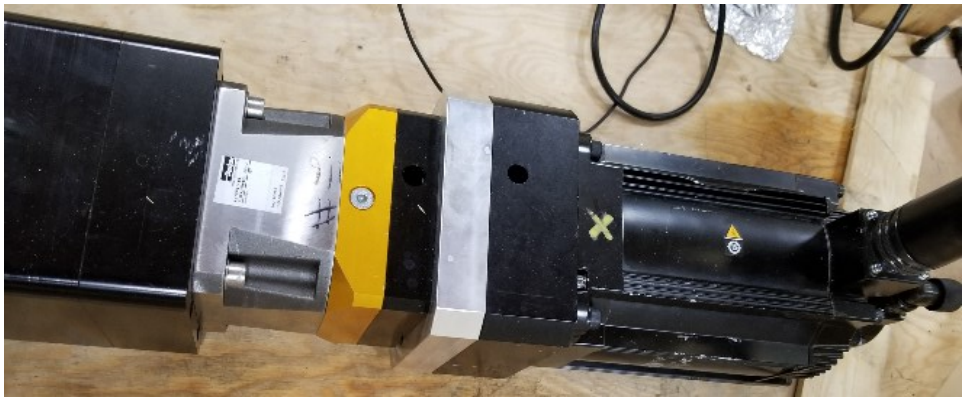

(a) Gearbox connected between the actuator and electric motor.

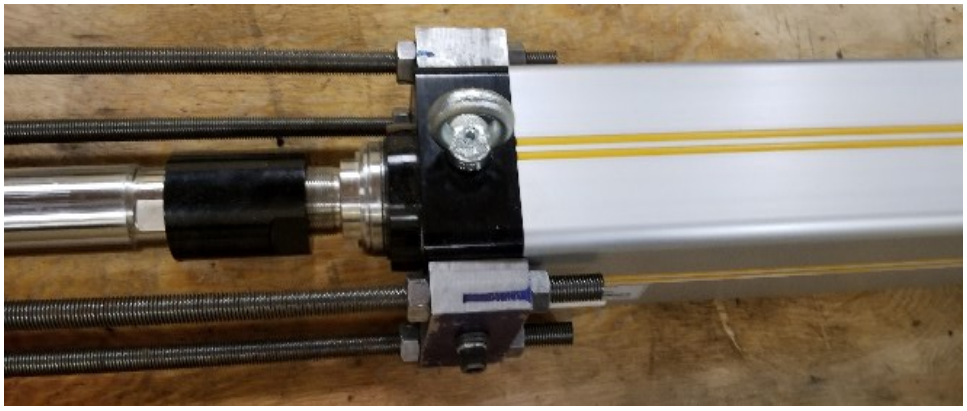

(b) Screw actuator that moves piston cylinder forward or backward for pressure generation.

Figure 4.4: Electric-driven pressurization system setup consists of a gearbox connected between an actuator and electric motor and a screw actuator that moves the piston cylinder.

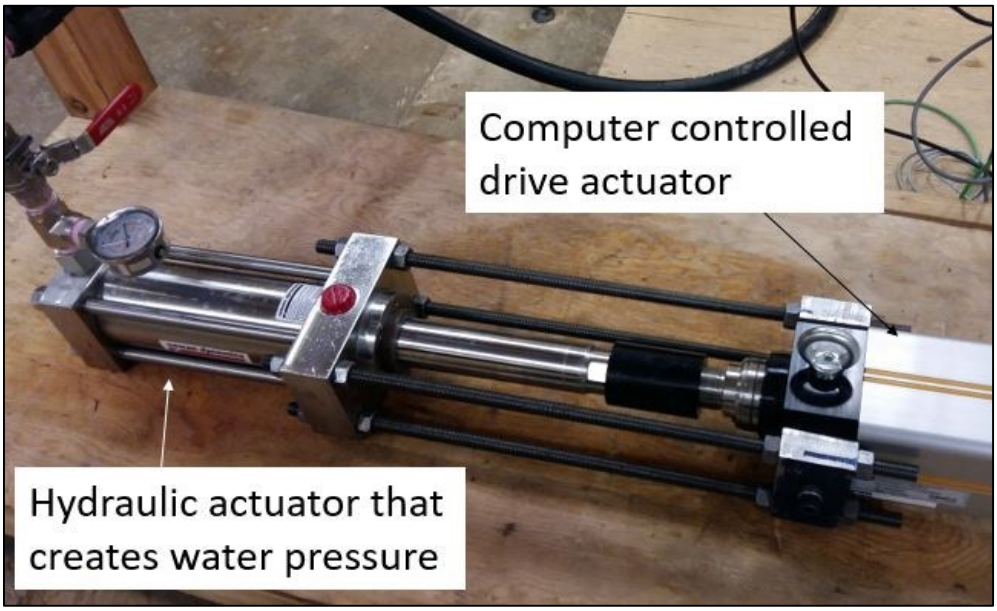

Figure 4.5: Water-filled hydraulic pressurization cylinder.

The manifold (see Figure 4.3) allowed several specimens to be simultaneously pressurized and monitored. To prevent pressure depletion of the system whenever any specimen failed, check valves were installed to ensure one-way flow. Internal pressure was measured via pressure sensors calibrated to ±0.01 MPa. The hydraulic cylinder, manifold, valves, and fitting were rated to withstand 13.8 MPa or higher and tested for pressure leaks to 13.8 MPa. The custom-built LabVIEW data acquisition system was programmed to control actuator movements, open and close solenoid valves, and monitor and store pressure sensor data at 100 samples per second.

To maintain the test specimens at a constant temperature, two 19-mm thick polypropylene plastic tanks, 2.4 m long and 1.5 m wide and 0.9 m deep, were manufactured to hold a maximum of 8 test specimens. The inside of the tanks was insulated to protect the plastic walls from damage should a test specimen fail catastrophically. To condition the specimens before testing and ensure constant temperature, the tank was filled with water and maintained at ±2°C.

4.4 Test Equipment Validation

4.4.1 PVC Theoretical Burst Pressure

The new test facility was commissioned and validated by completing short-term burst tests on some DR-18 PVC pipes with well-established burst pressure. PVC 1120 (or PVC-U) pipe is listed in PPI TR-4 [48] to have a 23°C hydrostatic design basis (HDB) and hydrostatic design stress (HDS) of 27.6 and 13.8 MPa, respectively.

The PVC pipe pressure rating (PR) can be determined using Equation 4.1.

$$PR = \frac{2 \times HDS}{DR - 1} \tag{4.1}$$

where:

DR = ratio of the pipe outside diameter to the pipe minimum wall thickness, and

HDS = hydrostatic design stress, taken as 13.8 MPa for this scenario.

Therefore, the pressure rating for the DR-18 PVC pipe was determined to be 1.62 MPa. Following available data for PVC in PPI TR-4 [48] and details provided by Boros [45] (see Table 4.1 and Figure 4.2), PVC burst stress (55.2 MPa) was determined by multiplying the pipe material PR (1.62 MPa) by a factor of 4. PVC burst pressure can then be computed using Equation 4.2, which is Barlow's Formula.

$$P = \frac{2 \times \sigma_h}{DR \times N} \tag{4.2}$$

where:

σ_h= Pipe hoop stress

DR = ratio of the pipe outside diameter to the pipe minimum wall thickness, and

N = factor of safety, taken as 1 in this study for burst scenario.

Thus, the estimated PVC burst pressure is 6.13 MPa

The burst pressure for a DR-18 PVC pipe can also be calculated using another theoretical equation. Moser [57] presents Equation 4.3, which is a modified Barlow's equation accounting for the thickness

in the midsection of the pipe, to determine the pipe burst pressure based on the pipe's ultimate tensile strength (σ_t).

$$P = \frac{2 \times \sigma_t}{(DR - 1) \times N} \tag{4.3}$$

where:

DR = ratio of the pipe outside diameter to the pipe minimum wall thickness, and

N = factor of safety, taken as 1 in this study for burst scenario.

Equation 4.3 was used with the typical ultimate tensile strength of 54 MPa for PVC, and the burst pressure of the DR-18 PVC pipe was estimated to be approximately 6.35 MPa.

4.4.2 PVC Experimental Burst Pressure

Six factory-manufactured PVC DR-18 pipes 150 mm diameter were cut to a length of approximately 1.5 m and shipped to Waterloo. Watertight mechanical joint cast iron end caps were installed on the pipe to allow pressurization of the test specimens. Since testing of large diameters can result in high-end cap forces being developed during pressurization, three high-yield threaded bars were installed to secure the ends should a failure occur. The end caps were held together using the threaded rods such that when the bolts were tightened, the rubber gaskets sandwiched in between the endcaps prevented the transfer of extra stress to the test pipe. The PVC specimens were filled with water by standing the pipes vertically and then attaching a hose to the valve at the back end to ensure no trapped air. Before pressurizing, PVC specimens were conditioned by completely immersing them in a water bath maintained at an approximate temperature of 23°C for at least a minimum of one hour.

The pressurizing system increased internal pipe pressure at a constant rate to burst the specimens within 60 to 70 seconds. While testing the first PVC pipe specimen, it was noted that internal water pressure would level off (or plateau) at about 5.8 to 6.2 MPa with no pipe failure. The plateauing was due to PVC pipe expansion during water pressurization and the inability of the hydraulic cylinder to have a sufficient volume of water to burst the PVC pipe specimens without recharging. Despite this water volume limitation, the design of the test apparatus allowed the test specimen's internal water pressure to be maintained while the hydraulic cylinder was refilled with water. After the cylinder was

refilled, a second pressure cycle was applied to the test specimen to get the test specimen to burst. This process was repeated multiple times at an increased pressurization rate to burst the specimen at a pressure ranging from 6.2 to 6.63 MPa. PVC burst pressure was then compared to typical PVC DR-18 burst values. Figure 4.6 shows two of the six tested PVC pipe specimens, and Table 4.2 presents the number of pressure cycles to burst and plateau pressure for the PVC burst test. Table 4.2 also compares the experimental PVC burst pressure obtained through multiple pressure cycles to the PVC pipe's expected burst pressure. The PVC burst pressure range (5.86 to 6.63 MPa) is experimentally determined to agree with the 6.13 MPa and 6.35 MPa burst pressure values determined using Equation 4.2 and Equation 4.3, respectively. Thus, the experimental data obtained for PVC burst pressures using multiple cycles (ranging from 5.86 to 6.63 MPa) is in good agreement with PVC theoretical burst pressure (ranging from 6.13 to 6.35 MPa). This testing validates the University of Waterloo CIPP liner burst testing facility, and the CIPP test facility limitations were noted.

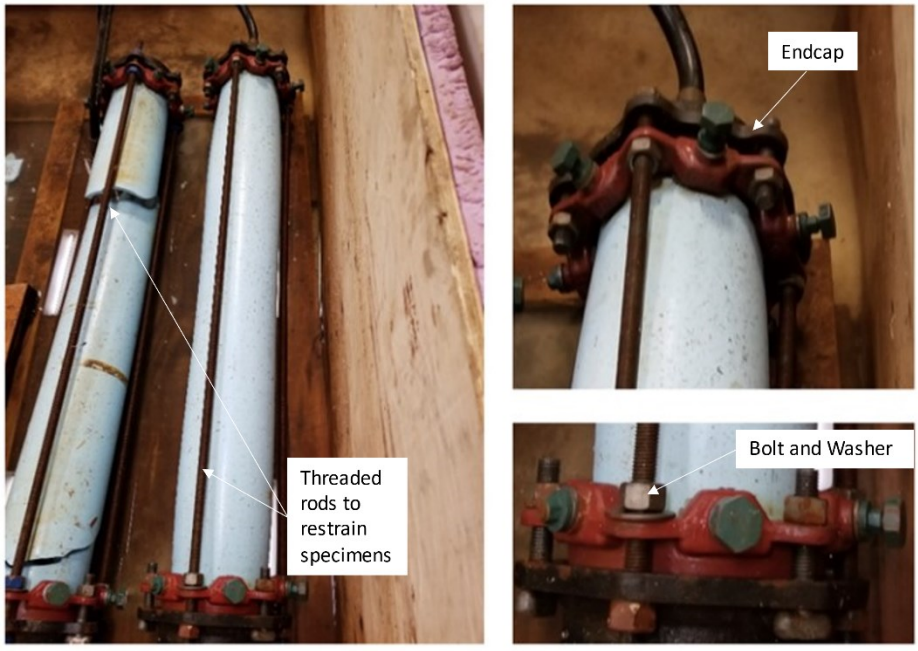

Figure 4.6: PVC burst testing conducted to validate the new CIPP test facility.

Table 4.2 Test results of Six PVC short-term burst tests.

ID	No. of Pressure Cycles to Burst	Maximum Plateau Pressure (MPa)	Min Plateau Pressure (MPa)	Mean Plateau Pressure (MPa)	Burst pressure (MPa)	Burst Time (min)	Equation 4.2 (MPa)	Equation 4.3 (MPa)
P1	4	6.55	6.21	6.38	6.21	3.9	6.13	6.35
P2	4	6.63	5.86	6.25	6.63	4.2	6.13	6.35
P3	5	6.61	6.38	6.50	5.86	4.1	6.13	6.35
P4	6	6.33	5.86	6.10	6.33	3.9	6.13	6.35
P5	8	6.67	6.61	6.64	6.55	4.2	6.13	6.35
P6	6	6.81	6.58	6.70	6.62	4.1	6.13	6.35

4.5 Test Equipment Commissioning

4.5.1 CIPP Burst Testing

For this research, CIPP installation was completed under controlled temperature and humidity conditions to reduce possible product variability. Using field-installed CIPP liner specimens was avoided to ensure consistency and reproducibility of the test result is possible. Thus, CIPP liner specimens were fabricated, installed, and supplied by Insituform Technologies Limited. The composite CIPP product is a redesigned version of the InsituMain^{TM} and is called the I-Main CIPP. Reinforcements were made to induce high tensile capacity to the CIPP product depending upon sliding overlaps of the fibreglass layer. The reinforcing tube incorporates short fibreglass strands in a layered form, which provides a construction improvement for improved liner wetting out and good expandability, thereby ensuring a close-fit liner can be formed within the host pipe. During the manufacturing process of the CIPP liner, the reinforcing tube was installed into an 18 m-long PVC pipe within the plant with a fibreglass pipe connector located every 1.5 meters. The choice of PVC as the host pipe was because CIPP liners have little to no bond with PVC, allowing the liner to be easily separated after curing.

A summary of the installation process for the CIPP liner is as follows:

1. The reinforced fabric was wet-out with epoxy resin and inserted into PVC pipes placed into pipes lying on the shop floor of the Insituform laboratory via the inversion method. This manufacturing process is unlike the typical CIPP installation process, where the liner installation is completed in the field within a buried pipe.
2. Inversion was done using hydrostatic pressure to expand the CIPP bag to fit the inner surface of the host pipe and cured using steam.
3. The cured CIPP product, free of any longitudinal wrinkles or folds, was cut mechanically into specimens with a desired length of 1.5 m.
4. Watertight Mechanical Joint (MJ) cast iron end caps were used with three high-yield threaded bars to secure the ends and create watertight end seals. Threaded rods were used to ensure the end caps did not blow off.

4.5.2 Test Procedure

Twelve 150-mm diameter CIPP specimens were prepared for short-time burst tests. All CIPP specimens were filled with tap water through the manifold, the ball valve, and the one-way flow valve. Ball valves were attached to the rear end of the test specimens to allow the removal of any entrapped air after standing up the pipe vertically to fill up with water. Once all air was removed, the ball valve located at the specimen end was closed. The test specimens were connected to the manifold, and the location of the ball valves, one-way flow check valves, and pressure transducers (see Figure 4.7). The specimens were then conditioned in a 19-mm thick constant-temperature polypropylene plastic tank at 23°C for at least one hour. The testing procedure was adopted from ASTM D1599 [55]. Figure 4.8 shows the end caps and restraints prepared by Insituform to facilitate adequate end enclosure.

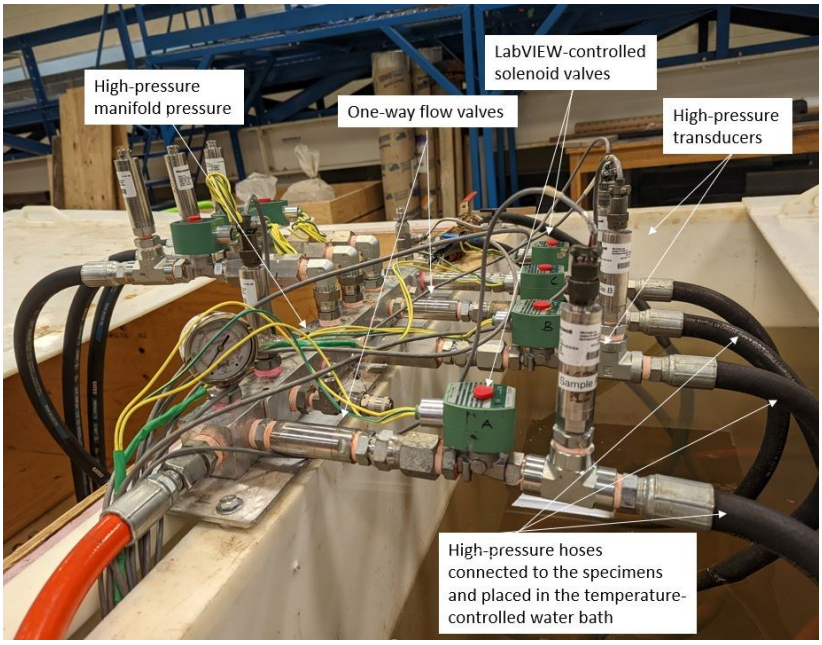

Figure 4.7: High-pressure hoses connected to the pressurization manifold.

Figure 4.8: CIPP specimens after prepping with the MJ end caps and high-yield threaded bars.

The pipe specimens were filled with water by connecting the test specimen to the lab building's potable water network. Any entrapped air was released by opening the ball valve on one of the end caps after standing up the pipe vertically. The specimens were then conditioned in a 19-mm thick constant-temperature polypropylene plastic tank at 23°C for at least one hour. The testing procedure was adopted from ASTM D1599 [55].

4.5.3 Test Results and Discussions

For short-term burst testing, the internal water pressure was increased to equalize with the lab building's water pressure of approximately 0.4 MPa. The inflow water source was shut to have a closed system for water pressurization, and then the internal water pressure was increased using the hydraulic cylinder. A trial-and-error method was used to obtain the appropriate pressurization rate to induce specimen failure within 60 to 70 seconds.

Table 4.3 provides the burst test results for the twelve CIPP liner specimens. The test specimen showed the pipe fractures at burst, and their burst failures occurred between 31 to 69 seconds. Most fractures were of the "wedge" shape, which initiated at a single point, and the wall was ripped across the circumference of the CIPP specimen. Other pipe bursts were in the form of an initial "line fracture," which continues with the ripping of the CIPP wall material.

Table 4.3 ASTM D1599 CIPP liner short-term burst test results.

Specimen ID	Time to Burst (sec)	Burst Pressure (MPa)	Failure Location	Failure Mode	Valid Test
SB02	31	3.09	Middle	Line Crack	No
SB03	69	6.05	Middle	Burst	Yes
SB04	62	5.22	Middle	Burst	Yes
SB05	52	5.04	End	Burst	No
SB06	60	5.30	Middle	Burst	Yes
SB07	47	3.92	End	Seam Failure	No
SB08	48	4.00	Middle	Burst	No
SB09	55	4.82	Middle	Burst	No
SB10	66	5.58	Middle	Burst	Yes
SB12	37	3.08	Middle	Seam Failure	No
SB13	64	5.04	Middle	Burst	Yes
SB14	68	5.59	Middle	Line Crack	Yes

Burst values noted in Table 4.3 were considered valid data, in conformity with ASTM D1599 standard requirements, when the burst failure occurred in the middle or near the middle of the test specimen. The six valid tests are marked “Yes” in Table 4.3 and have short-term burst pressures ranging from 5.04 to 6.05 MPa with a mean burst pressure of 5.47 MPa and a standard deviation of 0.36 MPa. ASTM D1599 [55] specifies that a good pipe burst test should be between 60 and 70 seconds. Figure 4.10 shows the internal water pressure versus the time to failure for all twelve CIPP liner test specimens. This figure shows a linear water pressure ramp rate with no pressure surges for all twelve test specimens. It also shows the inherent variability in the burst pressure as some specimens failed as low as 3.1 MPa with failure times as low as 31 and 37 seconds, while others failed as high as 6.05 MPa at failure times greater than 60 seconds. However, the linear sections of the curves show comparable loading rates for all CIPP test specimens.

The burst testing found that one in four test specimens consistently burst before the ASTM D1599 60 to 70 seconds failure time requirement, even though the internal water pressure loading rate was noted to be significantly close for all tests (see Figure 4.10). Further investigation into the reason for the large variability in CIPP burst testing found that there was no correlation between the CIPP burst pressures and failure modes. Figure 4.9 examines and compares the failure mode of four CIPP specimens. Specimens SB12 and SB10 are noted to be fractured in the same "middle" area of the specimen. However, their failure modes are not the same, and their burst pressures of 3.08 MPa and 5.58 MPa are significantly different (45% difference). Specimens SB07 and SB05 are noted to be fractured in the same "end" area of the specimen. However, their failure modes are not the same, and their burst pressures of 3.92 MPa and 5.04 MPa are significantly different (23% difference).

The large variability in burst pressure and time to failure noted were experimentally determined to be independent of the performance of the CIPP testing equipment, as the specimens were pressurized consistently. The liner variability may be attributed to invisible liner imperfections, resulting in a few early and low burst pressure data. Fractures may have been initiated at liner locations that possessed microscopic air voids inferred to be due to possible Quality Assurance and Quality Control (QA/QC) oversight during the liner saturation process.

The test results show that CIPP burst pressure can vary from a high value of 6.1 MPa to a value as low as 3.1 MPa. This test data and the test results reported by Knight and Bontus [2] and Almansour et al. [56] show the impact of CIPP material flaws, and the significant reduction in CIPP burst pressure is approximately 45 to 50%.

Figure 4.9: Examples of failure modes observed in the burst testing of the I-Main CIPP liner.

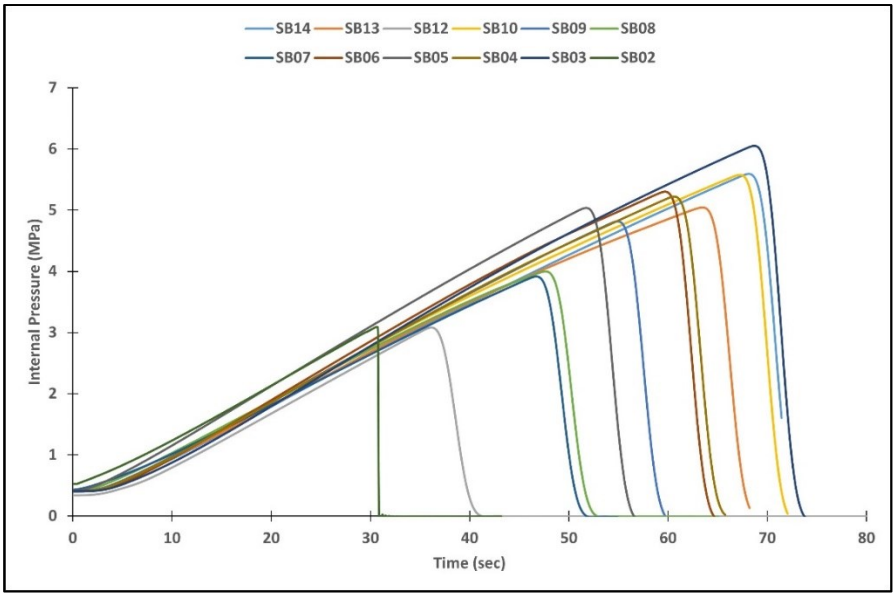

Figure 4.10: Pressure-time plots for all CIPP specimens showing similarities in the rate but different burst values and time.

PVC and HDPE pipe materials have HDS values approximately four times lower than the short-term burst stress, and both products exhibit different short-term burst strengths [48]. Applying the Safety Factor of 4 noted for PVC and PE to the CIPP minimum burst pressure of 3.1 MPa (see Table 4.3), CIPP maximum operating pressure can be estimated. Thus, the I-Main CIPP product will have a maximum working pressure of 0.78 MPa (i.e., 3.1/4). While this estimate shows that CIPP will have a high tensile capacity to withstand full pressure load for a system having the typical operating pressure of about 0.7 MPa, CIPP liners have the additional complexity of being field manufactured, which further increases the variability in CIPP product burst pressure.

PVC is a homogeneous material with no reinforcements and will, as a result, have a different pressure response. This material response is validated by the Equipment validation testing presented herein, where obtaining the failure pressure for PVC involved multiple cycles but was completed without reloading with CIPP testing. Owing to the noted difference in mechanical properties that is different from CIPP, dividing CIPP burst pressure value by four may provide misleading results. The findings herein demonstrate the need for North American standardized testing and design methods for all CIPP products to classify all CIPP products in line with other pressure pipe products. Embracing such advancement will classify different CIPP products based on their pressure pipe PR. CIPP long-term hydrostatic testing can be completed using a piece of test equipment (such as the test facility presented herein) that would be computer-programmed to ensure specimens are subjected to constant and uniform internal water pressure rate for an extended period and no pressure surges are induced during testing.

4.6 Conclusions

Although pressure liners such as PVC, HDPE, and GRP have standard testing guides using pressure testing and evaluation methods, there is currently no framework to guide the hydrostatic testing of CIPP formed within water supply pressure pipes. This study introduces an approach to advance pressure liner testing. It discusses challenges in ensuring all CIPP products can be tested using a similar full-scale burst testing approach. From this research, the following conclusions are drawn:

1) A unique test testing facility for pressure liners was constructed at the University of Waterloo, Canada. The new facility has completed short-term burst tests on Insituform I-Main

composite CIPP pressure liners. It can conduct long-term testing such as HDB testing and cyclic (or fatigue) testing on the tested product and other pressure liners.

2) The new test facility uses a custom-made pressurizing technique using water pressure and has been validated using PVC test specimens. Burst testing was completed using multiple cycles, and the burst pressure ranged from 5.86 MPa to 6.63 MPa and was experimentally determined to be in good agreement with available data and computed PVC burst pressure (ranging from 6.13 MPa to 6.35 MPa). The PVC testing revealed a limitation of the test equipment that involves dealing with pipe expandability in homogenous materials, as water demand for the test equipment will be significantly higher.

3) Short-term burst testing completed on the 150-mm I-Main CIPP liner found that their burst pressure values varied from 3.1 to 6.1 MPa when a linear constant internal water pressure loading rate was applied. Even though the liner tested did not have any visible defect or imperfection, there was no correlation between the failure mode and the failure pressure or location. Invisible imperfections, such as air voids in the liner, were believed to induce significant variability in the CIPP product and were not related to any malfunctioning test equipment. The liner imperfection decreased the liner burst pressure by approximately 50%, which agrees with the range of 45 to 50% from previous watermain CIPP research.

4) The tested CIPP pressure liner Pressure Rating (PR) was estimated using a Safety Factor of 4 based on available PVC, HDPE and GRP research data. From a pressure pipe design standpoint, the I-Main CIPP would have a PR of about 0.78 MPa following the application of a Safety Factor of 4 on the minimum burst pressure (3.1 MPa). While this approach provides engineers and designers with useful long-term mechanical properties, there is a high chance that a Safety Factor of 4 is not appropriate for all CIPP products owing to the significant amount of variability reported and considering the high consequence of failure in a watermain break. Hence the need for North American standardized testing and design methods for all CIPP products to classify each CIPP product in line with other pressure pipe products using long-term hydrostatic testing.

Chapter 5

Long-Term Hydrostatic Strength and Design of Pressure CIPP Liners for Watermain Renovation

5.1 Overview

The design of thermoplastics and thermoset pressure pipes such as HDPE, PVC and GRP involves the establishment of Long-term Hydrostatic Strength (LTHS) and pipe material Pressure Rating (PR) using an industry-recognized Hydrostatic Design Basis (HDB) approach. However, no design method currently addresses thermoset CIPP pressure considerations. This study provides an overview of the HDB design approach and its applicability to designing a 200-mm I-Main composite pressure CIPP liner. It discusses the challenges of using the well-established HDB design approach for CIPP pressure pipe liners. A University of Waterloo customized burst facility validated in previous research was modified to get unique CIPP HDB test data to develop the first known HDB regression line. Test results found that the CIPP design factor (ratio of the short-term burst strength to the 50-year LTHS) of 0.42 agrees with previous research on thermoplastics and GRP, which is 0.42-0.8. The tested CIPP pressure rating was determined to be 0.88 MPa using the predicted 50-year LTHS of 25 MPa. Therefore, this study provides valuable CIPP long-term data and a framework to advance and standardize pressure CIPP design methods.

5.2 Introduction

Pipelines are essential in transporting potable water from treatment plants to residents and businesses. As service duration increases, these pipelines deteriorate and corrode, significantly reducing pipe hoop strength. At this critical stage, there is a high probability of catastrophic pipe failure [3]. Since most potable water distribution networks are old and close to the end of their service lives, watermain renovation methods such as cured-in-place-pipe (CIPP) liners have been used to extend the life of the pipeline network [2], [4], [37].

5.2.1 AWWA Structural Classification

Watermain renovation methods in North America are classified into three structural categories and four classes. Table 5.1 details the differences and similarities between the structural classifications established by the American Water Works Association (AWWA) [58]. AWWA Class I Liners are non-structural systems, such as traditional Cement Mortar Lining (CML) and epoxy. The lining is applied to increase the service life by protecting the pipe's inner surface from corrosion. However, it does not improve the pipe's structural integrity or substantially reduce leakage. AWWA Class II Liners are close-fit semi-structural liners that can span holes and gaps in the host pipe. However, they have minimal thickness and require support from the host pipe to prevent collapse during depressurization. AWWA Class III Liners are similar to AWWA Class II liners. The difference is that AWWA Class III Liners have sufficient thickness to resist buckling from external hydrostatic load or vacuum. AWWA Class IV Liners are fully structural liners, which involve placing a self-supporting, watertight structure inside a pipe. Fully structural linings are typically used in situations requiring minimal disruption to repair structurally deteriorated pipes [58].

Table 5.1: Structural classification and AWWA Class of liners [58].

Liner Characteristics	**Non-Structural**	**Semi-Structural**		**Fully Structural**
	Class I	**Class II**	**Class III**	**Class IV**
Internal corrosion barrier	Yes	Yes	Yes	Yes
Bridges holes/gaps at pipe operating pressure	No	Yes	Yes	Yes
Inherent ring stiffness	No (Depends on adhesion)	No (Depends on adhesion)	Yes	Yes
Long-term independent pressure rating ≥ pipe operating pressure	No	No	No	Yes
Survives “burst” failure of the host pipe	No	No	No	Yes

CIPP liners are typically classified under Class IV or fully structural liners as they are independent of the host pipe. Therefore, they are designed as stand-alone pipes following the Non-Mandatory Appendix X1 in ASTM F1216 [1], *“Standard Practice for Rehabilitation of Existing Pipelines and*

Conduits By The Inversion And Curing Of A Resin-Impregnated Tube." Currently, there is an industry debate about whether watermain CIPP should or should not bond to the host pipe as a stand-alone pipe. For a Class IV design, provisions in the AWWA M28 rehabilitation manual do not specify how to quantify the ability of a liner to survive burst failure of the host pipe. There is currently no design standard for watermain CIPP to address this concern [37]. Other watermain renovation methods that involve installing high-density polyethylene (HDPE) and polyvinyl chloride (PVC) pipes have well-established AWWA standards (AWWA C906 and C900) and design procedures (AWWA M45 and M23). Their standards and design methods quantify the pipe's ability to independently withstand all system pressures and surge pressures (recurring or occasional surges).

5.2.2 Thermoplastic Pipe Pressure Design

HDPE and PVC are designed using an industry-accepted hydrostatic design basis (HDB) approach to determine the material pressure rating (PR) per ASTM D2837, *"Standard Test Method for Obtaining Hydrostatic Design Basis for Thermoplastic Pipe Materials or Pressure Design Basis for Thermoplastic Pipe Products."* The HDB refers to the categorized long–term hydrostatic strength (LTHS) in the circumferential or hoop direction for a given set of end-use conditions established by ASTM D2837 [47]. The LTHS is the estimated tensile stress in the wall of the pipe in the circumferential orientation that, when applied continuously, will cause the pipe failure at 100,000 hours and is the intercept of the stress regression line with the 100,000-hour coordinate (see Figure 5.1). The lower confidence limit (LCL) is the lowest value of the LTHS, based on a statistical analysis of the regression data that can be expected at 100,000 hours. The hydrostatic design stress (HDS) is the estimated maximum tensile stress the material can withstand continuously with a high degree of certainty that failure of the pipe will not occur [47]. This stress is circumferential when internal hydrostatic water pressure is applied. Figure 5.1 shows that the long-term HDS is significantly lower than the short-term burst stress determined using ASTM D1599 [55], *"Standard Test Method for Resistance to Short-Time Hydraulic Pressure of Plastic Pipe, Tubing, and Fittings."* For HDPE and PVC pipe materials, the available data in PPI TR-4 [48] provides the 50-year Long-term Hydrostatic Stress at 23°C ($LTHS_{50}$). Typically, the HDPE and PVC categorized $LTHS_{50}$ values (i.e., the HDB) are approximately two times greater than the HDS.

The pipe material PR is the estimated maximum water pressure the pipe is capable of withstanding continuously with a high degree of certainty that failure of the pipe will not occur [47].

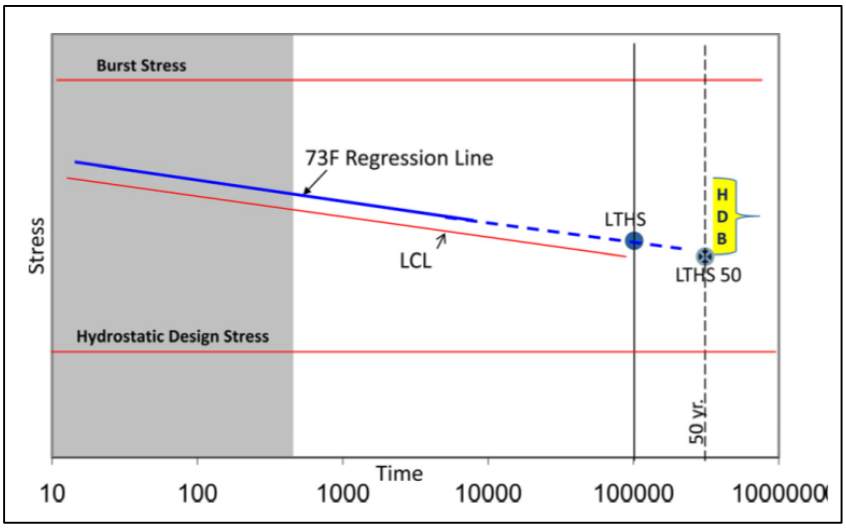

Figure 5.1: Typical regression line and extrapolation using ASTM D2837 [45].

The HDB design approach considers the stress-rupture response of the pipe after subjecting at least eighteen 25-mm extruded specimens under continuous stress levels until failure. The obtained data points are then used in a linear regression evaluation and extrapolated to a future point (typically 50 years) where the pipe's long-term strength can be forecast. The HDB design approach is a stress-based extrapolation method using the concept of allowable hoop stress and is based on the membrane theory of thin-walled tubes to calculate the hoop stresses in the pipe wall [59]. A suitable safety factor is applied to the long-term failure stress to account for critical parameters such as installation practices, operating conditions, and associated potential failure mechanisms of the material [48], [59]. This comprehensive method allows professionals to make informed and engineering-appropriate forecasts of the long-term strength of thermoplastic materials for pressure pipe applications [5]. Boros [45] details the HDB thermoplastic pipe methodology and determines PVC and HDPE long-term hydrostatic strength (LTHS) based on continuous pressure testing as per ASTM D2837 [45], [47]. The LTHS at 50 years ($LTHS_{50}$) was then categorized as the HDB and further reduced to a Hydrostatic Design Stress (HDS) or maximum working stress induced by internal pressure using a Safety Factor of 2 [2], [45].

5.2.3 GRP Pressure Design

Factory-manufactured composite pipes such as glass fibre reinforced plastic (GRP) also adopt the HDB design approach to quantify pipe structural classification via pressure rating determination. Similar testing is conducted using ASTM D2992 [49], "*Standard Practice for Obtaining Hydrostatic or Pressure Design Basis for "Fiberglass" (Glass-Fiber-Reinforced Thermosetting-Resin) Pipe and Fittings,"* and regression analysis is completed on at least eighteen specimens to determine the pipe's long-term hydrostatic strength at 50 years. Sung and Jin [50] evaluated the long-term structural performance of a GRP product by studying the failure pressure and time to failure after subjecting nineteen pipe specimens to hydrostatic pressure for 10,000 hours. They completed HDB tests to rate GRP based on the ratio of GRP 50-year failure pressure to the initial six-minute failure pressure. Failure pressures predicted using the linear equation developed from their regression analysis were 11.6 MPa and 5 MPa for the first six minutes and 50 years, respectively. The ratio of failure pressure for the first six minutes to the predicted 50-year failure pressure was 0.43 [50]. Faria and Guedes [51] presented long-term pressure test results for three GRP pipes. They evaluated the performance of in-plant manufactured 300-mm nominal diameter pipe specimens and 1.3-meter long. The reported regressions indicated that the ratios of the short-term burst pressures to the pipe's 50-year failure pressures were 0.42, 0.5, and 0.83 [51]. Chen et al. [53] discussed the structural performance of Kevlar fibre-reinforced flexible pipe subjected to long-term hydrostatic pressure. They conducted hydrostatic pressure tests for up to 10,000 hours following the ASTM D2992 method. They completed linear regression analysis on the pressure-time data to provide calibrated design pressures and a fast pipe qualification approach for engineering practices. Test specimens were 150 mm in diameter and 1.1 m long. The $LTHS_{50}/LTHS_{10}$ ratio was found to be 0.43 [49] - [51], [53].

5.2.4 CIPP Pressure Testing and Design

Unlike factory-manufactured plastic pipes, there are very limited studies on the long-term pressure testing and design of watermain pressure CIPP liners. Allouche et al. [54] conducted pressure testing to evaluate a CIPP liner. The sections of the CIPP liner spanned across circular perforations in a cast iron pipe since they aimed to investigate liner bending within a damaged area of the host pipe [54]. Thus, the liner was not tested independently, and CIPP 50-year failure pressure was not investigated

to determine the $LTHS_{50}$. Knight and Bontus [2] discussed short-term burst testing for two commercially available watermain pressure CIPP liners (Liner A and Liner B) per ASTM D1599 [55]. They noted a possibility of CIPP liners exhibiting different tensile capabilities to withstand internal pressure loads. They noted Liner B as a CIPP product with visible liner imperfections such as wrinkles and folds. Liner B, having a mean burst pressure of 2.92 MPa, was found to have burst pressures that are approximately 50% lower than Liner B, having a mean burst pressure of 5.45 MPa. [2], [55]. While Knight and Bontus [2] tested CIPP products independently, no CIPP 50-year failure pressure was investigated to determine the $LTHS_{50.}$ They did not state if the 50% reduction in burst pressure and material variability observed were directly related to the liner imperfections in Liner B. Almansour et al. [56] provided ASTM D1599 short-term failure burst data for another commercially available CIPP liner. The CIPP specimens, which have folds, were formed inside 150 mm PVC pipes, and then removed to burst independently. They evaluated the CIPP specimens to investigate the effect of folds and compared them with two control specimens (without folds). Test results indicated that inherent liner features such as folds could reduce CIPP burst pressure by 45%, as the mean burst pressure was 2.65 MPa with folds and 5.94 MPa without folds [56]. Although Almansour et al. [56] were able to investigate the effects of liner imperfections using pressure testing, no CIPP long-term testing was conducted to estimate the 50-year failure pressure and $LTHS_{50}$ Alam et al. [5] presented the results of burst pressure for multiple glass-reinforced thermosetting-resin CIPP specimens. They investigated the effect of CIPP liner configuration change. Nine 1.2-meter-long 300 mm diameter CIPP liners with three different configurations were tested following the ASTM D1599 procedure. Their results found that a CIPP liner having variations in the configuration of the glass reinforcements can significantly reduce CIPP burst pressure by up to 45% [5]. All available literature on pressure testing of CIPP liners discussed herein has detailed the bending capability of a pressure CIPP liner, the critical nature of imperfections (such as folds) in CIPP pressure performance, and the effect of variations in liner configuration. These studies involved short-term pressure testing and did not consider long-term pressure testing to determine critical mechanical properties of watermain CIPP liners.

In Europe, hydrostatic testing, such as short-term burst pressure testing and long-term HDB testing similar to the HDPE, PVC and GRP design approach, has been considered for CIPP. Beyond these, dynamic pressure testing to investigate CIPP fatigue life is now completed [60]. Their pressure testing

approach accounts for CIPP's inherent imperfections and material complexities using full-scale specimens. However, in North America, long-term mechanical properties used for ASTM F1216 design are based on flexural and tensile testing of flat plate specimens, which are not representative of the round field specimens. Conventional plate specimen testing also does not show possible effects of pressure loads, curvature, and small flaws [3], [4], [60]. The recommended long-term tests to be completed for ASTM F1216 design were based on gravity and low pressure (140 to 280 kPa) requirements and were not intended for the design of watermains, which are higher pressure systems (415 to 830 kPa) [4]. Based on a 2011 United States Environmental Protection Agency (USEPA) study [13], the responsibility to address CIPP quality assurance and quality control now lies with project owners or engineers since the ASTM F1216 design method is now considered to be well-established for the intended gravity application for sewers and forcemains [13]. Therefore, the International Organization for Standardization (ISO) and American Water Works Association (AWWA) have created a standard for pressure CIPP liners for watermain renovation. Currently, both organizations are working on standardized design methods for pressure liners. As such, there is an urgent demand for an approach to develop a unified design method for the various pressure CIPP commercially available products. Adopting existing HDB testing and design methodology for comparable pressure pipe products such as GRP appears reasonable in the context of glass-reinforced thermoset watermain CIPP liners.

This study presents experiment-based research to advance the development of a standardized design method for thermoset watermain CIPP liners. Following the HDB method of testing and design, various pressure levels were applied to induce failure of twenty-six Insituform I-Main CIPP specimens. A pressure testing equipment constructed and validated in previous research was used to complete long-term pressure testing to develop the first known CIPP HDB regression line. CIPP pressure performance was estimated using linear regression analysis, and the $LTHS_{50}$, HDS, and PR were determined.

5.3 Materials and Method

5.3.1 CIPP Specimen Configuration

CIPP liner specimens for this study were fabricated, installed, and supplied by Insituform Technologies Limited. The composite CIPP product is a redesigned version of the InsituMain^{TM} and is called the I-Main CIPP. Reinforcements were made to induce a high tensile capacity to the CIPP product depending upon sliding overlaps of the fibreglass layer. The reinforcing tube incorporates short fibreglass strands in a layered form, which provides a construction improvement for improved liner wetting out and good expandability, thereby ensuring a close-fit liner can be formed within the host pipe. The I-Main is designed so that the primary fibres are a $0^o/90^o$ glass in the hoop direction with an area weight of approximately 1 kg/m^2. It has an extra layer of randomly placed fibres on the bottom and has an area weight of approximately 0.2 kg/m^2. After constructing the I-Main, the final product is an epoxy composite with no distinct layers, similar to homogeneous liners. Figure 5.2 shows a cross-section of the glass-reinforced CIPP liner evaluated in this study. The zoomed image shows how the discontinuous short fibreglass strands are placed on top of each other in the hoop direction.

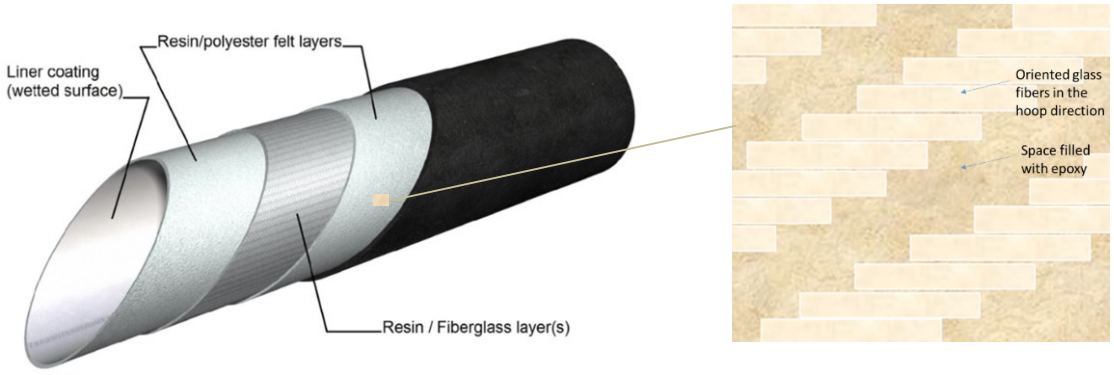

Figure 5.2: Liner configuration and fibreglass reinforcements in the composite CIPP liner [61].

CIPP test specimens were manufactured in a laboratory under controlled temperature and humidity conditions to reduce product variability and enhance test data consistency. The CIPP liner was installed within an 18-meter-long PVC pipe under controlled conditions. A PVC host pipe was chosen since CIPP liners are known to have little to no bond with PVC. Therefore, the liner can be easily chiselled out from the PVC pipe after curing. The installation process for the CIPP liner is as follows:

1. The reinforced fabric was wet-out with epoxy resin and inserted into PVC pipes placed into pipes lying on the shop floor of the Insituform laboratory via the inversion method. This manufacturing process is unlike the typical CIPP installation process, where the liner installation is completed in the field within a buried pipe.
2. Inversion was done using hydrostatic pressure to expand the CIPP bag to fit the inner surface of the host pipe and cured using steam.
3. The cured CIPP product, free of any longitudinal wrinkles or folds, was cut mechanically into specimens with the desired length of 1.5 m.
4. Watertight Mechanical Joint (MJ) cast iron end caps were used with three high-yield threaded bars to secure the ends and create watertight end seals. Threaded rods were used to ensure the end caps did not blow off.

5.3.2 CIPP Specimen Preparation

A total of forty fibre-reinforced thermoset CIPP liner specimens were prepared for short-term and long-term pressure tests. The specimens were 200 mm in diameter and 1.2 meters long so they are at least five times the diameter. Both ends of the specimens were placed within ductile iron steel rings, and the annular spaces between the inner surface of the ring and the outer surface of the CIPP liner were filled up to prevent any radial expansion of the liner. Cast iron mechanical joint (MJ) end caps were used with three high-yield threaded bars to secure the ends and create water-tight end seals. As the rods were tightened inward direction, a rubber seal inside the MJ caps pressed against the outer surface wall of the ductile iron steel ring, thereby creating a water-tight seal. Inlet and outlet tap connections were made on the MJ cap to let water in from one end and bleed out the inside air through the other. Figure 5.3 shows completed end seals, end caps, and restraints attached to CIPP specimens to facilitate adequate end enclosure.

Figure 5.3: CIPP specimens prepared for pressure testing.

5.3.3 CIPP Testing Procedure

Tests were conducted in the custom-built University of Waterloo test facility. A computer-controlled test apparatus continually monitored and maintained multiple test specimens at the target value over an approximate 10,000-hour testing period.

Testing involved the pressurization of a high-pressure manifold that was connected to various CIPP test specimens laid in a constantly controlled temperature water bath. Internal pressure was measured using high-pressure pressure sensors calibrated to ±0.01 MPa. The possible issue of reduction in the test pressure was addressed using solenoid valves that were electronically monitored using a custom-built LabVIEW data acquisition system, and several specimens were simultaneously pressured and monitored. The LabVIEW data acquisition system was programmed to control the actuator movements, open and close solenoid valves, monitor, and take up to 100 pressure sensor data samples per second. Figure 5.4 and Figure 5.5 shows the LabVIEW software interface and physical experimental setup of the CIPP specimens, respectively. The unique pipe pressurizing equipment and data acquisition system ensured that up to seven test specimens could be simultaneously tested using two constant temperature water baths and one pressurizing equipment.

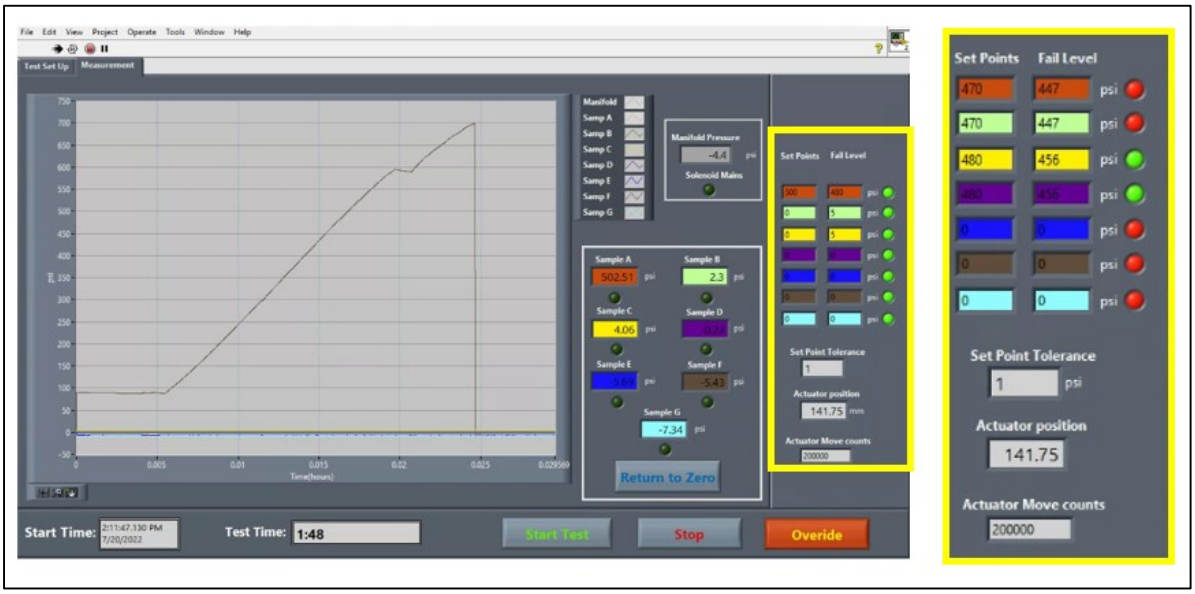

Figure 5.4: LabVIEW software interface for pressure testing at the University of Waterloo test facility.

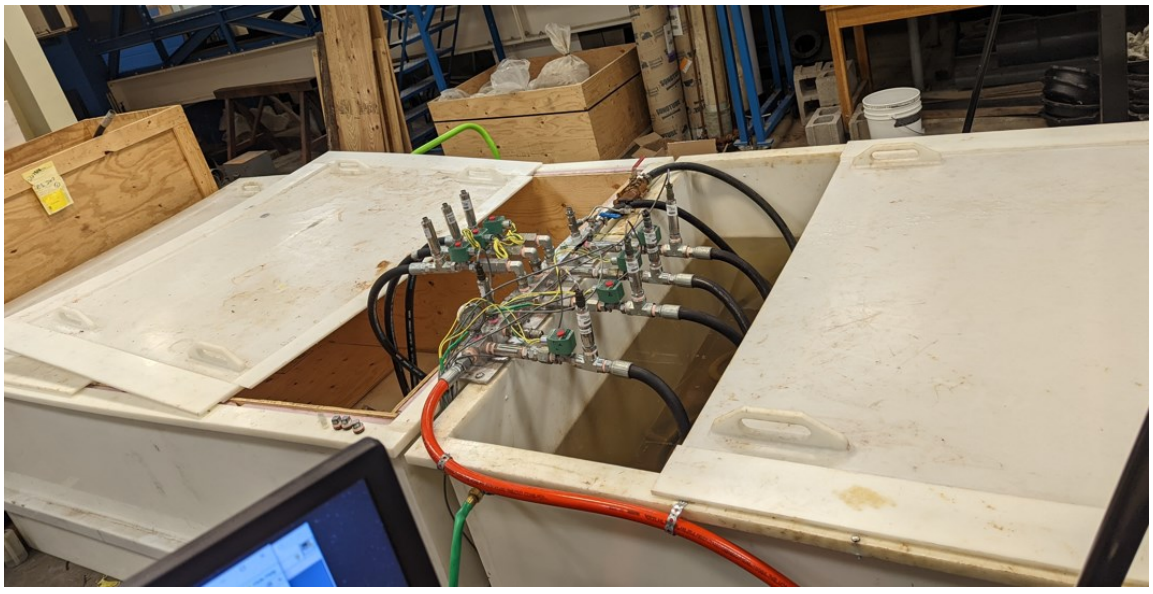

Figure 5.5: The University of Waterloo burst testing setup and water baths to condition the CIPP specimens.

5.3.4 HDB Test Methodology

Long-term hydrostatic tests are typically conducted for up to 10,000 hours while ensuring the internal pressure is maintained at less than 1% during the test required to fail within certain time intervals. The pressure data is typically converted to stress, and the PR is determined based on the HDS after extrapolating using linear regression [45], [47], [49].

Table 5.2 details the target time interval suggested for HDPE, PVC, and GRP. Thermoplastics and GRP HDB test methods involve pressurizing a minimum of eighteen pipe specimens. However, care should be taken when using conventional design approaches for a resin-based plastic product such as CIPP, which is susceptible to huge variations in burst performance. To develop the first known CIPP HDB regression line, time intervals given by ASTM D2837 and ASTM D2992 were incorporated, and multiple CIPP liner specimens (more than eighteen specimens) were experimentally required to be tested to establish failure points from Time Sections I to V.

Table 5.2: Test specification for long-term hydrostatic tests on HDPE, PVC, and GRP pipes.

Time Interval	**Hours to Failure**	**No. of Pipes**	
		GRP	HDPE/PVC
Time Section I	<1,000	At least 6	-
Time Section II	10 to 1,000	At least 3	At least 4
Time Section III	1,000 to 6,000	At least 3	At least 3
Time Section IV	After 6,000	At least 3	At least 3
Time Section V	After 10,000	At least 1	At least 1
Total		At least 18	At least 18

5.4 Results and Discussions

5.4.1 Short-Term Burst Testing

To investigate CIPP's long-term hydrostatic pressure performance, short-term burst tests were first conducted to establish the initial test data that was used as a reference throughout the testing process. Six 1.2-meter-long 200-mm diameter CIPP specimens, having a mean wall thickness of 8 mm, were filled with water ensuring that all air was removed. Three threaded rods were used to ensure

the end connectors did not blow off. The specimens were then conditioned in a temperature-controlled water bath at approximately 23°C for about an hour. Figure 5.6 and Table 5.3 provides the ASTM D1599 burst test results for the six CIPP specimens. The CIPP liner was noted to have short-term burst pressures that range between 4.65 to 5.42 MPa with a mean burst pressure of 5.19 MPa and a standard deviation of 0.31 MPa. All CIPP test specimen burst failures occurred between 69 to 97 seconds. Burst pressure values were considered valid, in conformity with ASTM D1599 standard requirements, when the burst failure happened in the middle or near the middle of the specimens.

The CIPP burst pressure value formed the basis for setting initial failure pressures, and a trial-and-error process was subsequently used since CIPP load-rate behaviour was unknown.

Table 5.3: ASTM D1599 CIPP liner short-term burst test results.

Specimen ID	**Time to Burst (sec)**	**Burst Pressure (MPa)**	**Failure Location**	**Failure Type**
SB_A	97	5.26	Middle	Burst
SB_B	80	5.36	Middle	Burst
SB_C	77	5.27	Middle-End	Burst
SB_D	70	5.42	Middle-End	Burst
SB_E	75	4.70	End	Burst
SB_F	69	4.65	Middle	Burst
Mean	78	5.11	-	-
St. Dev	10.2	0.34	-	-

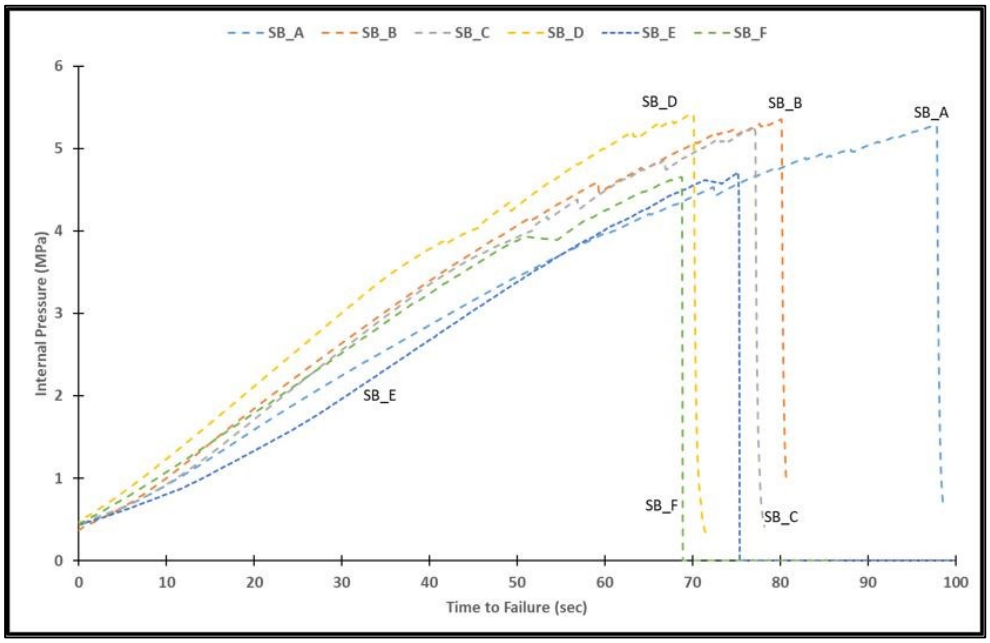

Figure 5.6: Pressure-time plots for six 200-mm diameter CIPP specimens.

5.4.2 Long-Term Hydrostatic Testing

Test pressures were selected to investigate the long-term hydrostatic strength and develop the HDB regression line for CIPP. The experiment was planned such that multiple failures occurred before 10 hours, between 10 and 1,000 hours, 1,000 and 6,000 hours, and then greater than 6,000 hours up to an approximate 10,000-hour period. Table 5.4 provides the CIPP experimental plan.

Table 5.4: Long-term hydrostatic tests experimental plan for the CIPP specimens.

Time Interval	Hours to Failure	No. of CIPP Specimens
Time Section I	<10	At least 6
Time Section II	10 to 1,000	At least 4
Time Section III	1,000 to 6,000	At least 3
Time Section IV	After 6,000	At least 3
Time Section V	After 10,000	At least 1
Total		At least 18

Since the mean short-term burst for the CIPP specimen was 5.2 MPa, test pressures were selected with a start point that is 85% of the CIPP burst pressure (4.25 MPa) and subsequently reduced by 5% to ensure a good spread of data to extrapolate to 50 years. However, the CIPP long-term hydrostatic testing did not go as planned. At 4.25 MPa test pressure, the CIPP specimen could not maintain constant internal pressure for an extended period. After approximately one hour, the specimen pressure dropped from the set pressure (4.25 MPa) to 3 MPa, thereby requiring constant re-pressurization of the specimen, which initiated some frequent “saw tooth waves” in the curves indicating dilation of CIPP (see Test_1 in Figure 5.7). Although no bubbles or fluid leaks were observed in the specimen's vicinity during the test, it was inferred that the CIPP specimen experienced significant circumferential expansion after the initiation of audible cracks in the test specimens. In two attempts, the pressurizing system could only ramp up the specimen pressure to approximately 3.65 MPa (< 4.25 MPa set pressure). Testing was stopped as this CIPP behaviour was unexpected and was not in line with ASTM D2992 methodology that requires the internal test pressure to be maintained within ±1%.

The 3.65 MPa pressure level (approximately 70% of the specimen burst pressure) was then investigated to note CIPP behaviour. The specimen (see Test_2 in Figure 5.7) experienced similar circumferential expansion to the first trial, with test pressure ranging from 3.61 to 3.69 MPa. Testing lasted about six hours, and then irregular pressure stabilization, which was different from the previous six hours, was noted until the pressure dropped again to approximately 2.8 MPa. Furthermore, no bubbles, leaks or liner burst was observed during the testing.

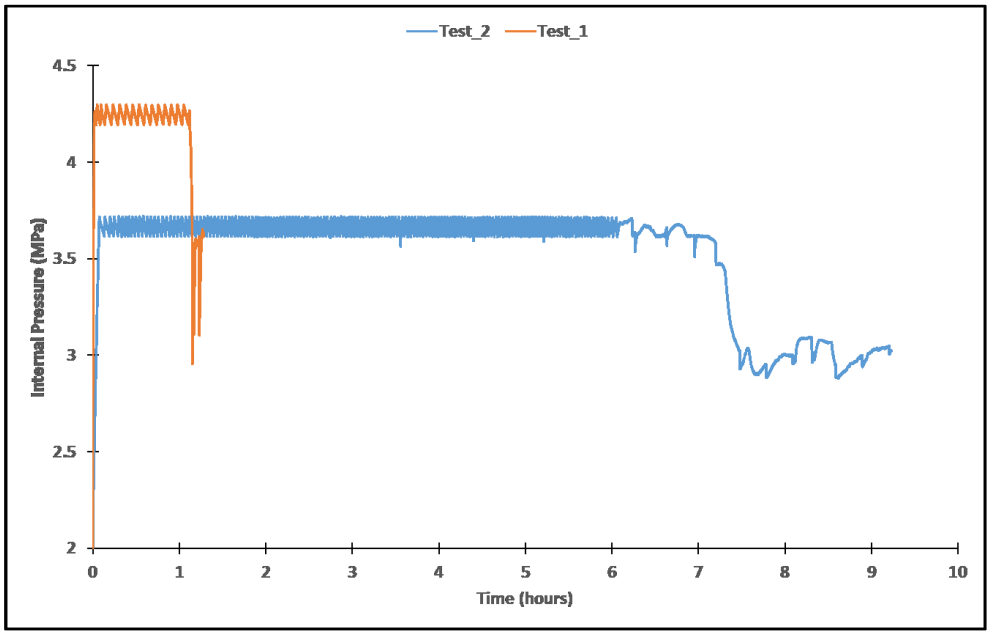

Figure 5.7: Pressure-time graph showing the unexpected pressure drops in the first two tested CIPP HDB specimens.

HBD regression lines for thermoplastic pipes were developed using 25 to 50-mm extruded tubes, which are significantly smaller than 200-mm full-scale CIPP specimens. Since the I-Main CIPP is constructed as a reinforced tube via the inversion method with limited ability to manufacture small tubes as used for HPPE and PVC testing, it was essential to resolve the testing challenges. Similar pressure testing research by Chen et al. [53] evaluated a 1.1-meter long 150-mm Kevlar fibre-reinforced flexible pi. They could not maintain the test pressure due to the failure of the machine control system and lack of system control with the use of pumps. Therefore, several modifications were made to the custom-built University of Waterloo test facilities to overcome this challenge of maintaining the system pressure within the specimens. The LabVIEW program was redesigned to automatically manipulate the pressurization rate to counteract the specimen's pressure loss rate. Also, the solenoid valve for refilling the hydraulic cylinder was upsized from a valve with a 6.35 mm opening to a value with a 19.05 mm opening to allow for an increased water flow. These modifications to the test equipment ensured the change in internal pressure was maintained within an acceptable limit of ±1% of the test pressure.

Following the lessons learned from specimens Test_1 and Test_2 creep and circumferential expansion characteristics, it was essential to have a specific definition for the failure of the CIPP specimens. Both ASTM D2837 and ASTM D2992 standards define specimen failures as the transmission of the test fluid through the body of the specimen in any manner. This specimen failure could be through bursting, cracking, splitting, or weeping (seepage of liquid) of the pipe during the test [47], [49]. The first two specimens (Test_1 and Test_2) were inferred to have failed under "weeping" as it was impossible to see the specimens when covered in water inside the water bath. Whenever a loud breaking sound was heard, or the pressure measurement on the LabVIEW data logger dropped abruptly to zero, such specimens were considered to have failed under "bursting," "cracking," or "splitting," depending on the appearance of the failure location.

After the modifications were made to the test facility, all other test specimens failed in "burst." Figure 5.8 shows a specimen burst failure location for one of the CIPP specimens subjected to sustained internal pressure.

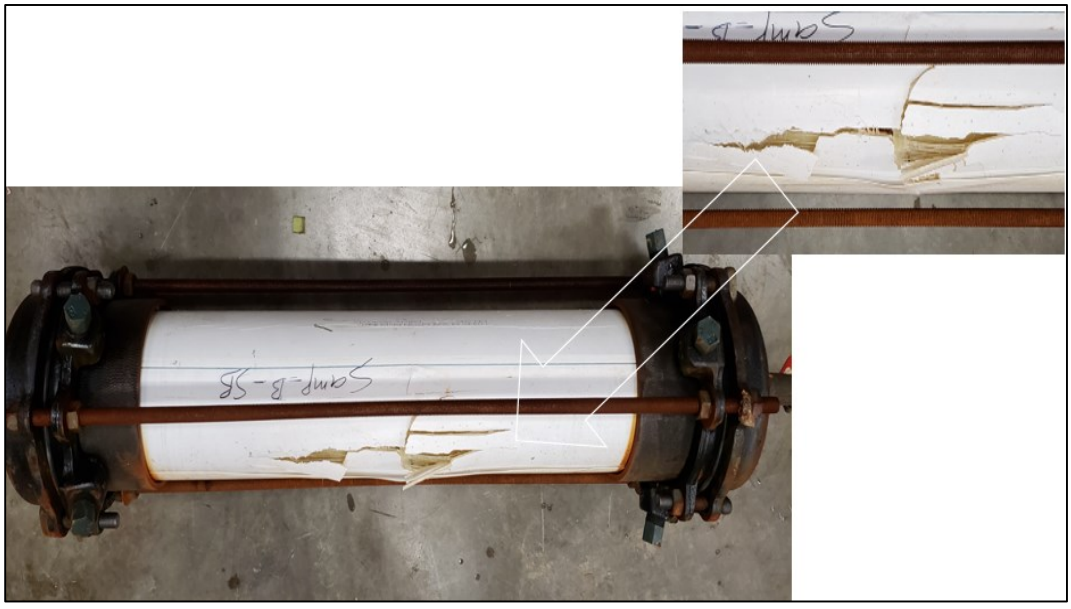

Figure 5.8: Failure that occurred in one of the CIPP specimens under sustained internal pressure.

Equation 5.1 was used to determine the pipe stress, σ_f, from the failure pressure using a Safety Factor of 1 and the dimension ratio of the CIPP specimens.

$$\sigma_f = \frac{P \times (D - t)}{2 \times t} \qquad (5.1)$$

where:

P = Failure pressure,

N = Safety Factor,

D = Pipe outside diameter, and

t = Pipe minimum wall thickness.

Table 5.5 shows the failure pressure and strength, time to failure, and failure location of twenty-six CIPP specimens for long-term performance prediction and design using the HDB approach. For the first eleven CIPP specimens tested, internal pressure ranging from 3.66 to 5.42 MPa was applied to induce failure within Time Section I (< 10 hours). Twelve CIPP specimens with a pressure range from 3.24 to 4.07 MPa caused damage within Time Section II (10 to 1,000 hours). For three CIPP specimens, test pressure ranging from 3.31 to 3.38 MPa was applied to induce damage within Time Section III (1,000 to 6,000 hours). Overall, long-term pressure tests were conducted on the composite CIPP specimens for up to 1635 hours.

Table 5.5: Distribution of time to failure for composite CIPP HDB regression line development.

Time Section	Hours to Failure (hr)	Failure Pressure (MPa)	Failure Strength (MPa)	Time to Failure (hr)	Failure Mode
Time section I	< 10	5.42	64.9	0.02	Burst
		5.36	64.1	0.02	Burst
		5.27	63.1	0.02	Burst
		5.26	63.0	0.03	Burst
		4.65	55.6	0.02	Burst
		4.38	52.4	1.38	Burst
		4.25	50.6	1.16	Weep
		4.14	49.6	1.45	Burst
		3.94	47.2	3.93	Burst
		3.65	43.7	7.31	Weep
Time section II	10 to 1,000	4.07	48.7	46.40	Burst
		3.97	47.5	10.15	Burst
		3.97	47.5	41.72	Burst
		3.66	43.7	64.12	Burst
		3.59	42.9	242.57	Burst
		3.52	42.1	12.64	Burst
		3.52	42.1	183.19	Burst
		3.45	41.3	309.86	Burst
		3.45	41.3	35.34	Burst
		3.38	40.4	714.10	Burst
		3.24	38.8	382.16	Burst
		3.24	38.8	454.48	Burst
Time section III	1,000 to 6,000	3.38	40.4	1041.00	Burst
		3.31	39.6	1634.82	Burst
		3.31	39.6	1386.82	Burst

Figure 5.9 shows the failure pressure points for CIPP specimens subjected to varying sustained internal pressure to cause different failure durations. The trend from the pressure-time graph suggests that with the reduction in test pressure, the CIPP failure time increases. The slope of the graph is noted to be initially steep, and the curve starts to decrease rather steadily beyond 400 hours of testing. This trend was considered to make an informed and reasonable test pressure selection for subsequent testing.

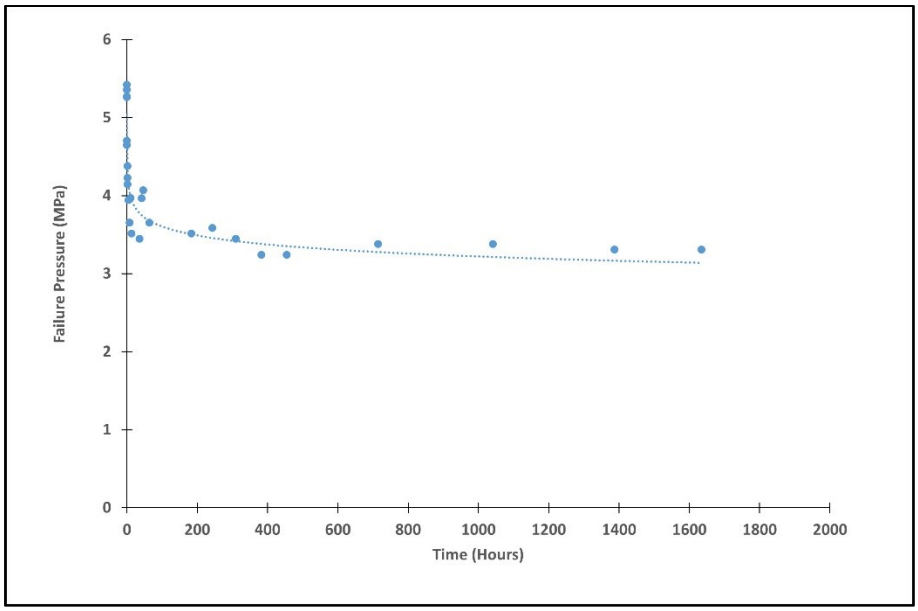

Figure 5.9: Failure pressure versus time to failure curves of CIPP pipes under sustained internal pressure.

To complete data points up to 10,000 hours, some CIPP HDB testing can be conducted by subjecting specimens to pressures ranging from 2.76 to 3.17 MPa so that they fail within Time Section IV (6,000 to 10,000 hours) and section V (> 10,000 hours).

5.4.3 CIPP HDB Regression Line

Data analysis was completed using a logarithmic treatment on the test data. A linear regression analysis was conducted using the failure stress (σ_f) as the independent variable on the y-axis for a least squares calculation and log time (t) as the dependent variable on the x-axis.

Long–term hydrostatic strength (LTHS) in the hoop direction was estimated at 50 years, which was then used to estimate the hydrostatic design stress (HDS). The long-term hydrostatic stress of the tested reinforced CIPP product was extrapolated using Equation 5.2.

$$\sigma_f = a \times \log(t) + b \quad (5.2)$$

where:

σ_f = failure stress,

t = time to failure, and

a and b are regression constants.

Figure 5.10 shows the regression line representing the long-term behaviour of the composite CIPP liner subjected to HDB testing of up to 2,000 hours. Using the linear equation (Equation 5.2) and residual analysis, a 95% lower confidence limit (LCL) line was included on the graph. The LCL line is the lowest value of the LTHS, based on a statistical analysis of the regression data that can be expected. The regression constants, a and b, were -4.6 and 52.3, respectively, and the correlation coefficient between the test results and the linear equation was 0.9 (greater than the minimum threshold of 0.495 for a linear equation to be applied).

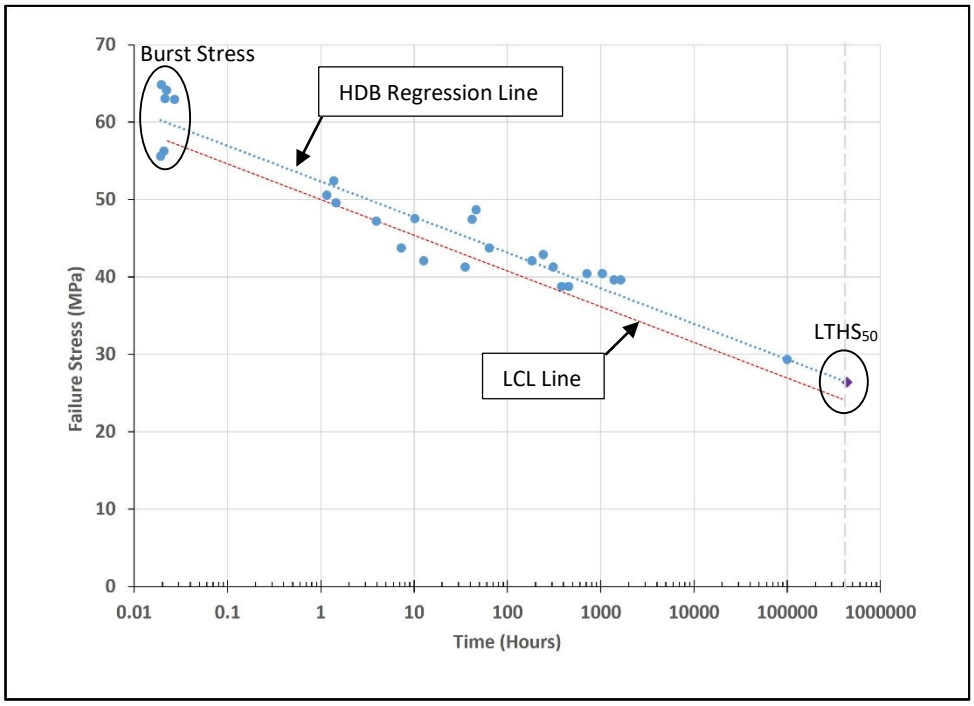

Figure 5.10: HDB Regression line and extrapolation to determine CIPP 50-year Long-Term Hydrostatic Strength and Hydrostatic Design Stress.

From the developed CIPP HDB regression line, a conservative approach was adopted using the LCL line, and it was noted that the 10,000-hour burst stress would be approximately 32 MPa. CIPP LTHS at the 100,000-hour coordinate was estimated to be 27 MPa, and CIPP 50-year LTHS ($LTHS_{50}$) was estimated to be 25 MPa.

5.4.3.1 Design Factor Considerations

Based on available data provided by PPI TR-4 [48] and Boros [45] for PVC and HDPE pipe materials, the typical design factor (DF) applied to the HDB value to estimate the pressure rating was based on the ratio of the short-term burst strength to the categorized $LTHS_{50}$ values. For example, PVC 1120 has a short-term burst strength of 55.2 MPa and a categorized $LTHS_{50}$ (HDB) of 27.6 MPa, allowing a typical DF of 0.5 (i.e., 27.6/55.2). Similarly, test results herein show that the 200-mm CIPP has a short-term burst strength of 60 MPa and a 50-year LTHS or $LTHS_{50}$ of 25 MPa, allowing an approximate DF of 0.42 (i.e., 25/60).

CIPP approximate DF of 0.42 is inferred to agree with DF of 0.43 by Sung and Jin [50] and Chen et al. [53]. CIPP DF also falls within the range of 0.42-0.83 based on research that was conducted by Boros [45] and Faria and Guedes [51].

5.4.3.2 CIPP Pressure Rating

By applying a DF of 0.42 to the extrapolated $LTHS_{50}$ value, CIPP HDS was determined. Then the liner pressure rating was computed using Equation 5.3, which estimated the maximum pressure the CIPP can withstand continuously without failure.

$$PR = \frac{2 \times HDS}{DR - 1} \quad (5.3)$$

where:

DR = ratio of the pipe outside diameter to the pipe minimum wall thickness, and

HDS = hydrostatic design stress for CIPP estimated to be 10.5 MPa (0.42 × 25 MPa)

Therefore, the 200-mm CIPP studied herein will have a PR of 0.88 MPa.

Available data provided by PPI TR-4 [48] shows that PVC and HDPE have burst stresses about four times their categorized $LTHS_{50}$ value. Using this Safety Factor on CIPP short-term burst pressure may be misleading as the tested CIPP had a PR of approximately 1.2 MPa (i.e., 4.65/4) when the minimum burst pressure value (with "middle" failure) was used. This 1.2 MPa PR value is overestimated by 25% as the CIPP PR value obtained from long-term hydrostatic testing was 0.88 MPa. Hence, all CIPP products must undergo individual long-term hydrostatic testing to determine their HDS and PR. This research has provided a unique dataset that can serve as a powerful engineering tool for numerical modelling researchers to explore CIPP pressure performance. It has also provided valuable CIPP long-term data and framework that ISO and AWWA can consider for watermain pressure CIPP liner design.

5.5 Conclusions

This study describes full-scale hydrostatic tests on a composite fibre-reinforced CIPP product for approximately 2,000 hours and extrapolates to 50 years. Following existing design methodologies, a framework to determine the long-term behaviour of CIPP under sustained internal pressure was presented. From this research, the following conclusions can be drawn:

1. A unique test equipment was set up at the University of Waterloo to complete HDB testing on pressure CIPP liners. Several modifications were made to the test facility since testing larger specimens is more challenging than HDPE or PVC 25 or 50-mm tubes. Overall, a thermoset CIPP HDB data has been provided using the new experimental setup. This data can serve as a valuable engineering tool for numerical modelling researchers to explore CIPP pressure performance and provide a framework that can be useful to ISO and AWWA for watermain pressure CIPP design consideration.

2. The I-Main CIPP 2,000-hour pressure-time graph trend suggested that with the reduction in test pressure, the CIPP failure time increased. The slope of the graph was initially steep, and the curve started to decrease rather steadily beyond 400 hours of testing. The correlation coefficient between the test results and the regression equation was 0.89, and most data sets fell above the 95% LCL line, showing that applying the linear equation was appropriate for the CIPP data set. This research found that the tested thermoset CIPP composite provided acceptable data after undergoing HDB testing similar to HDPE, PVC and GRP.

3. The CIPP HDB regression line was developed using failure pressure and time data. CIPP HDS was determined after extrapolation was completed to estimate the $LTHS_{50}$ and PR using a DF. CIPP approximate DF was 0.42, based on the ratio of the short-term burst strength to the categorized $LTHS_{50}$ values, and was in agreement with the DF obtained from previous research on thermoplastics and GRP ranging from 0.42-0.8. The tested CIPP pressure rating was determined to be 0.88 MPa using a CIPP DF of 0.42, and CIPP HDS was estimated to be 10.5 MPa using the predicted $LTHS_{50}$ of 25 MPa.

4. This study has shown that existing HDB testing and design methodology for comparable pressure pipes such as HDPE, PVC and GRP is appropriate for glass-reinforced watermain products such as the I-Main CIPP. Estimating CIPP PR by applying a Safety Factor of 4 to the short-term burst pressure significantly differed from the PR obtained based on CIPP long-term testing as it overestimated the PR by 25%. From a pressure pipe design standpoint, care should be taken when adopting a generalized Safety Factor considering the high consequence

of failure in a watermain break. Hence, there is a need for all CIPP products to undergo individual long-term hydrostatic testing to determine their HDS and PR.

Chapter 6

Conclusions and Recommendations

6.1 Research Findings and Contributions

In this thesis, an experimental investigation has been conducted to evaluate the long-term mechanical response of commercially available fully structural CIPP liners by quantifying the flexural and tensile creep properties, investigating the creep-rupture performance of the liner, and determining short and long-term hydrostatic burst performance.

The key findings and research contributions for each chapter are summarized below:

1. In Chapter 2, a unique set of data providing pressure CIPP long-term flexural and tensile mechanical properties was made available to engineers, researchers, and numerical modelling experts. All tested flat plate specimens exhibited linear viscoelastic behaviour within the investigated range of stress that is 25% of the yield strength (i.e., approximately 48 MPa for flexural creep testing and 33 MPa for tensile creep testing). In the presented work, the composite CIPP response, when pulled apart (in tension), was significantly different from when loaded as a beam (in flexure). Extrapolated creep moduli using linear regression on 1,000 to 10,000-hour experimental data agreed with the theoretical moduli estimated using Findley's model. However, the flexural Creep Retention Factor (CRF) of 35% did not agree with the tensile CRF of 50%. Thus, using the traditional 50% CRF to estimate the 50-year CIPP creep modulus for reinforced pressure CIPP liners are direction dependent and do not apply to flexural and tensile testing.
2. In Chapter 3, over 3,000 hours of experimental data for flexural creep-rupture testing of four unique CIPP products (two non-reinforced and two reinforced CIPP liners) were provided to determine CIPP long-term 50-year flexural strength. The high tensile capacity introduced to the CIPP liner by glass fibre reinforcements significantly impacted the long-term strength. Testing found that the SRF for the non-reinforced liners (55% and 65%) was lower than the reinforced CIPP specimens SRF (80% and 85%). All SRF values were found not to agree with the generalized CIPP 50% retention factor. When analyzed using the applicable ASTM F1216

equations that require long-term flexural strength, the traditional 50% SRF value produced more conservative design outputs with a difference of about 5-20%.

3. In Chapter 4, details about the construction and commissioning of a unique burst testing facility at the University of Waterloo were provided. The new facility completed short-term burst tests on full-scale 150-mm PVC pipes and CIPP liners and was stated to have the capability to complete long-term testing, such as HDB testing and cyclic (or fatigue) testing on pressure liners. Testing on a commercially available CIPP liner (without any visible imperfection) found the short-term burst pressure values to vary between 3.1 and 6 MPa. The noted variability reduced liner burst pressure by approximately 50%. Due to the liner saturation process, it was experimentally determined not to be related to any malfunctioning in the test equipment but to the presence of small, microscopic imperfections, such as air voids. The I-Main CIPP liner Pressure Rating (PR) was estimated to be 0.78 MPa using a Safety Factor of 4 based on available PVC, HDPE and GRP research data.

4. In Chapter 5, a framework to develop an HDB regression line for a commercially available CIPP liner was provided. This research provided details on modifications to a unique experimental setup to complete challenging pressure testing on a full-scale 200-mm CIPP liner. A logarithmic treatment of the 2,000-hour data set found that internal test pressure showed good linear relation to the log of time. The correlation coefficient between the test results and the linear equation was 0.89, and most data sets fell above the 95% LCL line. The tested CIPP pressure rating was determined to be 0.88 MPa using a CIPP DF of 0.42, and CIPP HDS was estimated to be 10.5 MPa using the predicted $LTHS_{50}$ of 25 MPa. This research found that a polymer-based composite such as the I-Main pressure CIPP liner provided acceptable data after undergoing long-term hydrostatic testing similar to HDPE, PVC and GRP. It also provided valuable data for numerical modelling researchers to explore CIPP pressure performance and a framework that ISO and AWWA would find helpful for watermain pressure CIPP design consideration.

6.2 Recommendations for Future Research

Although this research presented some significant findings, it also uncovers several research opportunities, which can be explored to further the understanding of the long-term behaviour of watermain CIPP liners. Supported by the conceptual framework presented herein, this research work may further be extended by including the following ideas:

1. Exploring the possibility of comparing testing conducted on full-scale CIPP samples using hydrostatic burst testing to ring testing using round specimens to determine the hoop strength of the pipe. Further coupon testing can also be considered using curved hoop direction samples for long-term (creep or creep-rupture) testing in three-point bending to ensure a better representation of the CIPP products and account for the effect of curvature and closely simulate the field conditions.

2. The correlation between field-manufactured and lab-manufactured CIPP hydrostatic design strength can be established. The aim will be to improve the pressure rating equation used in Chapter 4 (Equation 4.1) and Chapter 5 (Equation 5.3) to account for field-manufactured samples since lab-manufactured samples may produce higher long-term strength values.

3. Demonstrating the proposed framework's application to other kinds of CIPP products and applying the developed testing method to different pipe sizes will advance the current knowledge. For example, completing parametric analysis to determine the degree of difference when conducting HDB on other smaller diameter pipes ranging from 150 to 600 mm. The availability of such data can lead to the birth of a document similar to PPI TR-4 [48], where CIPP historical data can be found.

4. Validating the HDB line produced by running checks on multiple CIPP specimens and also by running a comparative testing program with other researchers and laboratories to replicate the test facility. Manufacturer-provided design numbers used for watermain renovation design can also be compared with experimental estimates.

References

[1] ASTM F1216, *Standard Practice For Rehabilitation Of Existing Pipelines And Conduits By The Inversion And Curing Of A Resin-Impregnated Tube,* West Conshohocken, PA: ASTM International, 2016.

[2] M. A. Knight and G. Bontus, "Pressure Testing of CIPP Liners to Failure," in *ASCE Pipelines*, 2018.

[3] K. Awe, M. Knight, A. Abdel-aal and G. Bontus, "Advances in CIPP Pressure Pipe Liner Testing and Design," in *ISTT 37th International No-Dig Conference*, Florence, Italy, 2019.

[4] M. A. Knight, K. Awe, A. Abdel-aal, R. Baxter and G. Bontus, "Design of CIPP Pressure Liners using the HDB Method," in *ASCE Pipelines 2019*, Nashville, TN, 2019.

[5] S. Alam, I. T, E. L and C. U, *Determination of Resistance to Short-Time Hydraulic Pressure of Resin Impregnated Fiberglass Liner Material following the ASTM D1599 Procedures,* Ruston, Louisiana: Trenchless Technology Center, 2015.

[6] J. Matthews, A. Selvakumar and W. Condit, "Demonstration and Evaluation of an Innovative Water Main Rehabilitation Technology: Cured-in-Place Pipe (CIPP) Lining," *Water Practice Technology,* vol. 7(2), p. 1–12, 2012.

[7] J. Matthews, W. Condit, R. Wensink and G. Lewis, "Performance Evaluation of Innovative Water Main Rehabilitation Cured-In-Place Pipe Lining Product," Battelle Memorial Institute, Cleveland, OH, 2012.

[8] D. Glock, "Post-critical Behaviour of a Rigidly Encased Circular Pipe Subject to External Water Pressure and Temperature Rise," Der Stahlbau, 1977.

[9] ATV, "Structural Design of Liner Pipes and Segments for Rehabilitation of Sewers and Drains," Merkblatt ATV-M127 Teil 2, Gesellschaft zur Fo¨rderung der Abwassertechnik, 2000.

[10] ATV-M 127-2, "Static Calculations for the Rehabilitation of Sewers with Lining and Assembly Procedures," Hennef, 2000.

[11] T. Oliver, "Structural Design of Close-fit Liners in Fractured Rigid Circular or Non-circular Gravity Pipes," *Journal of Pipeline Systems Engineering and Practice,* vol. 12(1): 04020065, 2021.

[12] ASCE MOP 145, *Design Of Close-Fit Liners For The Rehabilitation Of Gravity Pipes,* Reston, VA: American Society of Civil Engineers, 2021.

[13] EPA, "Quality Assurance and Quality Control Practices for Rehabilitation of Sewer and Water Mains," U.S. EPA, Office of Research and Development, Edison, NJ, 2011.

[14] ASTM D2990, "Standard Test Methods For Tensile, Compressive, And Flexural Creep And Creep-Rupture Of Plastics," ASTM International, West Conshohocken, PA, 2017.

[15] G. Spathis and E. Kontou, "Creep Failure Time Prediction of Polymers and Polymer Composites," *Composite Science and Technology ,* pp. 959-964, 2012.

[16] J. Kraft, A. Shaurav, D. Kozman, M. Chandler and B. Donohue, "Creep Evaluation of GFRP Pressurized Pipe Materials," in *North American Society for Trenchless Technology No-Dig Show*, Chicago, IL, 2019.

[17] E. J. Barbero, S. Makkapati and J. S. Tomblin, "Experimental Determination of the Compressive Strength of Pultruded Structural Shapes," *Composite Science Technology,* pp. 59(13), 2047–2054, 1999.

[18] G. Shanhai, E. Allouche, M. E. Baumert, R. L. Sterling and K. Bainbridge, "Numerical and Experimental Examination of the Long-Term Performance of a CIPP Pressure Pipe Liner," in *North American Society for Trenchless Technology 2007 No-Dig Conference & Exhibition*, San Diego, California, 2007.

[19] R. K. Lee and S. Ferry, "Long-Term Cured-In-Place Pipe (CIPP) Performance and Its Design Implications," in *NASTT's 2007 No-Dig Show April 16-19*, San Diego, California, 2007.

[20] W. T. Straughan, N. Tantirungrojchai, L. Guice and H. Lin, "Creep Test of Cured-In-Place Pipe Material Under Tension, Compression, and Bending," *Journal of Testing and Evaluation,* vol. 26, no. 6, pp. 594-601, 1998.

[21] S. Batra, *Creep Rupture and Life Prediction of Polymer Composites,* Masters thesis, West Virginia University., 2009.

[22] W. K. Goertzen and M. R. Kessler, "Creep Behavior of Carbon Fiber/Epoxy Matrix Composites," *J. Materials Science and Engineering,* vol. 421, no. 1-2, pp. 217-225, 2006.

[23] W. T. Straughan, L. Guice and C. Mal-Duraipandian, "Long-Term Structural Behavior of Pipeline Rehabilitation Systems," *Journal of Infrastructure Systems,* vol. 1, no. 4, pp. 214-220, 1995.

[24] S. Wang, *A New Long -Term Design Model for Rehabilitation Pipe Liners,* PhD thesis, Louisiana Tech University, 2002.

[25] E. Barbero and S. I. Rangarajan, "Long-Term Testing of Trenchless Pipe Liners," *Journal of Testing and Evaluation,* vol. 33, no. 6, pp. 378-384, 2005.

[26] B. R. Hazen, "Physical Properties and Flexural Creep Retention Factors of Reinforced CIPP Liners of Various Bag Materials and Thermoset Resins," in *North American Society for Trenchless Technology NASTT's 2015 No-Dig Show, March 15-19*, Denver, Colorado, 2015.

[27] A. Riahi, "Short-term and Long-term Mechanical Properties of CIPP Liners," University of Waterloo, Waterloo, ON, 2015.

[28] M. Knight, "Evaluation of SANEXEN Technologies AQUA-PIPE Watermain Rehabilitation Product," CATT Technical Report, Toronto, ON, 2005.

[29] B. Shannon, G. Fu, R. Azoor, R. Deo and J. Kodikara, "Long-Term Properties of Cured-in-Place Pipe Liner Material," *Journal of Materials in Civil Engineering 34(7),* pp. 1-9, 2022.

[30] GTI, *Photo of Tensile Creep Testing Equipment,* Des Plaines, IL, 2019.

[31] ASTM D790, "Standard Test Methods for Flexural Properties of Unreinforced and Reinforced Plastics and Electrical Insulating Materials," ASTM International, West Conshohocken, PA, 2017.

[32] ASTM D638, *Standard Test Method for Tensile Properties of Plastics,* West Conshohocken, PA: ASTM International, 2014.

[33] L. K. Guice, T. Straughan, C. R. Norris and R. D. Bennett, "Long-Term Structural Behavior of Pipeline Rehabilitation Systems," Trenchless Technology Centre, TTC Technical Report #302, Ruston, LA, 1994.

[34] W. N. Findley, Creep and Relaxation of Nonlinear Viscoelastic Materials with an Introduction to Linear Viscoelasticity, Amsterdam: North-Holland ISBN 9780444601926, 1976.

[35] W. N. Findley, "Creep Characteristics of Plastics," *ASTM Symposium on Plastics,* pp. 1-18, 1944.

[36] D. W. Scott, J. Lai and A. Zureick, "Creep Behavior of Fiber Reinforced Polymeric Composites: A Review of the Technical Literature," *ournal of Reinforced Plastics and Composites,* Vols. Vol 14, No 6, p. 558–617, 1995.

[37] AWWA Committee, "Classifications of Pressure Pipe Linings; Suggested Protocol for Product Classification," American Water Works Association, Denver, CO, 2019.

[38] J. Gumbel and D. Chrystie-Lowe, "Determination of Hoop Strength and Stiffness in Short and Long Term Testing of Pipes and Liners," in *No Dig Berlin*, Berlin, 2015.

[39] H. Lin, "Creep Characterization of CIPP Material Under Tension, Compression, and Bending," Dept. of Civil Engineering, Louisiana Tech University, 1995.

[40] P. Lystbaek, "Investigation of Lifetime Expectancy of Cured-In-Place Pipes," in *ISTT No Dig Conf. London: International Society for*, 2007.

[41] W. Zhao and L. G. Whittle, "Liner Buckling Design using Critical Buckling Strain," in *Pipeline Technology Conference*, Hannover, Gremany, 2007.

[42] A. P. Moser, O. K. Shupe and R. R. Bishop, "Is PVC pipe strain limited after all these years?," *American Society for Testing Materials, edited by G. S. Buczala and M. J. Cassady, West Conshohocken, PA,* 1990.

[43] ISO 11296-4, *Plastics piping systems for renovation of underground non-pressure drainage and sewerage networks — Part 4: Lining with cured-in-place pipes,* International Organization for Standardization, 2021.

[44] ISO/DIS 11298-4, *Plastics Piping Systems for Renovation of Underground Water Supply Networks — Part 4: Lining with Cured-in-Place Pipes,* 2019.

[45] S. Boros, "Long-term Hydrostatic Strength and Design of Thermoplastic Piping Compounds," *Journal of ASTM International, Vol. 8, No. 9,* 2011.

[46] G. Marshall and S. Brogden, "Design Against Surge and Fatigue Conditions for Thermoplastic Pipes," *Water Industry Information and Guidiance Note,* pp. 1-12, 1999.

[47] ASTM D2837, *Standard Test Method for Obtaining Hydrostatic Design Basis for Thermoplastic Pipe Materials or Pressure Design Basis for Thermoplastic Pipe Products,* West Conshohocken, PA: ASTM International, 2022.

[48] PPI TR-4, *Listing of Hydrostatic Design Basis (HDB), Hydrostatic Design Stress (HDS), Strength Design Basis (SDB), Pressure Design Basis (PDB) and Minimum Required Strength (MRS) Ratings for Thermoplastic Piping Materials or Pipe,* Irving, TX: Plastic Pipe Institute, 2018.

[49] ASTM D2992, *Standard Practice for Obtaining Hydrostatic or Pressure Design Basis for "Fiberglass" (Glass-Fiber-Reinforced Thermosetting-Resin) Pipe and Fittings,* West Conshohocken, PA: ASTM International, 2018.

[50] H. Y. Sung and O. O. Jin, "Prediction of Long-term Performance for GRP pipes under Sustained Internal Pressure," *Composite Structures,* pp. 185-189, 2015.

[51] H. Faria and R. Guedes, "Long-term Behaviour of GFRP pipes: reducing the Prediction Test Duration," *Polymer testing, Vol. 29,* pp. 337-345, 2010.

[52] R. Rafiee and B. Mazhari, "Modeling Creep in Polymeric Composites: Developing a General Integrated Procedure," *International Journal of Mechanical Science,* vol. 99, pp. 112-120, 2016.

[53] W. Chen, Y. Bai, H. Yan and H. Xiong, "Analysis on the Long-term Hydrostatic Strength of Kevlar Fibre Reinforced Flexible Pipe," *Ships and Offshore Structures, Vol. 13,* pp. 226-232, 2018.

[54] E. N. Allouche, K. Bainbridge and I. Moore, "Laboratory Examination of Cured in Place Pipe Liner for Potable Water Distribution System," in *No-Dig Conference Proceedings*, Orlando, Florida, 2005.

[55] ASTM D1599, *Standard Test Method for Resistance to Short-Time Hydraulic Pressure of Plastic Pipe, Tubing, and Fittings,* West Conshohocken, PA: ASTM International, 2018.

[56] H. Almansour, R. Smith, J. Margeson and O. Maadani, *Burst Pressure Test According to ASTM D1599 – Test Set-up, Procedures and Results, Client Report A1-004080,* Canada: National Research Council, 2015.

[57] M. A. P, "Design of Pressure Pipes," in *Buried Pipe Design*, New york, McGraw-Hill Companies, Inc., 2001, pp. 188-244.

[58] AWWA M28, M28 Rehabilitation of Water Mains, Third Edition. ISBN: 9781583219706., 2014.

[59] M. Farsad, "Two New Criteria for the Service Life Prediction of Plastics Pipes," *Polymer Testing,* pp. 967-972, 2004.

[60] A. Haacker, "The DLT-Method: Stress Test for Pressure Pipes," in *International No-Dig 37th International Conference and Exhibition*, Florence, Italy, 2019.

[61] Insituform, *The Cured-in-Place Pipe Solution for Force Main and other Pressure Pipe Rehabilitation,* St. Louis, MO: Insituform Technologies, LLC, 2017.

[62] A. Jaganathan, E. Allouche and B. M, "Experimental and Numerical Evaluation of the Impact of Folds on the Pressure Rating of CIPP Liners.," *Journal of Tunnelling and Underground Space Technology,* 2007.

[63] R. Sterling, S. Alam, W. Allouche, E. Condit, J. Matthews and D. Downey, "Studying the Life-Cycle Performance of Gravity Sewer Rehabilitation Liners in North America," in *Elsevier*, Amsterdam, Netherlands, 2016.

[64] A. Polito, M. Davison and M. Bureau, "Performance of a Water Main CIPP Product Following 15 Years of Service," in *North American Society for Trenchless Technology's 2017 No-Dig Show*, Washington, DC, 2017.

[65] D. Kleweno, "Long-Term Performance Comparison of Pipe Lining Systems Using Traditional Methodologies," in *North American Conference and Exhibition of Trenchless Technology, Albuquerque, New Mexico, 5-8 April*, Albuquerque, New Mexico, 1998.

[66] H. E. Stewart, O. T. D, W. B. P, N. A. N, C. Argyrou, X. Zeng and K. T. Bond, "Performance Testing of Field-aged Cured-In-Place (CIPL) Liners for Cast Iron Piping," Cornell University, Ithaca, NY, 2015.

Appendix A

Sample Calculation to Determination of Findley Constants and Theoretical Strain in Chapter 2

This section presents a step-by-step procedure to obtain the Findley constants and theoretical strains in Chapter 3. An example is presented below to obtain the theoretical strain in Specimen LF1 at 0.25 hr.

Findley's power law is a simple relationship between creep strain and time using Equation 2.3 to determine a theoretical strain, ε. Findley's power law is given via Equation 2.3:

$$\varepsilon = \varepsilon_o + mt^n$$

Findley's creep parameters, n and m, were obtained by expressing Equation 2.3 in logarithmic form and performing a linear regression analysis on the normal-log plot of strain against the log of time given by Equation 2.4.

$$\text{Log}(\varepsilon - \varepsilon_o) = n \times \text{Log}(t) + \text{Log}(m)$$

Step 1: Obtain the corresponding y-axis value for each time, t

$(\varepsilon - \varepsilon_o) = 0.8817\% - 0.8538\% = 0.0279\%$

Step 2: Perform a linear regression analysis on the normal-log plot of $(\varepsilon - \varepsilon_o)$ against time:

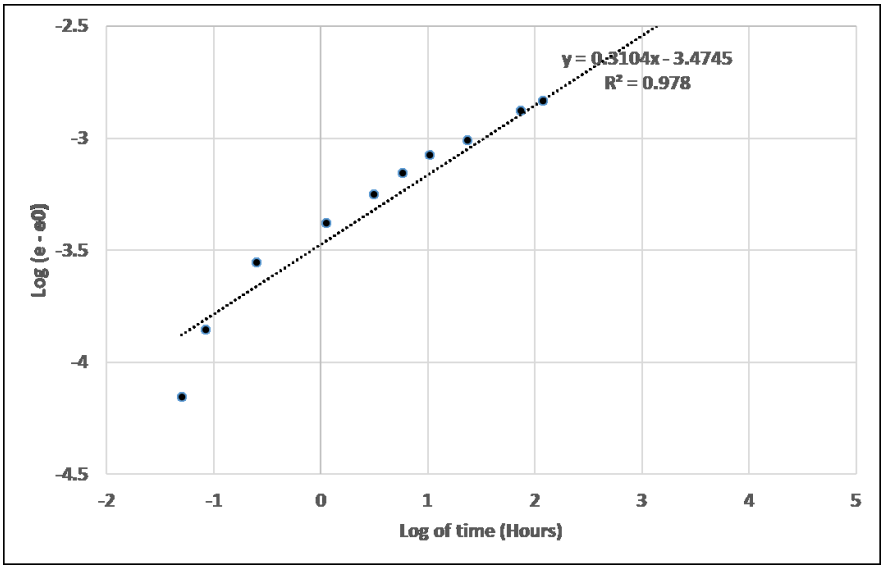

Figure C.1: Log-log plot showing Findley constants.

Step 3: Obtain constants m and n from the curve equation.

n = 0.31042

$\log(m) = -3.47453$, m = 0.00034

Step 4: Substitute constants n and m in Equation 2.3 to obtain theoretical strain at each time, t:

$\varepsilon(t) = 0.8538\% + (0.00034 \times 0.25^{0.31042})$

$\varepsilon(t) = 0.8756\%$

Appendix B

Supplementary Flexural Properties of the CIPP Liners in Chapter 3

Table A1: Depth, width, and flexural properties for each NC-L721 test specimen.

	L721-01	L721-02	L721-03	L721-04	L721-05	L721-06
Width	19.90	19.90	19.90	19.90	19.90	19.90
Average Depth (mm)	5.38	5.55	5.70	5.65	5.71	5.68
Span-to-Depth Ratio	16:1	16:1	16:1	16:1	16:1	16:1
Flexural Stress (Yield) (MPa)	42.66	40.52	36.96	36.13	39.95	34.06
Flexural Strain (Yield) (%)	0.80%	1.13%	1.02%	1.03%	1.10%	0.98%
Ultimate Flexural Strength (MPa)	64.90	61.07	62.59	52.35	50.70	54.45
Ultimate Flexural Strain (%)	4.78%	4.89%	5.00%	3.92%	3.81%	4.98%
Initial Tangent Modulus of Elasticity (MPa)	3,874	3,794	3,736	3,743	3,726	3,607

Table A2: Depth, width, and flexural properties for each NC-L758 test specimen.

	L758-01	L758-02	L758-03	L758-04	L758-05	L758-06
Width	19.80	19.80	19.80	19.80	19.80	19.80
Average Depth (mm)	5.63	5.66	5.64	5.58	5.61	5.60
Span-to-Depth Ratio	16:1	16:1	16:1	16:1	16:1	16:1
Flexural Stress (Yield) (MPa)	33.34	36.18	35.37	35.47	41.60	35.22
Flexural Strain (Yield) (%)	0.83%	0.90%	0.88%	0.91%	1.08%	0.96%
Ultimate Flexural Strength (MPa)	47.52	49.21	54.03	52.33	50.43	53.14
Ultimate Flexural Strain (%)	3.32%	3.56%	4.41%	4.40%	3.88%	4.27%
Initial Tangent Modulus of Elasticity (MPa)	3,946	4,078	4,041	3,926	3,966	4,139

Table A3: Depth, width, and flexural properties for each RC-IPLUS test specimen.

	IPLUS-01	IPLUS-02	IPLUS-03	IPLUS-04	IPLUS-05	IPLUS-06
Width	30.00	30.10	30.00	30.10	30.10	30.00
Average Depth (mm)	12.70	12.90	12.60	12.90	12.90	12.50
Span-to-Depth Ratio	16:1	16:1	16:1	16:1	16:1	16:1
Flexural Stress (Yield) (MPa)	73.08	64.46	71.02	67.53	67.53	75.44
Flexural Strain (Yield) (%)	1.38%	1.38%	1.28%	1.33%	0.48%	1.25%
Ultimate Flexural Strength (MPa)	215.76	206.51	223.06	207.75	201.01	210.21
Ultimate Flexural Strain (%)	4.95%	4.98%	4.91%	5.00%	5.00%	4.99%
Initial Tangent Modulus of Elasticity (MPa)	5,836	5,467	5,762	5,185	5,199	5,484

Table A4: Depth, width, and flexural properties for each RC-IMAIN test specimen.

	IMAIN-01	IMAIN-02	IMAIN-03	IMAIN-04	IMAIN-05	IMAIN-06
Width	30.10	30.00	30.00	30.00	30.00	30.00
Average Depth (mm)	12.60	12.70	13.00	13.10	12.80	12.60
Span-to-Depth Ratio	16:1	16:1	16:1	16:1	16:1	16:1
Flexural Stress (Yield) (MPa)	77.22	86.43	81.88	77.65	93.84	83.93
Flexural Strain (Yield) (%)	1.35%	1.63%	1.56%	1.46%	1.77%	1.44%
Ultimate Flexural Strength (MPa)	218.93	219.66	226.81	222.45	218.12	226.67
Ultimate Flexural Strain (%)	4.88%	5.02%	4.99%	5.00%	5.00%	5.00%
Initial Tangent Modulus of Elasticity (MPa)	5,567	5,333	5,488	5,379	5,451	5,641

Appendix C

Sample Calculation for CIPP Design Consideration in Chapter 3

Table B1: CIPP Liner Input Parameters.

	Value	Unit
Host Pipe ID, D	600	mm
Height of water, Hwo	1.2	m
Height of water, Hwi	1.9	m
Height of soil, Hso	1.3	m
Hole diameter, d	12.7	mm
Enhancement factor, K	7	
Poisson's ratio, v	0.3	
Safety factor, N	2	
Ovality, Δ	2	%
Soil density, w	1920	Kg/m3
Soil Modulus, E's	6.9	MPa
Internal Pressure, P	0.7	MPa
Vacuum Pressure, P	-0.07	MPa
Flexural Str, σ	50/201	MPa
SRF	50/55/80	%
Long-term FStr, σl		MPa

Equation X1.2

$$1.5\frac{\Delta}{100}\left(1+\frac{\Delta}{100}\right)DR^2-0.5\left(1+\frac{\Delta}{100}\right)DR=\frac{\sigma_L}{PN}$$

where:

Δ = ovality of the host pipe,

σ = 50 MPa

σ_L = Long-term Flex Strength = (Flex Strength Short-term) x (Long-term Retention Strength Factor)

P = external pressure on the liner

N = Safety Factor

Solve Eq. X1.2 for DR,

Where DR = $\frac{\left[0.5+\left\{0.25+\left(6\frac{\Delta}{100}\left[\frac{\sigma_L}{PN\left(1+\frac{\Delta}{100}\right)}\right]\right)\right\}^{0.5}\right]}{3\frac{\Delta}{100}}$

Liner thickness = Liner OD / DR

@SRF = 50%, t = 3.8 mm

@SRF = 55%, t = 3.66 mm (4.4% lower than t @ 50%SRF)

@SRF = 80%, t = 3.06 mm (20% lower than t @ 50%SRF)

Equation X1.6

$$P = \frac{5.33}{(DR-1)^2} \cdot \left(\frac{D}{d}\right)^2 \cdot \frac{\sigma_L}{N}$$

where:

DR = liner dimension ratio

D = Inside diameter of the existing pipe

d = diameter of the hole in the existing pipe

σ = 201 MPa

σ_L = Long-term Flex Strength = (Flex Strength Short-term) x (Long-term Retention Strength Factor)

N = Safety Factor

Liner thickness = Liner OD / DR

@SRF = 50%, t = 0.67 mm

@SRF = 55%, t = 0.64 mm (4.6% lower than t @ 50%SRF)

@SRF = 80%, t = 0.53 mm (20.9% lower than t @ 50%SRF)